THE AUTOPARAMETRIC

VIBRATION ABSORBER

ROBERT S. HAXTON

Thesis submitted for the degree of

Doctor of Philosophy

University of Edinburgh

July 1971

ACKNOWLEDGEMENTS

The author wishes to gratefully acknowledge the valuable guidance given by his supervisor, Dr. A.D.S. Barr of the Department of Mechanical Engineering, and the Studentship support of the Science Research Council, London, during the period of this research.

Special thanks are due to Mr. George Smith for his advice and skill in the construction of the apparatus and to Miss Avril Myles who typed the thesis.

SYNOPSIS

This thesis presents the basic steady-state operating characteristics of a device known as the autoparametric vibration absorber (or simply as the AVA). This is a two-degree of freedom system consisting of a main linear spring mass system and an attached absorber system. The motion of the main mass under external forcing, acts parametrically on the motion of the absorber. Terms, nonlinear in the absorber motion, act back on the main mass and with appropriate choice of tuning parameters, 'absorption' of the main mass response can be obtained.

Mathematically the analysis of the AVA under harmonic excitation of the main mass is the study of two coupled nonhomogeneous equations of the second order with quadratic nonlinearities. Three possible methods of solution are considered, each of which provides the same first order solution for the steady-state behaviour of the AVA. After a stability assessment, this theoretical solution is compared with the steady-state results of the experimental investigation.

A theoretical comparison is also made between the steady-state performance of the AVA and that of a linear tuned and damped absorber of the same mass ratio. The results of this comparison highlight the need for an AVA system possessing the optimum absorbing capabilities and consequently the design of several AVA mechanisms is studied.

A possible theoretical solution of the transient behaviour of the AVA is also presented. This transient solution is formulated using a technique similar to that used in the steady-state analysis. The merits of this transient solution are assessed by comparison with a digital computer simulation of the system equations of motion.

Finally a brief study is made of the response behaviour of the AVA system when the main mass is subjected to random excitation.

CONTENTS

CHAPTER 1

INTRODUCTION

1.1 Parametric and Autoparametric Excitation

The phenomenon of parametric excitation, in which an oscillatory system oscillates at its natural frequency ω if one of its parameters is made to vary at frequency 2ω, was first observed by Faraday* (1831). He noticed that the wine in a wineglass oscillated at half the frequency of the excitation caused by moving moist fingers around the edge of the glass. Later, Melde (1859) provided a more striking demonstration in which a stretched string was attached at one end to a prong of a tuning fork capable of vibrating in the direction of the string. It was observed that when the fork vibrated with frequency 2ω, lateral vibrations of the string occurred at frequency ω. In 1883 Lord Rayleigh explained this phenomenon mathematically.

From a mathematical standpoint the study of such phenomena may be reduced to the integration of differential equations with time-dependent (generally periodic) coefficients. Beliaev (1924) was, apparently, the first to provide an analysis of parametric resonance in a structure. His model was that of an elastic column, pinned at both ends, and subjected to an axial periodic force $F(t) = F_0+F_1\cos\omega t$. The equation which emerged was of the Mathieu-Hill type. However, the study of this type of linear differential equation contributes little to the understanding of parametric excitation phenomena which are essentially nonlinear in most cases.

* references are listed alphabetically in the Bibliography.

Parametric resonance is an integral part of the wider field of dynamic instability. In a linear system the amplitude grows indefinitely while in the nonlinear case, the instability decreases with increasing amplitude and vanishes when the system amplitude reaches a certain level for which the oscillations become stationary.

The distinction between parametric, or more specifically heteroparametric (the prefix 'hetero' is normally dropped), and autoparametric excitation is that in the former case, parameter variations are produced by external periodic excitation, and in the latter, by the system itself. The classical autoparametric problem is that of the elastic pendulum described by Minorsky.

Beliaev's findings were completed by Andronov and Leontovich (1927) and over the next thirty years a considerable volume of literature had amassed on various aspects of parametric resonance and stability. Notable among the researchers of this period were the Russians, Chelomei, Krylov and Bogolyubov and the Germans, Mettler and Weidenhammer.

With the expansion of this relatively young branch of dynamical studies there was an increasing demand for more powerful mathematical techniques. As early as 1944, Artem'ev applied the technique of expansion with respect to a small parameter to determine instability zones, but it was not until the early sixties that the asymptotic methods were firmly established in the literature. These methods are well documented by Bogolyubov and Mitropol'skii.

This brief survey of developments in the field of parametric resonance would not be complete without a mention of the significant contribution made by Bolotin.

The papers he wrote during the fifties on dynamic stability and, in particular, on parametric stability, are incorporated in his book, "The Dynamic Stability of Elastic Systems" which was published in English in 1964 and is considered a standard text in this field.

For several years this Department has been engaged in the study of parametric response with the aim of providing a better understanding of the nature of the phenomenon and a broader experimental basis for existing theoretical work. This thesis presents one such investigation into the interaction between dynamic and autoparametric response based on an original research idea suggested by Dr. A.D.S. Barr, at present Reader in this Department.

1.2 The Autoparametric Vibration Absorber

Within the context of this thesis, vibration absorbers are considered to be passive single degree of freedom systems, designed for addition to some larger vibrating system with a view to reducing its resonant response under external harmonic excitation. Falling into this class are such devices as the tuned and damped absorber, the gyroscopic vibration absorber and the pendulum absorber. They are basically linear devices because although in operation large amplitudes may introduce nonlinear stiffness or inertial effects the working of the device is not dependent on these. The effectiveness and response characteristics of these absorbers is well documented.

The subject of this research however, is a device which interacts in an essentially nonlinear manner with the main system to which it is attached. It is the manner in which the device is excited that leads to it being termed the 'autoparametric vibration absorber' (contracted to AVA) in keeping with the definition of autoparametric excitation given in the previous section.

In the usual forms of absorber the motion of the main mass acts effectively as a 'forcing' term on the absorber motion. In the autoparametric absorber however, the main mass motion causes variations in the absorber spring stiffness which, although time-varying, are not explicit functions of time but actually depend on the absorber motion itself which acts back on the main system through nonlinear terms.

The absorber-like response of an autoparametric system might have been anticipated from existing analysis. For example, the classical autoparametric problem, already mentioned, in which an elastic pendulum exhibits energy absorption in the high-frequency mode (2ω) followed by transference of this energy to the low frequency mode (ω). However in this research the absorber-like response was first noticed in the laboratory when during tests on the parametric excitation of simple structures under foundation motion, it was observed that in a region of parametric instability the structure could have considerable effect on the 'foundation'. The foundation was really another degree of freedom and autoparametric interaction was involved.

Mathematically the analysis of the autoparametric absorber under harmonic excitation of the main system is the study of two coupled nonhomogeneous equations of the second order with quadratic nonlinearities. A general study of this form of system using the averaging method has been given by Sethna. A system which is mathematically similar to the device presently under consideration is presented in a paper by Sevin and also in related papers by Struble and Heinbockel.

They discuss the parametric interaction of a vibrating beam with its pendulous supports, however, they confine their studies to the autonomous or free-vibration case.

The question naturally arises as to whether the AVA has any advantage in application over the more conventional types of absorber. This is an open question at present but in most cases it can be anticipated that the answer will be negative. However, the study of an absorber system combining the action of the AVA with that of the linear tuned and damped absorber does show some promise in this direction. From a fatigue point of view, any benefit gained from the operation of the AVA absorber system at half the frequency of the main system tends to be nullified by the increased stresses caused by the relatively large operational amplitudes of the absorber itself.

1.3 The Scope of the Present Investigation

This thesis presents the operating characteristics of the autoparametric vibration absorber. The theoretical model of the AVA system is that of a main linear spring mass system under periodic forcing the motion of which acts parametrically on the motion of an attached absorber system which consists of a cantilever beam with adjustable end mass.

For the mathematical analysis of the relevant equations of motion, the asymptotic method described by Struble is used in preference to the averaging method used by Sethna and the two-variable expansion procedure described by Cole and Kevorkian, but, for this problem at least, the results are the same. In the asymptotic method a general perturbational solution of the equations of motion is expressed in the form

$$u = A\cos(\omega t + \theta) + \epsilon u_1 + \epsilon^2 u_2 + \ldots + \epsilon^N u_N$$

where each of A, θ, u_1, u_2,..., u_N is in general, a function of time. The first term of the expansion is the principal part of the solution while the additive terms in powers of ϵ (a natural parameter of the system) provide for a perturbational treatment. Substitution of this solution into the equations of motion leads to sets of variational and perturbational equations of different orders in ϵ. It is the variational equations of the first order in ϵ which provide the steady-state solution of the behaviour of the AVA in this case.

Formulation of the steady-state solution requires that certain assumptions be made regarding the conditions of internal and external resonance. A solution is obtained assuming the condition of exact internal resonance in which the absorber frequency is tuned to half that of the main system while the main system is excited in the neighbourhood of its natural frequency by the external harmonic forcing (external resonance condition). Another, more general, solution is found by assuming that the absorber is slightly detuned so that the exact internal resonance condition is no longer valid. In both cases the stability of these theoretical steady-state solutions is studied and the results presented as a series of amplitude response curves for selected values of the system parameters.

On the completion of the analysis of the steady-state solution it was decided to effect a theoretical comparison between the AVA and the linear tuned and damped absorber in an attempt to assess the efficiency of the former. From this comparison it emerges that the ϵ parameter plays an important role in determining the absorbing power of the AVA.

It is because this ϵ parameter is a function of the construction of the absorber that consideration is given to other possible AVA systems with a view to obtaining an optimum design. (One such system is a combination of the AVA and the linear tuned and damped absorber).

To demonstrate the validity of the theoretical predictions regarding the nature of the steady-state solution, experiments are performed using a cantilever-type absorber mounted on a main spring mass system which is excited by an electromagnetic vibrator. From the data collected by monitoring the steady-state amplitudes of the absorber and the main mass it is possible to compile a series of amplitude response curves which are directly comparable with their theoretical counterparts.

A study of the operating characteristics of the AVA would not be complete without an inquiry into the nature of its transient behaviour. Consequently, a possible analytical solution of the transient motion is discussed which involves mathematical procedures very similar to those used in the steady-state analysis. The merits of this solution are then compared with a digital computer simulation of the AVA transient performance.

Although the present investigation is mainly concerned with the AVA's ability to absorb energy from a system subjected to harmonic excitation, a few experiments were performed to show the AVA's response to external random excitation.

Finally, a paper entitled "The Autoparametric Vibration Absorber" by R.S. Haxton and A.D.S. Barr, is appended at the end of this thesis.

CHAPTER 2

THEORETICAL ANALYSIS OF THE AUTOPARAMETRIC VIBRATION ABSORBER

2.1 Introduction

The mathematical analysis of the autoparametric absorber under harmonic excitation of the main mass system is the study of two coupled nonhomogeneous equations of the second order with quadratic nonlinearities. In this chapter these equations are derived from a basic theoretical model using the Lagrangian formulation. The application of an asymptotic method described by Struble provides an insight into the nature of the steady-state behaviour of the AVA. Finally a study is made of the stability of the steady-state solutions.

A possible analytical solution of the transient behaviour of the AVA system under external excitation is given in Appendix I together with the results of a digital computer system simulation.

2.2 Theoretical Model

Fig. 2.2.1 represents a schematic drawing of an AVA mounted on a single degree of freedom system under external forcing $F(t)$. The AVA consists of a weightless cantilever beam of length ℓ and flexural rigidity EI carrying a concentrated end mass m. The varying motion $X_d(t)$ (subscript d indicates 'dimensional', a nondimensional X is introduced later) of the main mass system (mass M, spring stiffness k) induces fluctuations in the effective lateral spring stiffness λ of the cantilever.

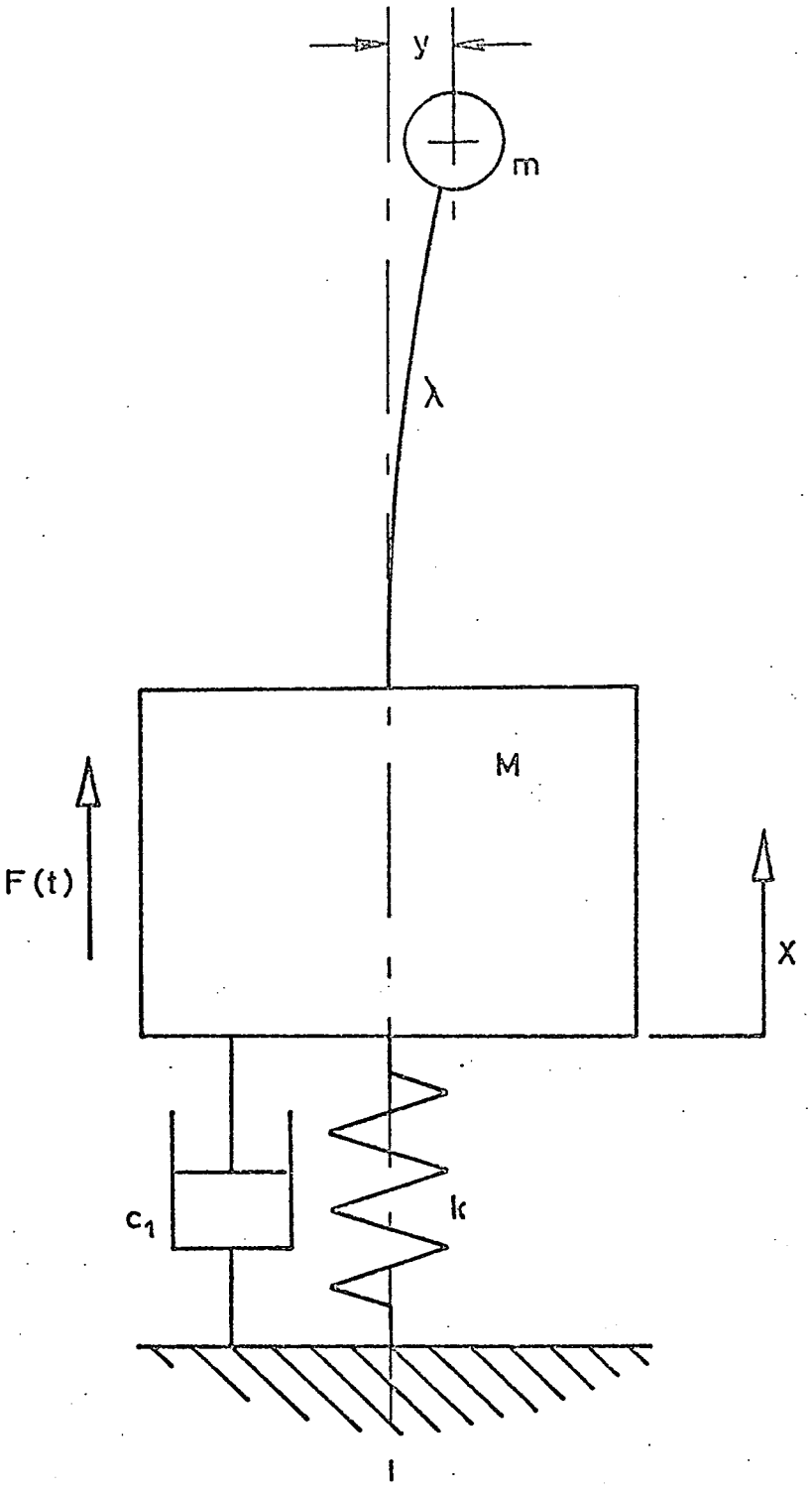

Fig. 2.2.1

Schematic Diagram of a Cantilever-Type
Autoparametric Absorber System.

It is this timewise variation in stiffness which initiates the motion of the absorber. However this motion of the absorber mass is not in a purely lateral mode (y_d) but is associated with an axial displacement which can be related to y_d from the geometry. Consequently the absorber feeds X-directed forces back on the main mass.

A factor which emerges from the analysis is the importance of this relationship between the axial and lateral displacements of the end mass in determining the effectiveness of the absorber. With this in mind, consideration was given to alternative mechanisations some of which are discussed briefly in Appendix II.

2.3 Equations of Motion

In deriving the equations of motion using the Lagrangian formulation it is essential to include terms due to the axial motion of the absorber mass in the evaluation of the expressions for kinetic energy, T, and potential energy, V, of the system.

If Z denotes the axial displacement of the absorber mass then

$$Z = \tfrac{1}{2} \int_0^{\ell} \left(\frac{dy}{dx}\right)^2 dx$$

where y is a function of the deflection form of the cantilever and x is the distance along the undeflected beam. (See S. Timoshenko's 'Strength of Materials', Part II). Assuming the cantilever to have a static form of displacement curve such that

$$y = \frac{y_d}{2\ell^3} (3\ell x^2 - x^3)$$

then the relationship between Z and y_d is

$$Z = \frac{3}{5\ell} y_d^2 \quad \text{with} \quad \dot{Z} = \frac{6}{5\ell} y_d \dot{y}_d$$

Dots indicate differentiation with respect to time t.

The expressions for T and V are then

$$T = \tfrac{1}{2}M\dot{X}_d^2 + \tfrac{1}{2}m(\dot{X}_d^2 + \frac{36}{25\ell^2} y_d^2 \dot{y}_d^2 - \frac{12}{5\ell} \dot{X}_d y_d \dot{y}_d + \dot{y}_d^2)$$

and

$$V = \tfrac{1}{2} kX_d^2 + \tfrac{1}{2} \lambda y_d^2 + Mg X_d + mg(X_d - \frac{3}{5\ell} y_d^2)$$

where g is the acceleration due to gravity.

The resulting equations of motion are

$$(1 + \frac{m}{M})\ddot{X}_d + \frac{k}{M} X_d + (1 + \frac{m}{M})g - \frac{m}{M} \frac{6}{5\ell} (\dot{y}_d^2 + y_d \ddot{y}_d) = \frac{F(t)}{M}$$

$$\ddot{y}_d + (\frac{\lambda}{m} - \frac{6}{5\ell} g - \frac{6}{5\ell} \ddot{X}_d) y_d + \frac{36}{25\ell^2} (\dot{y}_d^2 + y_d \ddot{y}_d) y_d = 0$$

Henceforth the gravitational effects will be ignored with the adoption of a horizontal configuration of the main mass and cantilever system. Also viscous damping will be assumed to act on the main mass (c_1) and the absorber mass (c_2).

Consequently the equations of motion take the form

$$(1 + \frac{m}{M})\ddot{X}_d + \frac{c_1}{M} \dot{X}_d + \frac{k}{M} X_d - \frac{m}{M} \frac{6}{5\ell} (\dot{y}_d^2 + y_d \ddot{y}_d) = \frac{F(t)}{M}$$

$$\ddot{y}_d + \frac{c_2}{m} \dot{y}_d + (\frac{\lambda}{m} - \frac{6}{5\ell} \ddot{X}_d) y_d + \frac{36}{25\ell^2} (\dot{y}_d^2 + y_d \ddot{y}_d) y_d = 0$$

It is now beneficial to perform a nondimensionalisation on the basis of the static deflection X_o of the main system under the force amplitude F_o of the external forcing function.

Thus when the external forcing is harmonic of the form $F(t) = F_o \cos 2\Omega t$ the nondimensional equations are

$$\ddot{X} + 2\epsilon\eta_1\omega_1\dot{X} + \omega_1^2 X - \epsilon R(\dot{y}^2 + y\ddot{y}) = \omega_1^2 \cos 2\Omega t$$

$$\ddot{y} + 2\epsilon\eta_2\omega_2\dot{y} + (\omega_2^2 - \epsilon\ddot{X})y + \epsilon^2 y(\dot{y}^2 + y\ddot{y}) = 0 \qquad 2.3.1$$

where $X_o = F_o/k$; $X = X_d/X_o$; $y = y_d/X_o$; $\epsilon = 6X_o/5\ell$; $\omega_1^2 = k/(M + m)$;

$\omega_2^2 = \lambda/m$; $\lambda = 3EI/\ell^3$; $R = m/(M + m)$; $\epsilon\eta_1 = c_1/2(M + m)\omega_1$;

$\epsilon\eta_2 = c_2/2m\ \omega_2$ 2.3.2

ω_1 is the free undamped natural frequency of the entire system with the absorber locked ($y = 0$) and ω_2 is the free undamped natural frequency of the absorber. R is a mass ratio and ϵ a natural small parameter of the system.

2.4 Steady-State Solution of the Perfectly Tuned AVA

Three possible methods of achieving an approximate solution to equations 2.3.1 have been examined. These are the method of averaging (as used by Sethna), the two-variable expansion procedure (Cole and Kevorkian), and an asymptotic method outlined by Struble. For this particular problem the asymptotic method lends itself most easily to analysis. The method of averaging, although providing identical results, tends to be rather tedious, while the two-variable expansion procedure is primarily a technique for singular perturbation problems. The asymptotic method is adopted here while the other two techniques are detailed in Appendix III.

As a prerequisite to further analysis the equations 2.3.1 are written in the form

$$\ddot{X} + 4\Omega^2 X = \epsilon[\epsilon^{-1}(4\Omega^2 - \omega_1{}^2)X - 2\eta_1\omega_1\dot{X} + R(\dot{y}^2 + y\ddot{y}) + P\cos 2\Omega t]$$

$$\ddot{y} + \Omega^2 y = \epsilon[\epsilon^{-1}(\Omega^2 - \omega_2{}^2)y - 2\eta_2\omega_2\dot{y} + \ddot{X}y - \epsilon y(\dot{y}^2 + y\ddot{y})] \qquad 2.4.1$$

This 'softening' of the forcing term through association with the small parameter ϵ such that $\omega_1{}^2$ is replaced by ϵP, enables the detailed structure of the solution close to external resonance to be obtained.

The solution of 2.4.1 is taken in the form

$$X = A(t)\cos[\omega_1 t + \phi(t)] + \epsilon X_1(t) + \epsilon^2 X_2(t) + \ldots$$

$$y = B(t)\cos[\omega_2 t + \theta(t)] + \epsilon y_1(t) + \epsilon^2 y_2(t) + \ldots \qquad 2.4.2$$

where A, B, ϕ and θ are slowly varying functions of t.

The first term in each asymptotic series represents the principal part of the solution while the additive terms in powers of ϵ provide for a perturbational treatment.

Substitution of 2.4.2, to the second order in ϵ, into the equations of motion yields the following two equations:-

$$[\ddot{A} - A(\omega_1 + \dot{\phi})^2]\cos(\omega_1 t + \phi) - [A\ddot{\phi} + 2\dot{A}(\omega_1 + \dot{\phi})]\sin(\omega_1 t + \phi)$$

$$+ \epsilon\ddot{X}_1 + \epsilon^2\ddot{X}_2 + 4\Omega^2 A\cos(\omega_1 t + \phi) + 4\Omega^2\epsilon X_1 + 4\Omega^2\epsilon^2 X_2$$

$$= \epsilon[\epsilon^{-1}(4\Omega^2 - \omega_1^2)\{A\cos(\omega_1 t + \phi) + \epsilon X_1 + \epsilon^2 X_2\}]$$

$$- \epsilon 2\eta_1\omega_1[\dot{A}\cos(\omega_1 t + \phi) - A(\omega_1 + \dot{\phi})\sin(\omega_1 t + \phi) + \epsilon\dot{X}_1]$$

$$+ \epsilon R[(B\ddot{B} + \dot{B}^2)\cos^2(\omega_2 t + \theta) - B^2(\omega_2 + \dot{\theta})^2\{\cos^2(\omega_2 t + \theta) -$$

$$- \sin^2(\omega_2 t + \theta)\} - \{B^2\ddot{\theta} + 4B\dot{B}(\omega_2 + \dot{\theta})\}\sin(\omega_2 t + \theta)\cos(\omega_2 t + \theta)]$$

$$+ \epsilon^2 R[\{B\ddot{y}_1 + 2\dot{B}\dot{y}_1 + \ddot{B}y_1 - B(\omega_2 + \dot{\theta})^2 y_1\}\cos(\omega_2 t + \theta) -$$

$$- \{2B\dot{y}_1(\omega_2 + \dot{\theta}) + B\ddot{\theta}y_1 + 2\dot{B}(\omega_2 + \dot{\theta})y_1\}\sin(\omega_2 t + \theta)] + \epsilon P\cos 2\Omega t$$

2.4.3

and

$$[\ddot{B} - B(\omega_2 + \dot{\theta})^2]\cos(\omega_2 t + \theta) - [B\ddot{\theta} + 2\dot{B}(\omega_2 + \dot{\theta})]\sin(\omega_2 t + \theta)$$

$$+ \epsilon\ddot{y}_1 + \epsilon^2\ddot{y}_2 + \Omega^2 B\cos(\omega_2 t + \theta) + \Omega^2\epsilon y_1 + \Omega^2\epsilon^2 y_2$$

$$= \epsilon[\epsilon^{-1}(\Omega^2 - \omega_2^2)\{B\cos(\omega_2 t + \theta) + \epsilon y_1 + \epsilon^2 y_2\}]$$

$$- \epsilon 2\eta_2\omega_2[\dot{B}\cos(\omega_2 t + \theta) - B(\omega_2 + \dot{\theta})\sin(\omega_2 t + \theta) + \epsilon\dot{y}_1]$$

$$+ \epsilon[\{B\ddot{A} - AB(\omega_1 + \dot{\phi})^2\}\cos(\omega_1 t + \phi)\cos(\omega_2 t + \theta) -$$

$$- \{AB\ddot{\phi} + 2B\dot{A}(\omega_1 + \dot{\phi})\}\sin(\omega_1 t + \phi)\cos(\omega_2 t + \theta)]$$

$$+ \epsilon^2[B\ddot{X}_1\cos(\omega_2 t + \theta) + y_1\{\ddot{A} - A(\omega_1 + \dot{\phi})^2\}\cos(\omega_1 t + \phi) -$$

$$- y_1\{A\ddot{\phi} + 2\dot{A}(\omega_1 + \dot{\phi})\}\sin(\omega_1 t + \phi)]$$

$$- \epsilon^2[\{B^2\ddot{B} + B\dot{B}^2 - B^3(\omega_2 + \dot{\theta})^2\}\cos^3(\omega_2 t + \theta) + B^3(\omega_2 + \dot{\theta})^2\sin^2(\omega_2 t + \theta).$$

$$. \cos(\omega_2 t + \theta) - \{B^3\ddot{\theta} + 4B^2\dot{B}(\omega_2 + \dot{\theta})\}\sin(\omega_2 t + \theta)\cos^2(\omega_2 t + \theta)]$$

2.4.4

Those terms in equations 2.4.3 and 2.4.4 of order zero in ϵ are called variational terms. However, equating these terms appropriately on each side simply implies that each of A, B, ϕ, θ is a constant. It is necessary then to consider the higher order terms in ϵ which give rise to sets of perturbational equations in the perturbational parameters X_1, y_1, X_2 and y_2. If there exists any term on the right-hand side of these perturbational equations which is likely to produce resonance in one of the perturbational parameters then this term must be removed for the solution to remain bounded. Such 'resonant' terms are transferred to the variational terms and provide for a set of variational equations in which A, B, ϕ and θ are not constants but functions of time.

Continuing the analysis, the first order terms in ϵ in 2.4.3 and 2.4.4 give the first order perturbational equations,

$$\begin{aligned}\ddot{X}_1 + \omega_1^2 X_1 = &- 2\gamma_1\omega_1[\dot{A}\cos(\omega_1 t + \phi) - A(\omega_1 + \dot{\phi})\sin(\omega_1 t + \phi)] \\ &+ R[(B\ddot{B} + \dot{B}^2)\cos^2(\omega_2 t + \theta) - B^2(\omega_2 + \dot{\theta})^2 . \\ &. \{\cos^2(\omega_2 t + \theta) - \sin^2(\omega_2 t + \theta)\} - \{B^2\ddot{\theta} + 4B\dot{B}(\omega_2 + \dot{\theta})\} . \\ &. \sin(\omega_2 t + \theta)\cos(\omega_2 t + \theta)] + P\cos 2\Omega t \qquad 2.4.5\end{aligned}$$

and

$$\begin{aligned}\ddot{y}_1 + \omega_2^2 y_1 = &- 2\gamma_2\omega_2[\dot{B}\cos(\omega_2 t + \theta) - B(\omega_2 + \dot{\theta})\sin(\omega_2 t + \theta)] \\ &+ [B\ddot{A} - AB(\omega_1 + \dot{\phi})^2]\cos(\omega_1 t + \phi)\cos(\omega_2 t + \theta) \\ &- [AB\ddot{\phi} + 2B\dot{A}(\omega_1 + \dot{\phi})]\sin(\omega_1 t + \phi)\cos(\omega_2 t + \theta) \qquad 2.4.6\end{aligned}$$

Both equation 2.4.5 and 2.4.6 have terms on the right which constitute resonant terms when certain conditions are imposed. Firstly, the periodic external forcing will have most effect when the frequency 2Ω is close to the system frequency ω_1, accordingly it is assumed that a condition of external resonance holds, defined by

$$(2\Omega/\omega_1) = 1 + O(\epsilon) \qquad 2.4.7$$

Secondly, to ensure that the absorber is excited parametrically in its principal region of instability the internal resonance or tuning condition,

$$\omega_1 = 2\omega_2 \qquad 2.4.8$$

is imposed. (This is the perfectly tuned or exact internal resonance condition, the effect of a slight detuning will be discussed later). Consequently, many of the terms on the right-hand side of 2.4.5 and 2.4.6 produce resonance in the perturbational parameters when the above conditions hold. By way of example, consider the term $\cos^2(\omega_2 t + \theta)$. Now using the standard trigonometric formulas $\cos^2(\omega_2 t + \theta) = \frac{1}{2}(1 + \cos 2(\omega_2 t + \theta))$ but $\cos 2(\omega_2 t + \theta)$ can be written as $\cos\{(\omega_1 t + \phi) + (2\theta - \phi)\}$ which is equivalent to $\cos(\omega_1 t + \phi)\cos(2\theta - \phi) - \sin(\omega_1 t + \phi)\sin(2\theta - \phi)$, and so the term $\cos^2(\omega_2 t + \theta)$ provides two fundamental harmonics which must be removed to the variational equations. This is a direct consequence of the exact internal resonance condition 2.4.8. Another, in the same category, is the $\cos(\omega_1 t + \phi)\cos(\omega_2 t + \theta)$ term which provides a resonant part $\cos\{(\omega_1 - \omega_2)t + (\phi - \theta)\}$ and a nonresonant part $\cos\{(\omega_1 + \omega_2)t + (\phi + \theta)\}$, the resonant $\cos\{(\omega_1 - \omega_2)t + (\phi - \theta)\}$ produces two harmonics,

$\cos(\omega_2 t + \theta)\cos(2\theta - \phi)$ and $\sin(\omega_2 t + \theta)\sin(2\theta - \phi)$ which again must be removed. Finally, the forcing term $\cos 2\Omega t$ is written as $\cos\{(\omega_1 t + \phi) - \phi\}$ thereby producing two harmonics of the form $\cos(\omega_1 t + \phi)\cos\phi$ and $\sin(\omega_1 t + \phi)\sin\phi$. This shows the effect of the external resonance condition 2.4.7

The resulting first order perturbational equations are

$$\ddot{X}_1 + \omega_1^2 X_1 = \tfrac{1}{2} R(B\ddot{B} + \dot{B}^2) \qquad 2.4.9$$

$$\ddot{y}_1 + \omega_2^2 y_1 = \tfrac{1}{2}[B\ddot{A} - AB(\omega_1 + \dot{\phi})^2]\cos\{(\omega_1 + \omega_2)t + (\phi + \theta)\}$$

$$- \tfrac{1}{2}[AB\ddot{\phi} + 2B\dot{A}(\omega_1 + \dot{\phi})]\sin\{(\omega_1 + \omega_2)t + (\phi + \theta)\} \qquad 2.4.10$$

Now as previously stated A, B, ϕ and θ are slowly varying functions of time so that their first derivatives with respect to time are assumed small of the first order in ϵ. This means that 2.4.9 and 2.4.10 need not be treated precisely. Equation 2.4.9 simply becomes

$$\ddot{X}_1 + \omega_1^2 X_1 = 0 \qquad 2.4.11$$

while 2.4.10 reduces to

$$\ddot{y}_1 + \omega_2^2 y_1 = -\tfrac{1}{2}AB\omega_1^2 \cos\{(\omega_1 + \omega_2)t + (\phi + \theta)\} \qquad 2.4.12$$

and the particular integral solutions to 2.4.11 and 2.4.12 can be taken as

$$X_1 = 0$$

$$y_1 = \tfrac{1}{2} AB[\omega_1/(\omega_1 + 2\omega_2)]\cos\{(\omega_1 + \omega_2)t + (\phi + \theta)\} \qquad 2.4.13$$

With these solutions for X_1 and y_1 the second order perturbational equations may be written following the same procedure of removing the resonant terms to the variational equations then simplifying the remaining terms by eliminating those of order greater than ϵ^0. The reduced second order perturbational equations are

$$\ddot{X}_2 + \omega_1{}^2 X_2 = -\tfrac{1}{4} AB^2 R\omega_1(\omega_1 + 2\omega_2)\cos\{(\omega_1 + 2\omega_2)t + (\phi + 2\theta)\} \qquad 2.4.14$$

and

$$\ddot{y}_2 + \omega_2{}^2 y_2 = \tfrac{3}{2}AB[\omega_1\omega_2(\omega_1 + \omega_2)/(\omega_1 + 2\omega_2)]\sin\{(\omega_1 + \omega_2)t + (\phi + \theta)\} - \tfrac{1}{4} A^2 B[\omega_1{}^3/(\omega_1 + 2\omega_2)]\cos\{(2\omega_1 + \omega_2)t + (2\phi + \theta)\} + \tfrac{1}{2} B^3\omega_2{}^2\cos 3(\omega_2 t + \theta)$$

Once again particular integral solutions to 2.4.14 are required before formulating the third order perturbational equations. However these need not be found as the present analysis requires variational equations of the second order only.

The Variational Equations

Returning to equations 2.4.3 and 2.4.4, the variational equations comprise the coefficients of the fundamental harmonic terms together with the coefficients of the resonant terms brought up from the first and second order perturbational equations.

Thus the coefficients of $\cos(\omega_1 t + \phi)$ give,

$$\ddot{A} - A(\omega_1 + \dot{\phi})^2 + 4\Omega^2 A$$

$$= \epsilon[\epsilon^{-1}(4\Omega^2 - \omega_1{}^2)A] - \epsilon 2\gamma_1\omega_1\dot{A}$$

$$+ \epsilon R[\tfrac{1}{2}(B\ddot{B} + \dot{B}^2) - B^2(\omega_2 + \dot{\theta})^2]\cos(2\theta - \phi)$$

$$- \epsilon R[\tfrac{1}{2}B^2\ddot{\theta} + 2B\dot{B}(\omega_2 + \dot{\theta})]\sin(2\theta - \phi) + \epsilon P\cos\phi$$

$$+ \epsilon^2[R\omega_1 AB/4(\omega_1 + 2\omega_2)][\ddot{B} - B(\omega_2 + \dot{\theta})^2 + 2B(\omega_2 + \dot{\theta})(\omega_1 + \omega_2)] \qquad 2.4.15$$

The coefficients of $\sin(\omega_1 t + \phi)$ give

$$- A\ddot{\phi} - 2\dot{A}(\omega_1 + \dot{\phi})$$

$$= \epsilon 2\gamma_1\omega_1 A(\omega_1 + \dot{\phi}) - \epsilon R[\tfrac{1}{2}B^2\ddot{\theta} + 2B\dot{B}(\omega_2 + \dot{\theta})]\cos(2\theta - \phi)$$

$$- \epsilon R[\tfrac{1}{2}(B\ddot{B} + \dot{B}^2) - B^2(\omega_2 + \dot{\theta})^2]\sin(2\theta - \phi)$$

$$+ \epsilon P\sin\phi + \epsilon^2[R\omega_1 AB/4(\omega_1 + 2\omega_2)][B\ddot{\theta} + 2\dot{B}(\omega_2 + \dot{\theta})] \qquad 2.4.16$$

The coefficients of $\cos(\omega_2 t + \theta)$ give

$$\ddot{B} - B(\omega_2 + \dot{\theta})^2 + \Omega^2 B$$

$$= \epsilon[\epsilon^{-1}(\Omega^2 - \omega_2{}^2)B] - \epsilon 2\gamma_2\omega_2\dot{B}$$

$$+ \epsilon[\tfrac{1}{2}B\ddot{A} - \tfrac{1}{2}AB(\omega_1 + \dot{\phi})^2]\cos(2\theta - \phi)$$

$$+ \epsilon[\tfrac{1}{2}AB\ddot{\phi} + B\dot{A}(\omega_1 + \dot{\phi})]\sin(2\theta - \phi)$$

$$+ \epsilon^2[\omega_1 AB/4(\omega_1 + 2\omega_2)][\ddot{A} - A(\omega_1 + \dot{\phi})^2]$$

$$- \tfrac{1}{4}\epsilon^2[3B^2\ddot{B} + 3B\dot{B}^2 - 2B^3(\omega_2 + \dot{\theta})^2] \qquad 2.4.17$$

Completing the four variational equations, the coefficients of $\sin(\omega_2 t + \theta)$ yield,

$$- B\ddot{\theta} - 2\dot{B}(\omega_2 + \dot{\theta})$$

$$= \epsilon 2\eta_2\omega_2 B(\omega_2 + \dot{\theta}) - \epsilon[\tfrac{1}{2}AB\ddot{\phi} + B\dot{A}(\omega_1 + \dot{\phi})]\cos(2\theta - \phi)$$

$$+ \epsilon[\tfrac{1}{2}B\ddot{A} - \tfrac{1}{2}AB(\omega_1 + \dot{\phi})^2]\sin(2\theta - \phi)$$

$$+ \epsilon^2[\omega_1 AB/4(\omega_1 + 2\omega_2)][A\ddot{\phi} + 2\dot{A}(\omega_1 + \dot{\phi})]$$

$$+ \tfrac{1}{4}\epsilon^2[B^3\ddot{\theta} + 4B^2\dot{B}(\omega_2 + \dot{\theta})] \qquad 2.4.18$$

Again, because of the assumed slow variation of A, B, ϕ and θ, and since it is sufficient to obtain solutions correct to the second order in ϵ, the above four variational equations can be simplified. Accordingly, each of the omitted terms will be of the third order in ϵ.

Hence 2.4.15 becomes

$$- A\dot{\phi} = (\epsilon/2\omega_2)[2\epsilon^{-1}(\Omega^2 - \omega_2^2)A - 2\eta_1\omega_2\dot{A} - \tfrac{1}{2}RB^2\omega_2^2\cos(2\theta - \phi) +$$

$$+ \tfrac{1}{2}P\cos\phi + \epsilon RAB^2 5\omega_2^2/8] \qquad 2.4.19$$

where ω_1 has been eliminated using the internal resonance condition $\omega_1 = 2\omega_2$.

Similarly 2.4.16 becomes

$$- \dot{A} = (\epsilon/2\omega_2)[4\eta_1\omega_2^2 A + \tfrac{1}{2}RB^2\omega_2^2\sin(2\theta - \phi) + \tfrac{1}{2}P\sin\phi] \qquad 2.4.20$$

While 2.4.17 yields

$$- B\dot{\theta} = (\epsilon/2\omega_2)[\epsilon^{-1}(\Omega^2 - \omega_2^2)B - 2\eta_2\omega_2\dot{B} - 2AB\omega_2^2\cos(2\theta - \phi) -$$

$$- \epsilon A^2 B\omega_2^2 + \epsilon\tfrac{1}{2}B^3\omega_2^2] \qquad 2.4.21$$

Finally 2.4.18 gives

$$-\dot{B} = (\epsilon/2\omega_2)[2\eta_2\omega_2^2 B - 2AB\omega_2^2\sin(2\theta - \phi)] \qquad 2.4.22$$

The term in $\dot{A}$ in equation 2.4.19 and that in $\dot{B}$ in equation 2.4.21 can be eliminated using equations 2.4.20 and 2.4.22, respectively. Thus 2.4.19 becomes

$$-A\dot{\phi} = (\epsilon/2\omega_2)[2\epsilon^{-1}(\Omega^2 - \omega_2^2)A - \tfrac{1}{2}RB^2\omega_2^2\cos(2\theta - \phi) + \tfrac{1}{2}P\cos\phi]$$
$$+ (\epsilon/2\omega_2)^2[8\eta_1^2\omega_2^3 A + RB^2\eta_1\omega_2^3\sin(2\theta - \phi) + P\eta_1\omega_2\sin\phi +$$
$$+ RAB^2 5\omega_2^3/4] \qquad 2.4.23$$

and 2.4.21 becomes

$$-B\dot{\theta} = (\epsilon/2\omega_2)[\epsilon^{-1}(\Omega^2 - \omega_2^2)B - 2AB\omega_2^2\cos(2\theta - \phi)]$$
$$+ (\epsilon/2\omega_2)^2[4\eta_2^2\omega_2^3 B - 4AB\eta_2\omega_2^3\sin(2\theta - \phi) - 2A^2B\omega_2^3 + B^3\omega_2^3] \qquad 2.4.24$$

Equations 2.4.23, 2.4.20, 2.4.24, 2.4.22 constitute the four second order variational equations from which the steady-state solution may be obtained. Before further analysis however, it is convenient to introduce a change of variables. This transformation takes the form

$$t = 4\tau/\epsilon\sqrt{PR} \;;\; \gamma = (\omega_2^2 - \Omega^2)/\epsilon\omega_2\sqrt{PR} \;;$$
$$A = b_1\sqrt{P}/\omega_2\sqrt{R} \;;\; B = b_2\sqrt{P}/\omega_2\sqrt{R} \;;\; \phi = \psi_1 \;;\; \theta = \psi_2 \qquad 2.4.25$$

Note, $\epsilon P = \omega_1^2 = 4\omega_2^2$ as previously stated.

The resulting variational equations are,

$$b_1\,\psi_1' = 4\gamma b_1 + b_2^2\cos(2\psi_2 - \psi_1) - \cos\psi_1$$
$$+ \epsilon\zeta_1[-4\zeta_1(\epsilon/R)^{\frac{1}{2}}b_1 - b_2^2\sin(2\psi_2 - \psi_1) - \sin\psi_1]$$
$$- \tfrac{5}{4}(\epsilon/R)^{\frac{1}{2}}\,b_1 b_2^2$$

$$b_1' = -4\zeta_1(\epsilon/R)^{\frac{1}{2}}b_1 - b_2^2\sin(2\psi_2 - \psi_1) - \sin\psi_1$$

$$b_2\,\psi_2' = 2\gamma b_2 + (4/R)b_1 b_2\cos(2\psi_2 - \psi_1)$$
$$+ \epsilon\zeta_2[-2\zeta_2(\epsilon/R)^{\frac{1}{2}}b_2 + (4/R)b_1 b_2\sin(2\psi_2 - \psi_1)]$$
$$+ (2/R)(\epsilon/R)^{\frac{1}{2}}[2b_1^2 b_2 - b_2^3]$$

and

$$b_2' = -2\zeta_2(\epsilon/R)^{\frac{1}{2}}b_2 + (4/R)b_1 b_2\sin(2\psi_2 - \psi_1)$$

... 2.4.26

where primes denote differentiation with respect to the slow time τ.

The steady-state solutions for b_1, b_2, ψ_1 and ψ_2 are found by equating the right-hand sides of equations 2.4.26 to zero.

Thus $b_1' = b_2' = b_1\,\psi_1' = b_2\,\psi_2' = 0$ and after some algebra, eliminating ψ_1 and ψ_2, there results two rather complicated relationships between b_1 and b_2, namely

$$4b_1^2 = \epsilon\zeta_2^2 R + \gamma^2 R^2 + 2\gamma R(\epsilon/R)^{\frac{1}{2}}(2b_1^2 - b_2^2)$$
$$+ (\epsilon/R)(2b_1^2 - b_2^2)^2 \qquad 2.4.27$$

and

$$16(\epsilon/R)\gamma_1^2 b_1^2 + \tfrac{1}{4}\epsilon R\gamma_2^2 \frac{b_2^4}{b_1^2} + 4\epsilon\gamma_1\gamma_2 b_2^2 + 16\gamma^2 b_1^2 + \tfrac{1}{4}\gamma^2 R^2 \frac{b_2^4}{b_1^2} -$$
$$- 4\gamma^2 R b_2^2 + \tfrac{1}{4}(\epsilon/R)\frac{b_2^8}{b_1^2} + \frac{81}{16}(\epsilon/R)b_1^2 b_2^4 - 4\gamma(\epsilon/R)^{\frac{1}{2}} b_2^4 -$$
$$- 18\gamma(\epsilon/R)^{\frac{1}{2}} b_1^2 b_2^2 + \tfrac{1}{2}\gamma(\epsilon R)^{\frac{1}{2}} \frac{b_2^6}{b_1^2} + \frac{9}{4}\gamma(\epsilon R)^{\frac{1}{2}} b_2^4 +$$
$$+ \frac{9}{4}(\epsilon/R) b_2^6 = 1 \qquad 2.4.28$$

Although an approach to the steady-state solutions for b_1 and b_2 through the second order variational equations provides a more detailed insight into the nature of those solutions, the algebra required becomes rather excessive. In the present study, therefore, a solution to the first order variational equations will suffice, in the knowledge that 2.4.27 and 2.4.28 would yield more accurate predictions.

The first order variational equations comprise the fundamental harmonic terms of 2.4.3 and 2.4.4 together with the resonant terms of the first order perturbation equations. They are, after simplification and transformation,

$$b_1\psi_1' = 4\gamma b_1 + b_2^2\cos(2\psi_2 - \psi_1) - \cos\psi_1$$
$$b_1' = -4\gamma_1(\epsilon/R)^{\frac{1}{2}} b_1 - b_2^2 \sin(2\psi_2 - \psi_1) - \sin\psi_1$$
$$b_2\psi_2' = 2\gamma b_2 + (4/R)b_1 b_2\cos(2\psi_2 - \psi_1)$$
and $$b_2' = -2\gamma_2(\epsilon/R)^{\frac{1}{2}} b_2 + (4/R)b_1 b_2\sin(2\psi_2 - \psi_1)$$
... 2.4.29

Regarding the form of the above four equations it is seen that they are directly derivable from the second order variational equations 2.4.26, the terms emanating from the second order perturbation equations are simply eliminated.

Once more, equating the right-hand sides of equations 2.4.29 to zero such that $b_1' = b_2' = b_1\psi_1' = b_2\psi_2' = 0$, produces a set of four steady-state equations

$$4\gamma b_1 + b_2^2\cos(2\psi_2 - \psi_1) - \cos\psi_1 = 0$$

$$-4\zeta_1(\epsilon/R)^{\frac{1}{2}}b_1 - b_2^2\sin(2\psi_2 - \psi_1) - \sin\psi_1 = 0$$

$$2\gamma b_2 + (4/R)b_1 b_2\cos(2\psi_2 - \psi_1) = 0$$

and $$-2\zeta_2(\epsilon/R)^{\frac{1}{2}}b_2 + (4/R)b_1 b_2\sin(2\psi_2 - \psi_1) = 0 \quad \ldots 2.4.30$$

which yield, on the elimination of ψ_1 and ψ_2, two explicit relations for b_1 and b_2, both nonzero. These are

$$b_1 = \pm\tfrac{1}{2}(R)^{\frac{1}{2}}[\epsilon\zeta_2^2 + \gamma^2 R]^{\frac{1}{2}} \qquad 2.4.31$$

and $$b_2^2 = 2(\gamma^2 R - \epsilon\zeta_1\zeta_2) \pm [1 - 4\gamma^2\epsilon R(\zeta_1 + \zeta_2)^2]^{\frac{1}{2}} \qquad 2.4.32$$

Equations 2.4.31 and 2.4.32 represent the theoretical solution of the steady-state behaviour of a perfectly tuned AVA system in the neighbourhood of external resonance. From 2.4.32 it is clear that b_2 is dependent on both ζ_1 and ζ_2, however, 2.4.31 suggests that b_1 is dependent only on ζ_2 and not ζ_1. This apparent ambiguity is dispelled when the results of the second order analysis are recalled. Clearly equations 2.4.27 and 2.4.28 show a direct relationship between b_1 and b_2 and consequently b_1 must also be dependent on ζ_1. This illustrates one advantage of working to a higher order of approximation.

2.5 Steady-State Solution of a Slightly Detuned AVA

This section considers the more realistic case (from a physical standpoint) of an AVA which has a certain degree of detuning. In other words the exact internal resonance condition $\omega_1 = 2\omega_2$ is no longer deemed to hold, instead it must be replaced by a new and more general assumption that

$$2\omega_2 - \omega_1 = \delta \qquad 2.5.1$$

where δ is a small parameter, referred to as the detuning factor. (The external resonance condition 2.4.7 still holds).

With this new internal resonance condition it is necessary, once again, to obtain the first order variational equations. The equations of motion (2.4.1) are unaltered and the same solution (2.4.2) is adopted. Substitution of the solution into the equations of motion leads to the two equations 2.4.3 and 2.4.4. Equating the coefficients of the terms of the first order in ϵ produces the first order perturbation equations 2.4.5 and 2.4.6 which, for convenience, are rewritten here,

$$\begin{aligned}\ddot{X}_1 + \omega_1^2 X_1 = &- 2\eta_1\omega_1[\dot{A}\cos(\omega_1 t + \phi) - A(\omega_1 + \dot{\phi})\sin(\omega_1 t + \phi)] \\ &+ R[(B\ddot{B} + \dot{B}^2)\cos^2(\omega_2 t + \theta) - B^2(\omega_2 + \dot{\theta})^2 \cdot \\ &\cdot \{\cos^2(\omega_2 t + \theta) - \sin^2(\omega_2 t + \theta)\} - \{B^2\ddot{\theta} + 4B\dot{B}(\omega_2 + \dot{\theta})\} \cdot \\ &\cdot \sin(\omega_2 t + \theta)\cos(\omega_2 t + \theta)] + P\cos 2\Omega t \qquad 2.5.2\end{aligned}$$

and

$$\begin{aligned}\ddot{y}_1 + \omega_2^2 y_1 = &- 2\eta_2\omega_2[\dot{B}\cos(\omega_2 t + \theta) - B(\omega_2 + \dot{\theta})\sin(\omega_2 t + \theta)] \\ &+ [B\ddot{A} - AB(\omega_1 + \dot{\phi})^2]\cos(\omega_1 t + \phi)\cos(\omega_2 t + \theta) \\ &- [AB\ddot{\phi} + 2B\dot{A}(\omega_1 + \dot{\phi})]\sin(\omega_1 t + \phi)\cos(\omega_2 t + \theta) \qquad 2.5.3\end{aligned}$$

Imposing internal and external resonance conditions necessitates the removal of certain terms from the right of equations 2.5.2 and 2.5.3. For example the term $\sin(\omega_2 t + \theta)\cos(\omega_2 t + \theta)$ can be written as $\frac{1}{2}\sin 2(\omega_2 t + \theta)$ or $\frac{1}{2}\sin(\omega_1 t + \phi + \delta t + 2\theta - \phi)$ and two harmonics result, $\sin(\omega_1 t + \phi)\cos\omega$ and $\cos(\omega_1 t + \phi)\sin\omega$ where a new variable ω is defined as

$$\omega = \delta t + 2\theta - \phi \qquad 2.5.4$$

The resulting first order variational equations are

$(\cos(\omega_1 t + \phi))$:

$$\ddot{A} - A(\omega_1 + \dot{\phi})^2 + 4\Omega^2 A$$
$$= \epsilon[\epsilon^{-1}(4\Omega^2 - \omega_1^2)A] - \epsilon 2\gamma_1\omega_1\dot{A}$$
$$+ \epsilon R[\tfrac{1}{2}(B\ddot{B} + \dot{B}^2) - B^2(\omega_2 + \dot{\theta})^2]\cos\omega$$
$$- \epsilon R[\tfrac{1}{2}B^2\ddot{\theta} + 2B\dot{B}(\omega_2 + \dot{\theta})]\sin\omega + \epsilon P\cos\phi \qquad 2.5.5$$

$(\sin(\omega_1 t + \phi))$:

$$- A\ddot{\phi} - 2\dot{A}(\omega_1 + \dot{\phi})$$
$$= \epsilon 2\gamma_1\omega_1 A(\omega_1 + \dot{\phi}) - \epsilon R[\tfrac{1}{2}B^2\ddot{\theta} + 2B\dot{B}(\omega_2 + \dot{\theta})]\cos\omega$$
$$- \epsilon R[\tfrac{1}{2}(B\ddot{B} + \dot{B}^2) - B^2(\omega_2 + \dot{\theta})^2]\sin\omega + \epsilon P\sin\phi \qquad 2.5.6$$

$(\cos(\omega_2 t + \theta))$:

$$\ddot{B} - B(\omega_2 + \dot{\theta})^2 + \Omega^2 B$$
$$= \epsilon[\epsilon^{-1}(\Omega^2 - \omega_2^2)B] - \epsilon 2\gamma_2\omega_2\dot{B}$$
$$+ \epsilon[\tfrac{1}{2}B\ddot{A} - \tfrac{1}{2}AB(\omega_1 + \phi)^2]\cos\omega$$
$$+ \epsilon[\tfrac{1}{2}AB\ddot{\phi} + B\dot{A}(\omega_1 + \dot{\phi})]\sin\omega \qquad 2.5.7$$

$(\sin(\omega_2 t + \theta))$:

$$- B\ddot{\theta} - 2\dot{B}(\omega_2 + \dot{\theta})$$

$$= \epsilon 2\eta_2\omega_2 B(\omega_2 + \dot{\theta}) - \epsilon[\tfrac{1}{2}AB\ddot{\phi} + B\dot{A}(\omega_1 + \dot{\phi})]\cos\omega$$

$$+ \epsilon[\tfrac{1}{2}B\dot{A} - \tfrac{1}{2}AB(\omega_1 + \dot{\phi})^2]\sin\omega \qquad 2.5.8$$

Assuming the first derivatives of A, B, ϕ and θ to be of the first order in ϵ, the simplified equations are

$$- 2A\omega_1\dot{\phi} = \epsilon[\epsilon^{-1}(4\Omega^2 - \omega_1^2)A] - \epsilon RB^2\omega_2^2\cos\omega + \epsilon P\cos\phi$$

$$- 2\dot{A}\omega_1 = \epsilon 2\eta_1\omega_1^2 A + \epsilon RB^2\omega_2^2\sin\omega + \epsilon P\sin\phi$$

$$- 2B\omega_2\dot{\theta} = \epsilon[\epsilon^{-1}(\Omega^2 - \omega_2^2)B] - \epsilon\tfrac{1}{2}AB\omega_1^2\cos\omega$$

$$- 2\dot{B}\omega_2 = \epsilon 2\eta_2\omega_2^2 B - \epsilon\tfrac{1}{2}AB\omega_1^2\sin\omega \qquad \ldots 2.5.9$$

Transforming the variables as follows

$$t = 4\tau/\epsilon\sqrt{PR} \;;\; \gamma = (\omega_2^2 - \Omega^2)/\epsilon\omega_2\sqrt{PR} \;;$$

$$A = b_1\sqrt{P}/\omega_2\sqrt{R} \;;\; B = b_2\sqrt{P}/\omega_2\sqrt{R} \;;\; \phi = \psi_1 \;;\; \theta = \psi_2 \;;\; \omega = \omega \;; \qquad 2.5.10$$

remembering that $\epsilon P = \omega_1^2$ and $\omega_1 = 2\omega_2 - \delta$, the four variational equations assume their final form

$$b_1\psi_1' = 8\gamma b_1\omega_2/(2\omega_2 - \delta) + 2b_1(\delta^2 - 4\delta\omega_2)/(\epsilon R)^{\frac{1}{2}}(2\omega_2 - \delta)^2$$

$$+ (2b_2^2\omega_2\cos\omega)/(2\omega_2 - \delta) - (2\omega_2\cos\psi_1)/(2\omega_2 - \delta)$$

$$b_1' = - 4\eta_1(\epsilon/R)^{\frac{1}{2}} b_1 - (2b_2^2\omega_2\sin\omega)/(2\omega_2 - \delta)$$

$$- (2\omega_2\sin\psi_1)/(2\omega_2 - \delta)$$

$$b_2\psi_2' = 2\gamma b_2 + [b_1 b_2(2\omega_2 - \delta)^2\cos\omega]/R\omega_2^2$$

$$b_2' = - 4\eta_2\omega_2(\epsilon/R)^{\frac{1}{2}} b_2/(2\omega_2 - \delta) + [b_1 b_2(2\omega_2 - \delta)^2\sin\omega]/R\omega_2^2 \qquad \ldots 2.5.11$$

As before, primes denote differentiation with respect to the slow time τ.

Equating the right-hand sides of equations 2.5.11 to zero provides the steady-state solution of the detuned AVA system. However, it is advisable in subsequent analysis to replace the detuning factor δ, which is small of order ϵ, by the frequency ratio

$$\rho = 2\omega_2/\omega_1 \qquad 2.5.12$$

which is in the neighbourhood of unity. Hence the four steady-state equations are

$$\begin{aligned}
&4\rho\gamma b_1 + 2(1-\rho^2)b_1/(\epsilon R)^{\frac{1}{2}} + \rho b_2^{\,2}\cos\omega - \rho\cos\psi_1 = 0\\
&-4\eta_1(\epsilon/R)^{\frac{1}{2}}b_1 - \rho b_2^{\,2}\sin\omega - \rho\sin\psi_1 = 0\\
&2\gamma b_2 + (4/\rho^2 R)b_1 b_2\cos\omega = 0\\
&-2\rho\eta_2(\epsilon/R)^{\frac{1}{2}}b_2 + (4/\rho^2 R)b_1 b_2\sin\omega = 0
\end{aligned} \qquad \ldots\ 2.5.13$$

On the elimination of ω and ψ_1 there results two expressions for b_1 and b_2

$$b_1 = \pm\tfrac{1}{2}\rho^2(R)^{\frac{1}{2}}[\epsilon\rho^2\eta_2^{\,2} + \gamma^2 R]^{\frac{1}{2}} \qquad 2.5.14$$

and

$$\begin{aligned}
b_2^{\,2} = {}&2\rho^2[\gamma^2 R - \epsilon\eta_1\eta_2] + \rho(1-\rho^2)(R/\epsilon)^{\frac{1}{2}}\gamma\\
&\pm[1 - 4\rho^2\gamma^2\epsilon R(\eta_1 + \rho^2\eta_2)^2 - \rho^4(1-\rho^2)^2\eta_2^{\,2} -\\
&- 4\rho^3(1-\rho^2)(\epsilon R)^{\frac{1}{2}}\gamma\eta_2(\eta_1 + \rho^2\eta_2)]^{\frac{1}{2}}
\end{aligned} \qquad 2.5.15$$

These expressions represent the first order approximation to the steady-state behaviour of a detuned AVA system in the region of external resonance. They may be compared with their counterparts in the previous section, equations 2.4.31 and 2.4.32.

So far, analysis has provided the steady-state solutions for an AVA system both perfectly tuned and slightly detuned. In the remainder of this chapter the stability of these solutions will be examined by observing the behaviour of the parameters b_1, b_2, ψ_1 and ψ_2 when given small displacements about their equilibrium position.

2.6 Stability of Steady State Solutions : Exact Internal Resonance

Case 1 : b_1, b_2 nonzero.

The first order variational equations for a perfectly tuned absorber are given by equations 2.4.29 which, for convenience, are re-written here

$$\begin{aligned} b_1' &= -4\eta_1(\epsilon/R)^{\frac{1}{2}}b_1 - b_2^2\sin(2\psi_2 - \psi_1) - \sin\psi_1 \\ b_2' &= -2\eta_2(\epsilon/R)^{\frac{1}{2}}b_2 + (4/R)b_1 b_2\sin(2\psi_2 - \psi_1) \\ b_1\psi_1' &= 4\gamma b_1 + b_2^2\cos(2\psi_2 - \psi_1) - \cos\psi_1 \\ b_2\psi_2' &= 2\gamma b_2 + (4/R)b_1 b_2\cos(2\psi_2 - \psi_1) \end{aligned} \qquad \ldots 2.6.1$$

The parameters b_1, b_2, ψ_1 and ψ_2 of the above system equations are given small displacements from their equilibrium configurations such that

$$b_1 = b_1^{\circ} + \delta b_1 \; ; \; b_2 = b_2^{\circ} + \delta b_2, \; \psi_1 = \psi_1^{\circ} + \delta\psi_1, \; \psi_2 = \psi_2^{\circ} + \delta\psi_2 \qquad 2.6.2$$

where the b_i° and ψ_i° satisfy the equilibrium solutions.

The substitutions 2.6.2 are made in the variational equations 2.6.1 and, with the retention of linear terms in δb_i and $\delta\psi_i$, there emerges a set of four first order equations,

$$\begin{aligned}\delta b_1' &= -[4\gamma_1(\epsilon/R)^{\frac{1}{2}}]\delta b_1 - [2b_2{}^{o}\sin(2\psi_2{}^{o} - \psi_1{}^{o})]\delta b_2 \\ &\quad + [b_2{}^{o2}\cos(2\psi_2{}^{o} - \psi_1{}^{o}) - \cos\psi_1{}^{o}]\,\delta\psi_1 \\ &\quad - [2b_2{}^{o2}\cos(2\psi_2{}^{o} - \psi_1{}^{o})]\delta\psi_2\end{aligned}$$

$$\begin{aligned}\delta b_2' &= [(4/R)b_2{}^{o}\sin(2\psi_2{}^{o} - \psi_1{}^{o})]\delta b_1 \\ &\quad + [(4/R)b_1{}^{o}\sin(2\psi_2{}^{o} - \psi_1{}^{o}) - 2\gamma_2(\epsilon/R)^{\frac{1}{2}}]\delta b_2 \\ &\quad - [(4/R)b_1{}^{o}b_2{}^{o}\cos(2\psi_2{}^{o} - \psi_1{}^{o})]\,\delta\psi_1 \\ &\quad + [(8/R)b_1{}^{o}b_2{}^{o}\cos(2\psi_2{}^{o} - \psi_1{}^{o})]\,\delta\psi_2\end{aligned}$$

$$\begin{aligned}b_1{}^{o}\delta\psi_1' &= [4\gamma]\delta b_1 + [2b_2{}^{o}\cos(2\psi_2{}^{o} - \psi_1{}^{o})]\delta b_2 \\ &\quad + [b_2{}^{o2}\sin(2\psi_2{}^{o} - \psi_1{}^{o}) + \sin\psi_1{}^{o}]\,\delta\psi_1 \\ &\quad - [2b_2{}^{o2}\sin(2\psi_2{}^{o} - \psi_1{}^{o})]\,\delta\psi_2\end{aligned}$$

$$\begin{aligned}b_2{}^{o}\delta\psi_2' &= [(4/R)b_2{}^{o}\cos(2\psi_2{}^{o} - \psi_1{}^{o})]\delta b_1 \\ &\quad + [(4/R)b_1{}^{o}\cos(2\psi_2{}^{o} - \psi_1{}^{o}) + 2\gamma]\delta b_2 \\ &\quad + [(4/R)b_1{}^{o}b_2{}^{o}\sin(2\psi_2{}^{o} - \psi_1{}^{o})]\,\delta\psi_1 \\ &\quad - [(8/R)b_1{}^{o}b_2{}^{o}\sin(2\psi_2{}^{o} - \psi_1{}^{o})]\,\delta\psi_2\end{aligned}$$

... 2.6.3

Further, if a solution for the δb_i and $\delta\psi_i$ is taken in the form

$$\delta b_i = \delta b_i^{\,T} \exp \lambda t \; ; \quad \delta\psi_i = \delta\psi_i^{\,T} \exp \lambda t$$

then the four equations 2.6.3 may be written in matrix form

$$(M - \lambda D)r = 0$$

where M is the matrix of the coefficients of the $\delta b_i^{\,T}$ and $\delta\psi_i^{\,T}$, D is a diagonal matrix and r is the column vector of the $\delta b_i^{\,T}$ and $\delta\psi_i^{\,T}$. It follows that the nature of the roots of the 4 x 4 stability determinant,

$$|M - \lambda D| = 0 \qquad 2.6.4$$

determines the stability of the solutions. Once expanded, 2.6.4 provides a characteristic equation of the form

$$J_4 \lambda^4 + J_3 \lambda^3 + J_2 \lambda^2 + J_1 \lambda + J_o = 0 \qquad 2.6.5$$

where

$$J_4 = 1 \quad ; \quad J_3 = 4(\epsilon/R)^{\frac{1}{2}}(2\eta_1 + \eta_2) \; ;$$

$$J_2 = (16/R)[\gamma^2 R + \epsilon\eta_1^{\,2} + (b_2^{\,o})^2 + 2\epsilon\eta_1\eta_2] \; ;$$

$$J_1 = 32(\epsilon^{\frac{1}{2}}/R^{\frac{3}{2}})[(2\eta_1 + \eta_2)(b_2^{\,o})^2 + 2\eta_2(\gamma^2 R + \epsilon\eta_1^{\,2})] \; ;$$

and

$$J_o = (64/R^2)(b_2^{\,o})^2[(b_2^{\,o})^2 - 2(\gamma^2 R - \epsilon\eta_1\eta_2)]$$

... 2.6.6

It should be noted that considerable calculations are involved in the expansion of the determinant 2.6.4 and the final expressions for the coefficients of lambda (2.6.6) are only obtained after the elimination of $\psi_1^{\,o}$, $\psi_2^{\,o}$ and $b_1^{\,o}$ using the results of the steady-state analysis (2.4.30 and 2.4.31).

The Routh-Hurwitz criteria provide the necessary and sufficient conditions for the characteristic equation 2.6.5 to have roots with negative real parts and consequently, for the solutions to be stable. They are J_i positive and $H \equiv J_1J_2J_3 - J_1^2J_4 - J_0J_3^2$ positive for stability.

Now by inspection of 2.6.6 J_1, J_2, J_3 and J_4 are positive (only positive damping is considered) and by calculation H is also positive. The only remaining condition to be considered is that J_0 be positive, which yields the inequality

$$(b_2^{\circ})^2 > 2(\gamma^2 R - \epsilon\beta_1\beta_2) \qquad 2.6.7$$

as the required stability condition. If this inequality is now compared with the steady-state solution for b_2^2 given by equation 2.4.32, namely

$$b_2^2 = 2(\gamma^2 R - \epsilon\beta_1\beta_2) \pm [1 - 4\gamma^2\epsilon R(\beta_1 + \beta_2)^2]^{\frac{1}{2}}$$

then it is seen that the stability condition becomes

$$\pm [1 - 4\gamma^2\epsilon R(\beta_1 + \beta_2)^2]^{\frac{1}{2}} > 0 \qquad 2.6.8$$

It is evident therefore that the steady-state solutions for b_1 and b_2 both nonzero, are stable over the frequency range spanned by the upper branches of the b_2 response curves, and are bounded by the points of vertical tangency on these curves.

Case 2 : b_1 nonzero, b_2 zero

The substitutions

$$b_1 = b_1^{\circ} + \delta b_1;\ b_2 = \delta b_2 (b_2^{\circ} = 0);\ \psi_1 = \psi_1^{\circ} + \delta\psi_1;\ \psi_2 = \psi_2^{\circ} + \delta\psi_2 \qquad 2.6.9$$

are made in the system equations 2.6.1 where once again b_1°, $b_2^{\circ} = 0$, ψ_1° and ψ_2° satisfy the equilibrium conditions.

For $b_2^{\,o} = 0$, the steady-state equations 2.4.30 yield the following expression for $b_1^{\,o}$,

$$b_1^{\,o} = \pm \frac{1}{4[\gamma^2 + (\epsilon/R)\eta_1^{\,2}]^{\frac{1}{2}}} \qquad 2.6.10$$

Thus with $b_2^{\,o} = 0$ and $b_1^{\,o}$ given by 2.6.10 there results four first order equations in the δb_i and $\delta\psi_i$. These are

$$\delta b_1' = -[4\eta_1(\epsilon/R)^{\frac{1}{2}}]\delta b_1 - [\cos\psi_1^{\,o}]\,\delta\psi_1$$

$$\delta b_2' = [(4/R)b_1^{\,o}\sin(2\psi_2^{\,o} - \psi_1^{\,o}) - 2\eta_2(\epsilon/R)^{\frac{1}{2}}]\delta b_2$$

$$b_1^{\,o}\,\delta\psi_1' = [4\gamma]\delta b_1 + [\sin\psi_1^{\,o}]\,\delta\psi_1$$

and

$$0 = [(4/R)b_1^{\,o}\cos(2\psi_2^{\,o} - \psi_1^{\,o}) + 2\gamma]\delta b_2$$

... 2.6.11

As there are no linear terms in $\delta\psi_2$ the stability determinant reduces to a 3 x 3 in the coefficients of δb_1, δb_2 and $\delta\psi_1$. The fourth of equations 2.6.11 provides an expression for $\cos(2\psi_2^{\,o} - \psi_1^{\,o})$. Expanding the determinant results in a cubic characteristic equation of the form

$$J_3\lambda^3 + J_2\lambda^2 + J_1\lambda + J_o = 0 \qquad 2.6.12$$

where

$$J_3 = 1;\ J_2 = 8(\epsilon/R)^{\frac{1}{2}} + 2\{(\epsilon/R)^{\frac{1}{2}}\eta_2 - [(2/R)^2(b_1^{\,o})^2 - \gamma^2]^{\frac{1}{2}}\};$$

$$J_1 = 16[\gamma^2 + (\epsilon/R)\eta_1^{\,2}] + 16(\epsilon/R)^{\frac{1}{2}}\eta_1\{(\epsilon/R)^{\frac{1}{2}}\eta_2 - [(2/R)^2(b_1^{\,o})^2 - \gamma^2]^{\frac{1}{2}}\};$$

$$J_o = 32[\gamma^2 + (\epsilon/R)\eta_1^{\,2}]\{(\epsilon/R)^{\frac{1}{2}}\eta_2 - [(2/R)^2(b_1^{\,o})^2 - \gamma^2]^{\frac{1}{2}}\}$$

... 2.6.13

($\psi_1^{\,o}$ and $\psi_2^{\,o}$ have been eliminated using steady-state equations 2.4.30).

For a cubic characteristic equation the Routh-Hurwitz criteria are J_i positive and $J_1J_2 - J_o$ positive for stability. After calculation $J_1J_2 - J_o$ has the form

$$J_1J_2-J_o = 128(\epsilon/R)^{\frac{1}{2}}\eta_1[\gamma^2 + (\epsilon/R)^{\frac{1}{2}}\eta_1^2]$$
$$+ 32(\epsilon/R)^{\frac{1}{2}}\eta_1\{(\epsilon/R)^{\frac{1}{2}}\eta_2 - [(2/R)^2(b_1^o)^2 - \gamma^2]^{\frac{1}{2}}\}^2$$
$$+ 128(\epsilon/R)\eta_1^2\{(\epsilon/R)^{\frac{1}{2}}\eta_2 - [(2/R)^2(b_1^o)^2 - \gamma^2]^{\frac{1}{2}}\} \qquad 2.6.14$$

By inspection of 2.6.13 and 2.6.14 it is clear that stable solutions require

$$(\epsilon/R)^{\frac{1}{2}}\eta_2 \geq [(2/R)^2(b_1^o)^2 - \gamma^2]^{\frac{1}{2}} \qquad 2.6.15$$

Further, the bounds of stability are defined by the equality

$$\gamma^2 = (2/R)^2(b_1^o)^2 - (\epsilon/R)\eta_2^2 \qquad 2.6.16$$

which becomes, on substituting for b_1^o using 2.6.10,

$$\gamma^2 = -(\epsilon/2R)(\eta_1^2 + \eta_2^2) \pm (1/2R)[\epsilon^2(\eta_1^2 - \eta_2^2)^2 + 1]^{\frac{1}{2}} \qquad 2.6.17$$

2.6.17 defines the frequency range within the solution is unstable.

Considering once again the stability criterion 2.6.15 it is evident on rearranging the inequality thus

$$(b_1^o)^2 \leq (R/2)^2\gamma^2 + (\epsilon R/4)\eta_2^2$$

that the right-hand side represents the square of the two-degree of freedom solution for b_1, given by 2.4.31. In other words the stability criterion is simply stating that the zero b_2 solution is stable while the one-degree of freedom solution for b_1 ($b_2 = 0$, see equation 2.6.10) remains below its two-degree of freedom solution (b_1 and b_2 nonzero, equation 2.4.31).

Consequently the frequency expression 2.6.17 defines the 'cross-over' points in the main mass response found by equating the one-degree of freedom solution to the two-degree of freedom solution.

Returning to the steady-state solution for b_2 given by equation 2.4.32 it is seen that for $b_2 = 0$ this same expression 2.6.17 is obtained and that the slope $\frac{db_2}{d\gamma}$ is infinite. Therefore the bounds of zero b_2 stability coincide with the points of vertical tangency in the lower branches of the b_2 response curves.

In summary then, the stability criterion 2.6.15 provides a frequency expression 2.6.17 which defines

(a) the bounds of zero b_2 stability,

(b) the cross-over points of the b_1 response curves, and

(c) the points of vertical tangency in the lower branches of the b_2 response curves.

Clearly the cross-over points could be renamed the entry points as they signify the beginning of absorber action.

2.7 Stability of Steady-State Solutions : Detuned Absorber

A study of the stability of the solutions 2.5.14 and 2.5.15 for a detuned absorber follows the same procedure as detailed in the previous section. It is necessary only to quote the results of such an analysis for the detuned case.

Case 1 : b_1, b_2 nonzero.

The condition which emerges from the Routh-Hurwitz criteria is that

$$(b_2^{\,o})^2 > 2\rho^2(\gamma^2 R - \epsilon\beta_1\beta_2) + \rho(1-\rho^2)(R/\epsilon)^{\frac{1}{2}}\gamma \qquad 2.7.1$$

for stable solutions.

Comparing this inequality with the result 2.5.15 it can be concluded that

$$\pm [1 - 4\rho^2\gamma^2\epsilon R(\beta_1 + \rho^2\beta_2)^2 - \rho^4(1 - \rho^2)^2\beta_2^2 - 4\rho^3(1 - \rho^2)(\epsilon R)^{\frac{1}{2}}\gamma\beta_2(\beta_1 + \rho^2\beta_2)]^{\frac{1}{2}} > 0 \qquad 2.7.2$$

and therefore that the lower branches of the b_2 response curves are unstable.

Case 2 : b_1 nonzero, b_2 zero .

Here the Routh-Hurwitz stability criteria require that

$$\rho^3(\epsilon/R)^{\frac{1}{2}}\beta_2 \geq [(2/R)^2(b_1^{\,o})^2 - \rho^4\gamma^2]^{\frac{1}{2}} \qquad 2.7.3$$

for stability where the steady-state expression for $b_1^{\,o}(b_2^{\,o} = 0)$ is given by

$$b_1^{\,o} = \pm \frac{\rho}{2\left\{4[\rho^2\gamma^2 + (\epsilon/R)\beta_1^2] + [4\rho(1 - \rho^2)\gamma/(\epsilon R)^{\frac{1}{2}}] + (1 - \rho^2)^2/(\epsilon R)\right\}^{\frac{1}{2}}} \qquad 2.7.4$$

2.7.4 is obtained from the steady-state equations 2.5.13 with $b_2 = 0$, and its substitution into 2.7.3 gives a frequency relationship which defines the frequency band inside which the zero b_2 solution is unstable. Thus the bounds of stability are determined by the roots of the expression

$$[4\rho^4R^2]\gamma^4 + [4\rho^3(1 - \rho^2)(R^{\frac{3}{2}}/\epsilon^{\frac{1}{2}})]\gamma^3 + [4\rho^2\epsilon R(\beta_1^{\,2} + \rho^4\beta_2^{\,2}) + \rho^2(1 - \rho^2)(R/\epsilon)]\gamma^2 + [4\rho^5(1 - \rho^2)(\epsilon R)^{\frac{1}{2}}\beta_2^{\,2}]\gamma + [4\rho^4\epsilon^2\beta_1^{\,2}\beta_2^{\,2} + \rho^4(1 - \rho^2)^2\beta_2^{\,2} - 1] = 0 \qquad 2.7.5$$

However, 2.7.4 only provides a hypothetical one-degree of freedom response which, while it ensures the correct mathematical formulation of the stability bounds (2.7.5), does not represent the true b_1 response. To understand this it is necessary to consider what detuning means in a physical sense.

If the absorber system is not perfectly tuned to half of the main mass frequency it is considered to be in a detuned condition. The degree of this detuning may be reduced by suitable adjustments to the absorbers' stiffness or to the magnitude of its end mass. In the present study the system mass (M + m) is maintained constant and so any detuned condition stems from incorrect adjustment of the absorber stiffness for a given amount of damping $\epsilon\beta_2$. In this case it is obvious that the system cannot differentiate between perfect tuning or any amount of detuning when performing one-degree of freedom motion. Thus the one-degree of freedom response is given by equation 2.6.10, that is

$$b_1^{\,o} = \pm \frac{1}{4[\gamma^2 + (\epsilon/R)\beta_1^{\,2}]^{\frac{1}{2}}}$$

Consequently the cross-over points found by equating 2.6.10 with the two-degree of freedom solution 2.5.14 do not coincide with the bounds of zero b_2 stability.

Finally, the expression 2.7.5 is also derivable from equation 2.5.15 for $b_2 = 0$, while the slope $\frac{db_2}{d\gamma}$ becomes infinite. Thus 2.7.5 also defines the points of vertical tangency in the lower branches of the b_2 response curves.

Summarising the foregoing comments it may be said that the stability criterion 2.7.3 provides a frequency expression 2.7.5 which defines,

(a) the bounds of zero b_2 stability,

and (b) the points of vertical tangency in the lower branches of the b_2 response curves,

but which does not define the cross-over points. Because the cross-over and entry points for a detuned absorber system do not coincide, jumps in the main mass response are to be expected on the commencement of absorber action.

CHAPTER 3

THEORETICAL AMPLITUDE RESPONSE OF THE AVA

3.1 Introduction

With the completion of the stability analysis it is now possible to assimilate the findings of the preceding chapter and present them in graphical form. The drawing of a series of theoretical amplitude response curves for the main mass and absorber systems provides for easy interpretation of the steady-state results and forms a basis for comparison with known experimental data.

For the most part only the response curves of a perfectly tuned absorber system are presented although the effects of detuning are shown.

The chapter ends with a theoretical comparison of the autoparametric absorber and the linear tuned and damped absorber.

3.2 Theoretical Response Curves: Perfectly Tuned Absorber

To provide response curves which may be compared more readily with experimental data, the steady-state solutions for b_1 and b_2 given by equations 2.4.31 and 2.4.32 are transformed thus

$$\left|X_d/X_o\right| = \pm \left[\gamma_2^2 + (1 - n^2)^2/4\epsilon^2\right]^{\frac{1}{2}} \qquad 3.2.1$$

$$\left|(y_d/X_o)^2\right| = (8/\epsilon R)\left[\left\{(1 - n^2)^2/4\epsilon\right\} - \epsilon\gamma_1\gamma_2\right]$$

$$\pm (4/\epsilon R)\left[1 - (1 - n^2)^2(\gamma_1 + \gamma_2)^2\right]^{\frac{1}{2}} \qquad 3.2.2$$

Using these nondimensional expressions together with the stability conditions previously derived for the perfectly tuned case, the nondimensional quantities (X_d/X_o) and (y_d/X_o) can be plotted against the forced frequency ratio, $n = 2\Omega/\omega_1$, for various values of viscous damping $\epsilon\gamma_1$ and $\epsilon\gamma_2$. Known experimental values are assigned to the constants X_o, ϵ and R, while the ratio of the damping parameters γ_1 and γ_2 is varied over a range thought likely to be encountered in practice.

Adopting the following values for the system constants,

$$X_o = 0.0030 \text{ in}, \quad \epsilon = 0.0005 \text{ and } R = 0.0196$$

the Figs. 3.2.1 to 3.2.6 show the effect of varying γ_2 (for a given γ_1) on the amplitude response of the system. Each of these figures presents the amplitude response of the main mass, (1), together with the corresponding absorber response, (2). It should be noted that the lower branches of the absorber response curves are unstable as indicated by the broken lines and that the amplitudes of the absorber mass are approximately ten times greater than those experienced by the main mass.

An examination of equation 3.2.2 reveals the following properties of the absorber response curves:

1. For real (y_d/X_o), $[1 - 1/(\gamma_1 + \gamma_2)]^{\frac{1}{2}} \leq n \leq [1 + 1/(\gamma_1 + \gamma_2)]^{\frac{1}{2}}$.

Thus, absorber action occurs for a limited range of excitation frequencies in the neighbourhood of ω_1 when the damping is not too large.

2. For $0 < (\gamma_1 + \gamma_2) < \epsilon^{-\frac{1}{2}}$ the response curves have two maxima, one minimum and four points of vertical tangency (two for $(y_d/X_o) = 0$).

3. For $\epsilon^{-\frac{1}{2}} < (\gamma_1 + \gamma_2) < \frac{1}{2}\epsilon^{-1}(\gamma_1\gamma_2)^{-\frac{1}{2}}$ the response curves have only one maximum, no minima, and four points of vertical tangency.

4. For $(\gamma_1 + \gamma_2) > \frac{1}{2}\epsilon^{-1}(\gamma_1\gamma_2)^{-\frac{1}{2}}$ the response curves have only one maximum, no minima, and no points of vertical tangency. This means that the equality

$$(\gamma_1 + \gamma_2) = \frac{1}{2}\epsilon^{-1}(\gamma_1\gamma_2)^{-\frac{1}{2}} \qquad 3.2.3$$

defines the maximum permissible damping for stable absorber action (see Fig. 3.2.6).

To provide a measure of the effectiveness of the absorber Figs. 3.2.1 and 3.2.2 also show one-degree of freedom responses (absorber locked, $y_d = 0$) for $\epsilon\gamma_1 = 0$ and $\epsilon\gamma_1 = 0.0035$, respectively.

The points of vertical tangency on the absorber response curves are important as they define the boundaries of the region of parametric instability of the absorber. They coincide with the discontinuities and jumps observed in the main mass displacements. In subsequent discussion the forcing frequency at which a nonzero absorber amplitude becomes unstable will be referred to as a 'collapse frequency' and the associated main mass amplitude just prior to this will be referred to as its 'collapse amplitude'.

To follow the details of the action of the AVA consider the set of curves depicted in Fig. 3.2.3. It is seen that following the path of increasing frequency (indicated by arrows) the system behaves as a normal one-degree of freedom system (region A) until it reaches the cross-over point (point B) previously discussed. This corresponds to a point of vertical tangency in the absorber solution ($b_2^{\,o} = 0$ solution unstable) and so absorber action begins.

The main mass system then follows the two-degree of freedom solution (region C), its amplitude reaching a minimum value at n = 1. It then climbs steadily until the collapse amplitude is reached (point D). This corresponds to a vertical tangency in the absorber solution which defines the collapse frequency and marks the bound of absorber action. The result is that absorber action ceases and the main mass amplitude drops to its one-degree of freedom level (point E).

Following a path of decreasing frequency (again arrowed) the main system behaves in a similar fashion tracing the path F, G (absorber entry point), C, H (collapse amplitude), K and A.

The corresponding regions and points on the absorber response curve are similarly illustrated using lower case letters, the jumps bb and gg coinciding with the entry points B and G on the main mass response.

To complete the graphical presentation of the perfectly tuned AVA system, the amplitude response curves for both the main mass and the absorber can be combined to form the three-dimensional plots of Fig. 3.2.7 and Fig. 3.2.8. Fig. 3.2.7 shows the 3-d surface of main mass response formed when the additional parameter axis η_2/η_1 is introduced. The effect of viscous damping on the response is immediately apparent while any point on the wedge-shaped surface defines a main mass response for which there exists stable absorber action. The locus of the collapse amplitude, which is shown by chain line, has as asymptotes the two-degree of freedom response for $\epsilon\eta_1 = 0$ and $\epsilon\eta_2 = 0$ and, for increasing η_2/η_1, terminates when the maximum damping condition (3.2.3) is satisfied (in this case when $\epsilon\eta_1 = 0.0035$ and $\epsilon\eta_2 = 0.0238$).

This locus is seen to have a minimum value which defines that ratio of γ_2/γ_1 which will produce the minimum collapse amplitude.

Expressed mathematically, the equation of the locus is

$$(X_d/X_o)^2 = \gamma_2^2 + 1/4\epsilon^2(\gamma_1 + \gamma_2)^2$$

and it has a minimum value defined by

$$\gamma_2(\gamma_1 + \gamma_2)^3 - 1/4\,\epsilon^2 = 0$$

Finally, the locus of the minimum amplitude of the two-degree of freedom solution may also be drawn, it is a straight line of gradient $1/\gamma_1$ and is shown by chain line.

The 3-d surface of the absorber response is shown in Fig. 3.2.8 where the unstable lower branches of the solutions have been omitted for clarity and every point on the U-shaped surface defines a state of stable absorber action. There are a number of interesting loci in this figure which are identified as follows,

(a) the locus of maximum amplitude (chain line),

(b) the locus of collapse amplitude (dash line),

(c) the locus of zero b_2 stability which defines the entry points (chain line),

(d) the projection on the $b_2 = 0$ plane of the locus of collapse amplitude (dash line).

Now it has already been mentioned in this section that the absorber response curves fall into three distinct groups. The boundaries separating these groups occur at $(\gamma_1 + \gamma_2) = \epsilon^{-\frac{1}{2}}$ and $(\gamma_1 + \gamma_2) = \frac{1}{2}\,\epsilon^{-1}(\gamma_1\gamma_2)^{-\frac{1}{2}}$.

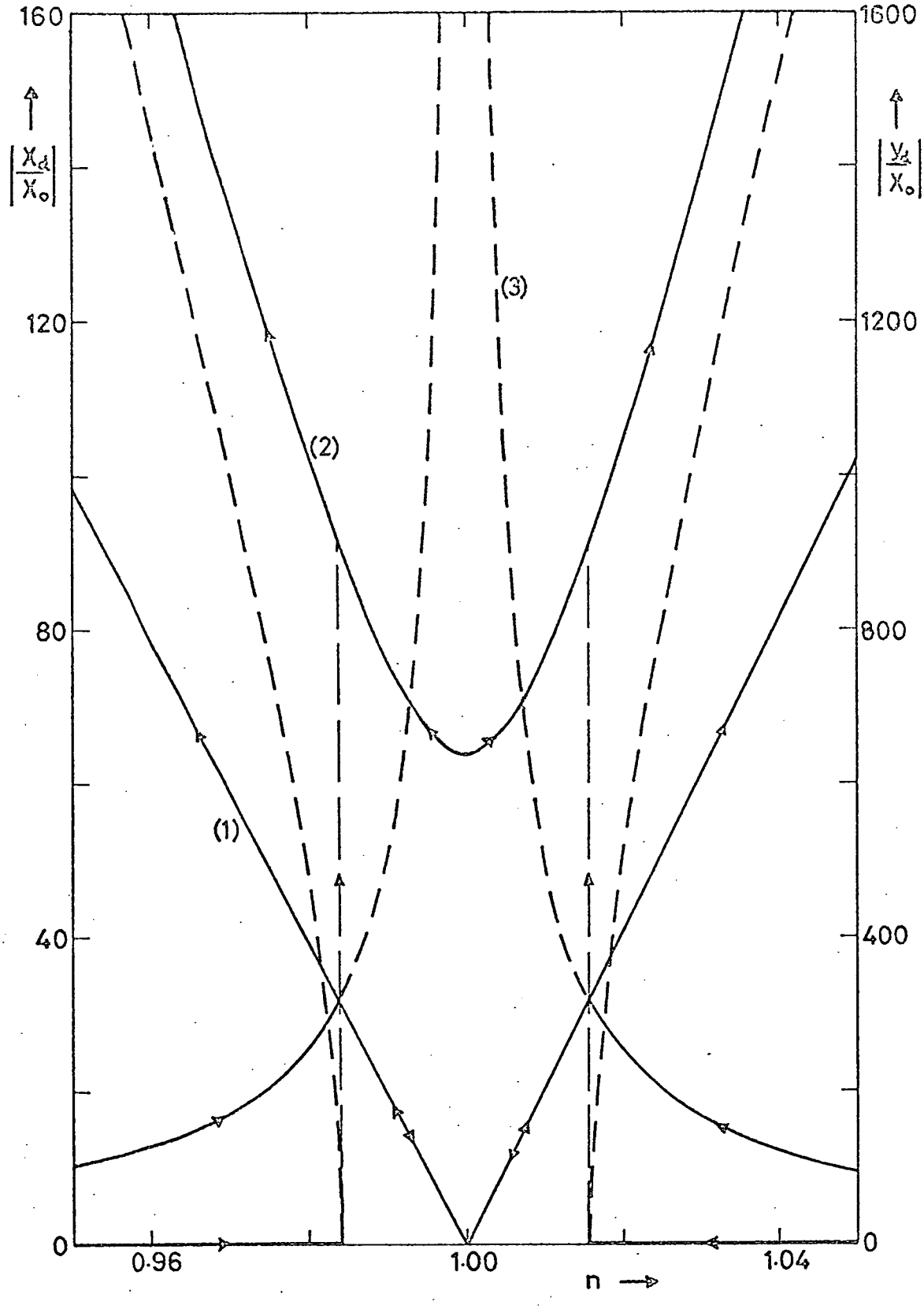

Fig. 3.2.1

Theoretical Amplitude Response Curves for $\epsilon\eta_1 = 0$, $\epsilon\eta_2 = 0$, (Perfectly Tuned Absorber, $\rho = 1.0$).

(1) main mass response,

(2) absorber response,

(3) main mass response (absorber locked).

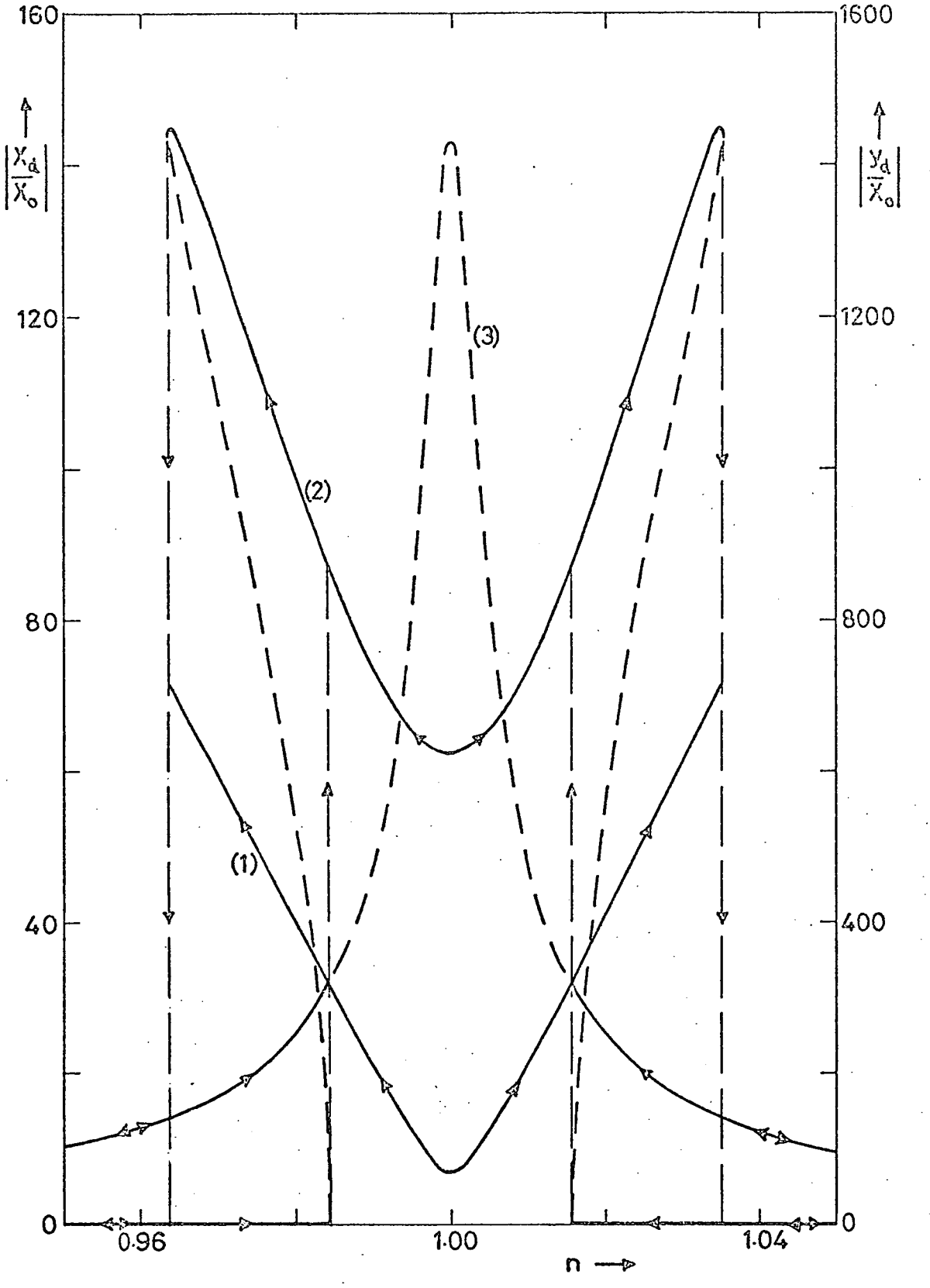

Fig. 3.2.2

Theoretical Amplitude Response Curves
for $\epsilon\eta_1 = 0.0035$, $\epsilon\eta_2 = 0.0035$, $(\rho = 1.0)$.

(1) main mass response,

(2) absorber response,

(3) main mass response (absorber locked).

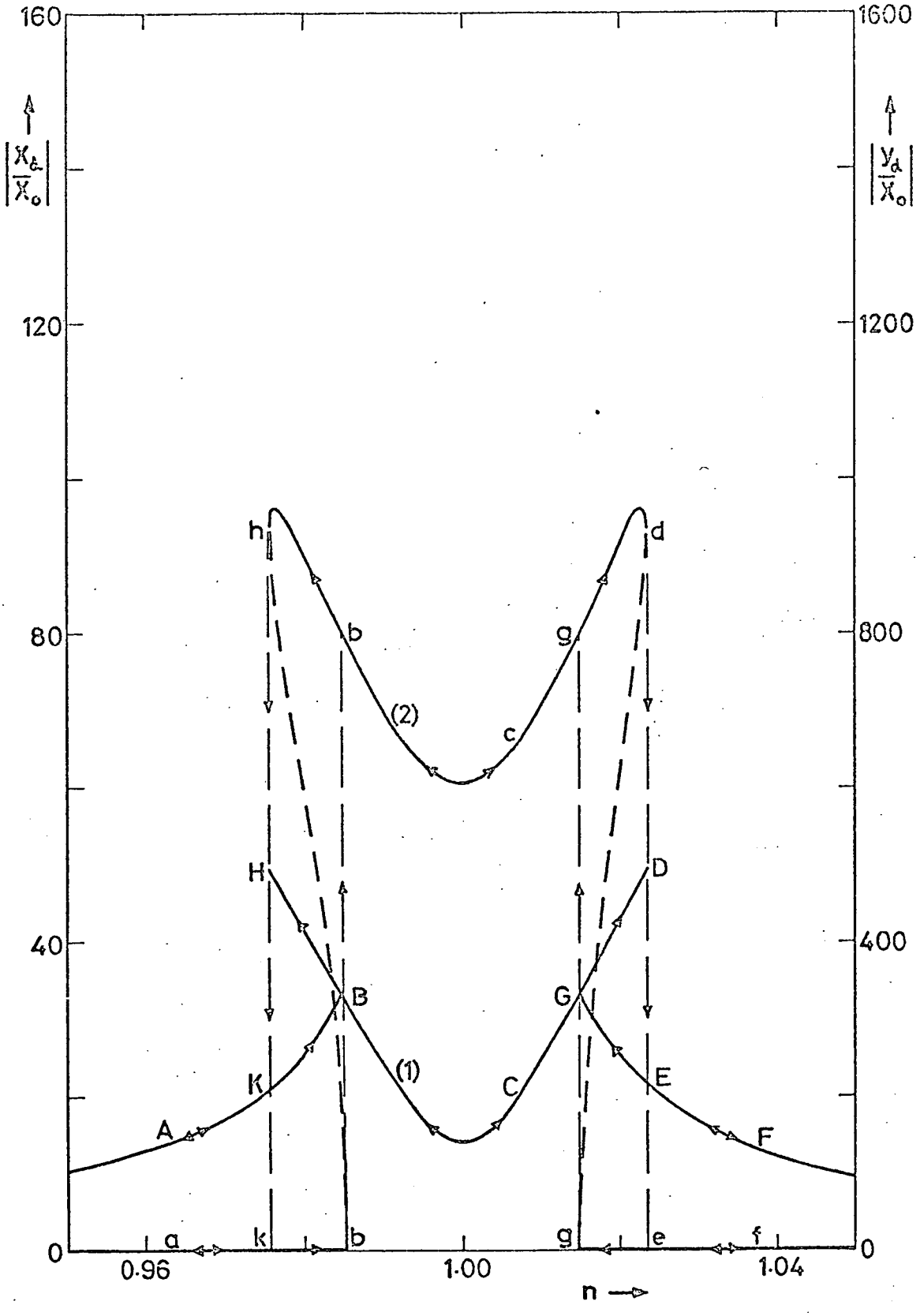

Fig. 3.2.3

Theoretical Amplitude Response Curves
for $\epsilon\eta_1 = 0.0035$, $\epsilon\eta_2 = 0.0070$, $(\rho = 1.0)$.

(1) main mass response,

(2) absorber response.

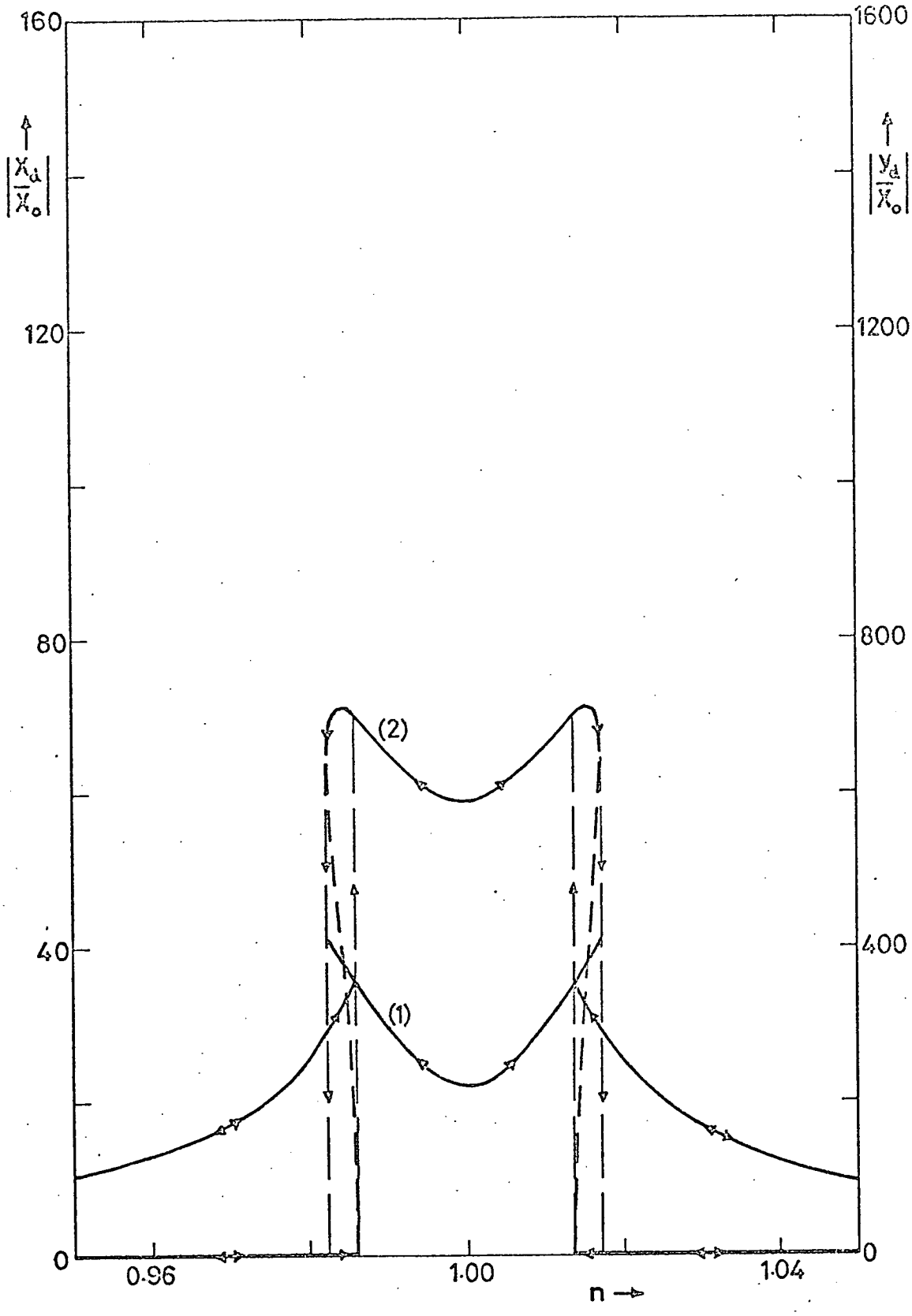

Fig. 3.2.4

Theoretical Amplitude Response Curves
for $\epsilon\gamma_1 = 0.0035$, $\epsilon\gamma_2 = 0.0110$, $(\rho = 1.0)$.

(1) main mass response,

(2) absorber response.

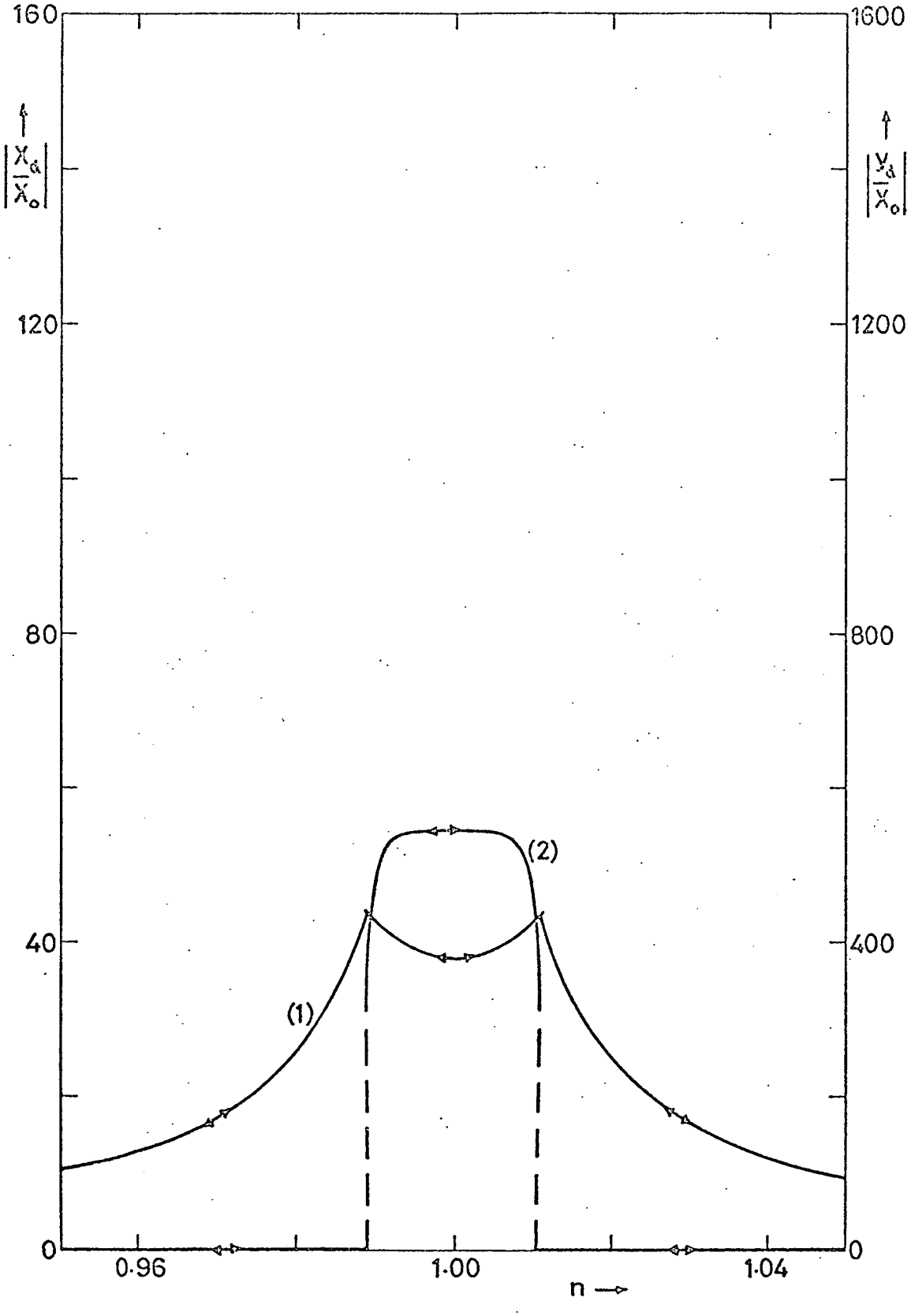

Fig. 3.2.5

Theoretical Amplitude Response Curves
for $\epsilon\gamma_1 = 0.0035$, $\epsilon\gamma_2 = 0.0189$, ($\rho = 1.0$).

(1) main mass response,

(2) absorber response.

(Details of jumps omitted for clarity).

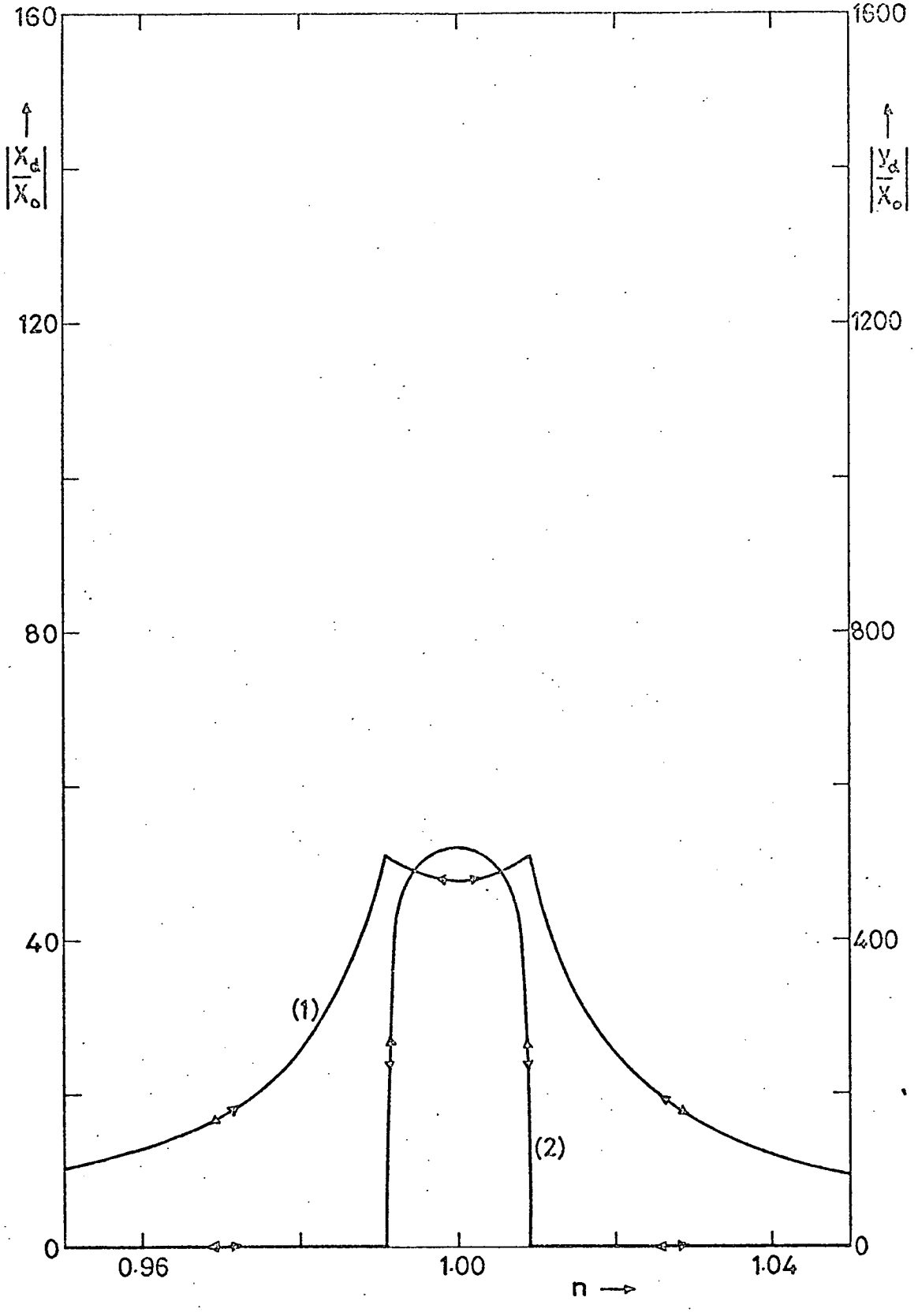

Fig. 3.2.6

Theoretical Amplitude Response Curves
for $\epsilon\eta_1 = 0.0035$, $\epsilon\eta_2 = 0.0238$, $(\rho = 1.0)$.

(1) main mass response,

(2) absorber response.

(Note : no jumps).

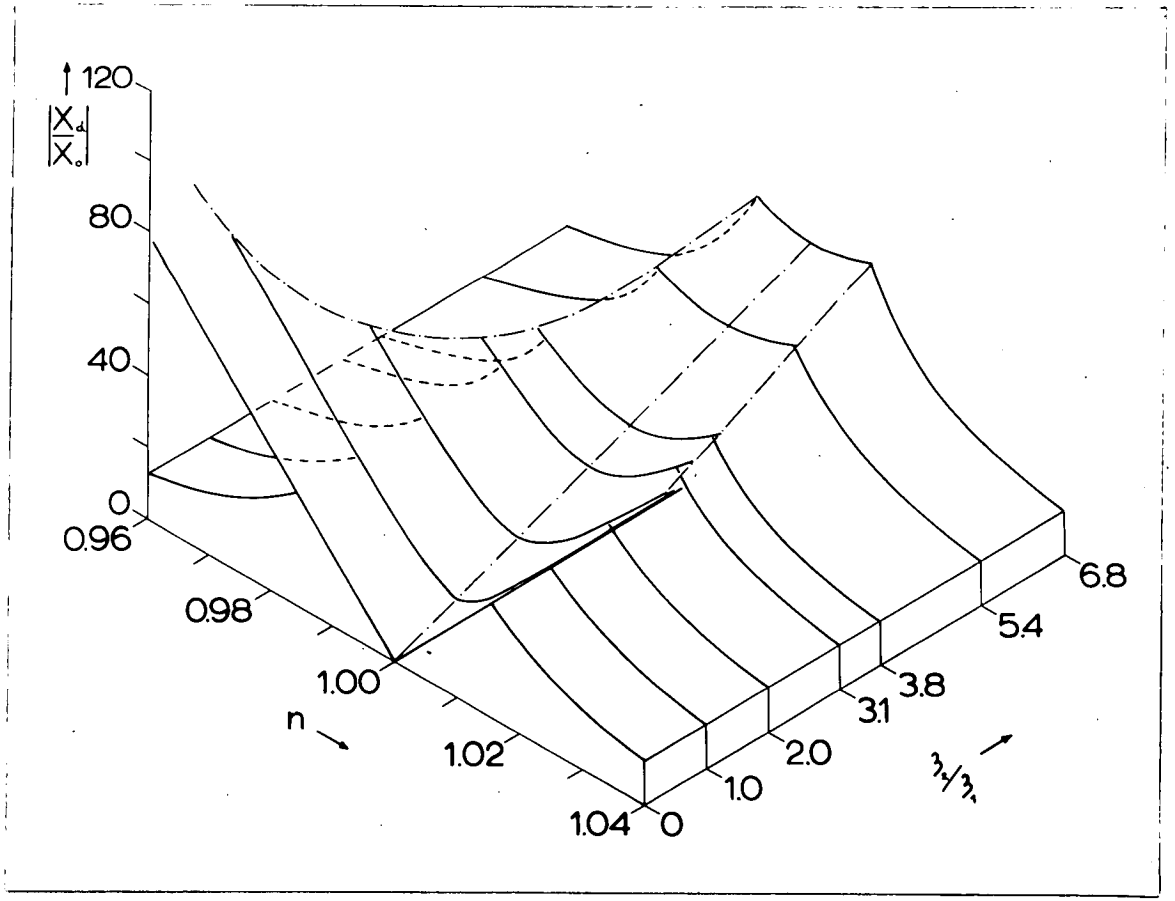

Fig. 3.2.7

3-d Plot of Theoretical Response Amplitude of Main Mass under the Action of the AVA.

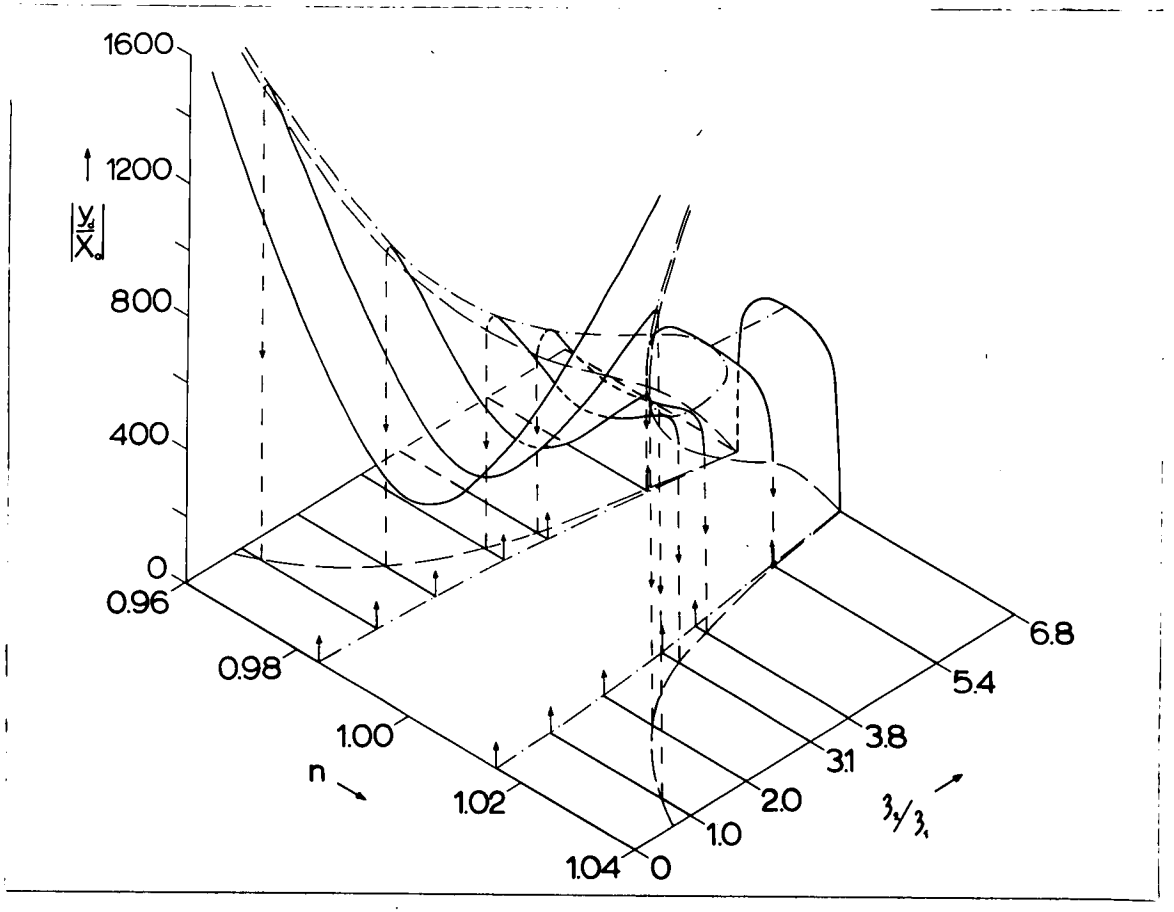

Fig. 3.2.8

3-d Plot of Theoretical Response Amplitude of the Absorber.

When $(\gamma_1 + \gamma_2) = \epsilon^{-\frac{1}{2}}$ the locus of maximum amplitude exhibits a bifurcation, a transition point from two maxima (and a minimum) to one maximum. For the values ascribed to the system parameters this occurs when $\gamma_2/\gamma_1 = 5.39$, i.e. $\epsilon\gamma_1 = 0.0035$ and $\epsilon\gamma_2 = 0.0189$ (see Fig. 3.2.5).

When $(\gamma_1 + \gamma_2) = \frac{1}{2}\epsilon^{-1}(\gamma_1\gamma_2)^{-\frac{1}{2}}$ the two sets of vertical tangency points coincide so that the locus of collapse amplitude intersects the zero b_2 plane. For the given system this occurs when $\gamma_2/\gamma_1 = 6.80$, i.e. $\epsilon\gamma_1 = 0.0035$ and $\epsilon\gamma_2 = 0.0238$ (see Fig. 3.2.6). An infinitesimal increase in damping beyond these values results in imaginary absorber action (negative collapse amplitude) and so the system reverts to its one-degree of freedom response.

3.3 Theoretical Response Curves: Detuned Absorber

Once more it is convenient to transform the steady-state solutions for b_1 and b_2, given by equations 2.5.14 and 2.5.15, to provide expressions suitable for graphical presentation, thus

$$|X_d/X_o| = \pm[\rho^4\gamma_2^2 + (\rho^2 - n^2)^2/4\epsilon^2]^{\frac{1}{2}} \qquad 3.3.1$$

$$\begin{aligned}|(y_d/X_o)^2| &= (8/\epsilon R\rho^2)[\{(\rho^2-n^2)^2/4\epsilon\} - \epsilon\rho^2\gamma_1\gamma_2 + R(1-\rho^2)(\rho^2-n^2)/4\epsilon] \\ &\pm (4/\epsilon R\rho^2)[1 - (\rho^2-n^2)^2(\gamma_1 + \rho^2\gamma_2)^2 - \rho^4(1 - \rho^2)^2\gamma_2^2 - \\ &- 2\rho^2(1 - \rho^2)(\rho^2 - n^2)(\gamma_1\gamma_2 + \rho^2\gamma_2^2)]^{\frac{1}{2}} \qquad 3.3.2\end{aligned}$$

These expressions may be compared with their counterparts in the previous section, 3.2.1 and 3.2.2. They are very similar in form and, of course, identical when $\rho = 1$.

Using 3.3.1 and 3.3.2 together with the restraints of the stability conditions for the detuned case, it is possible to produce a series of response curves similar to those already drawn for the perfectly tuned absorber. However, to avoid unnecessary duplication it is sufficient to simply highlight the effects of detuning with the aid of Figs. 3.3.1 and 3.3.2. The value of the detuning factor ρ is taken as 1.01 to emphasis these effects although closer tuning can be obtained in practice. The same values are chosen for the system constants, namely, $X_o = 0.0030$ in, $\epsilon = 0.0005$ and $R = 0.0196$.

Fig. 3.3.1 is drawn for $\epsilon\gamma_1 = \epsilon\gamma_2 = 0$ and may be compared directly with Fig. 3.2.1 for the perfectly tuned case. Similarly Fig. 3.3.2, for $\epsilon\gamma_1 = \epsilon\gamma_2 = 0.0035$, is directly comparable with Fig. 3.2.2. The features which emerge from this visual comparison may be listed as follows:

1. The two-degree of freedom solutions for X_d and y_d shift bodily to centre themselves about $n = 1.01$.

2. The symmetry of the perfectly tuned response no longer exists due to the term in $(1 - \rho^2)(\rho^2 - n^2)$ which reduces the collapse amplitudes when $n > \rho > 1.0$ and increases them when $n < \rho > 1.0$. (Note the opposite effect occurs for $\rho < 1.0$).

3. Because the one-degree of freedom response of the system is unchanged, the cross-over and entry points do not coincide with the result that the main mass response now exhibits jumps on the entry of absorber action.

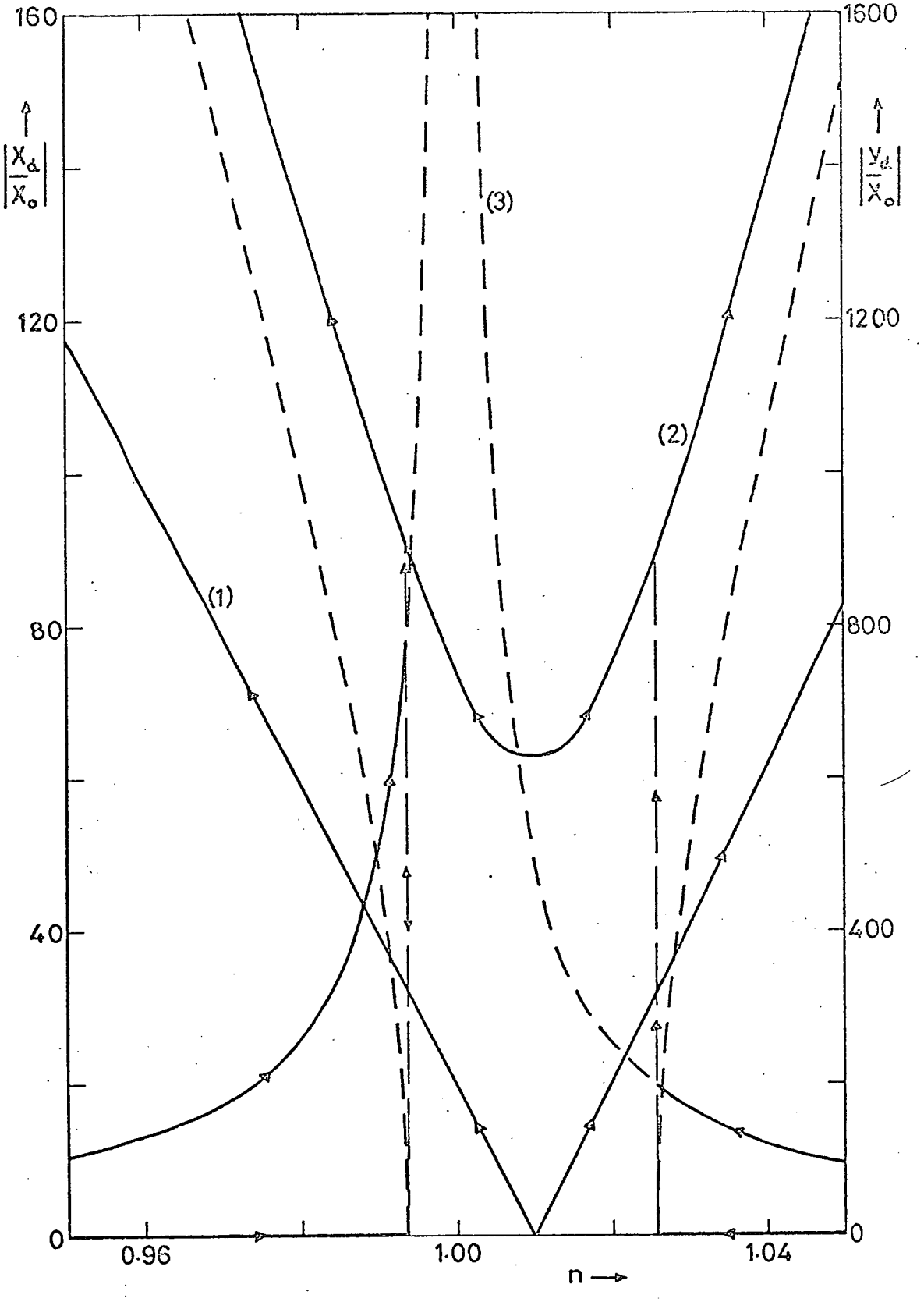

Fig. 3.3.1

Theoretical Amplitude Response Curves for $\epsilon\eta_1 = 0$, $\epsilon\eta_2 = 0$.
(Detuned Absorber, $\rho = 1.01$).

(1) main mass response,

(2) absorber response,

(3) main mass response (absorber locked).

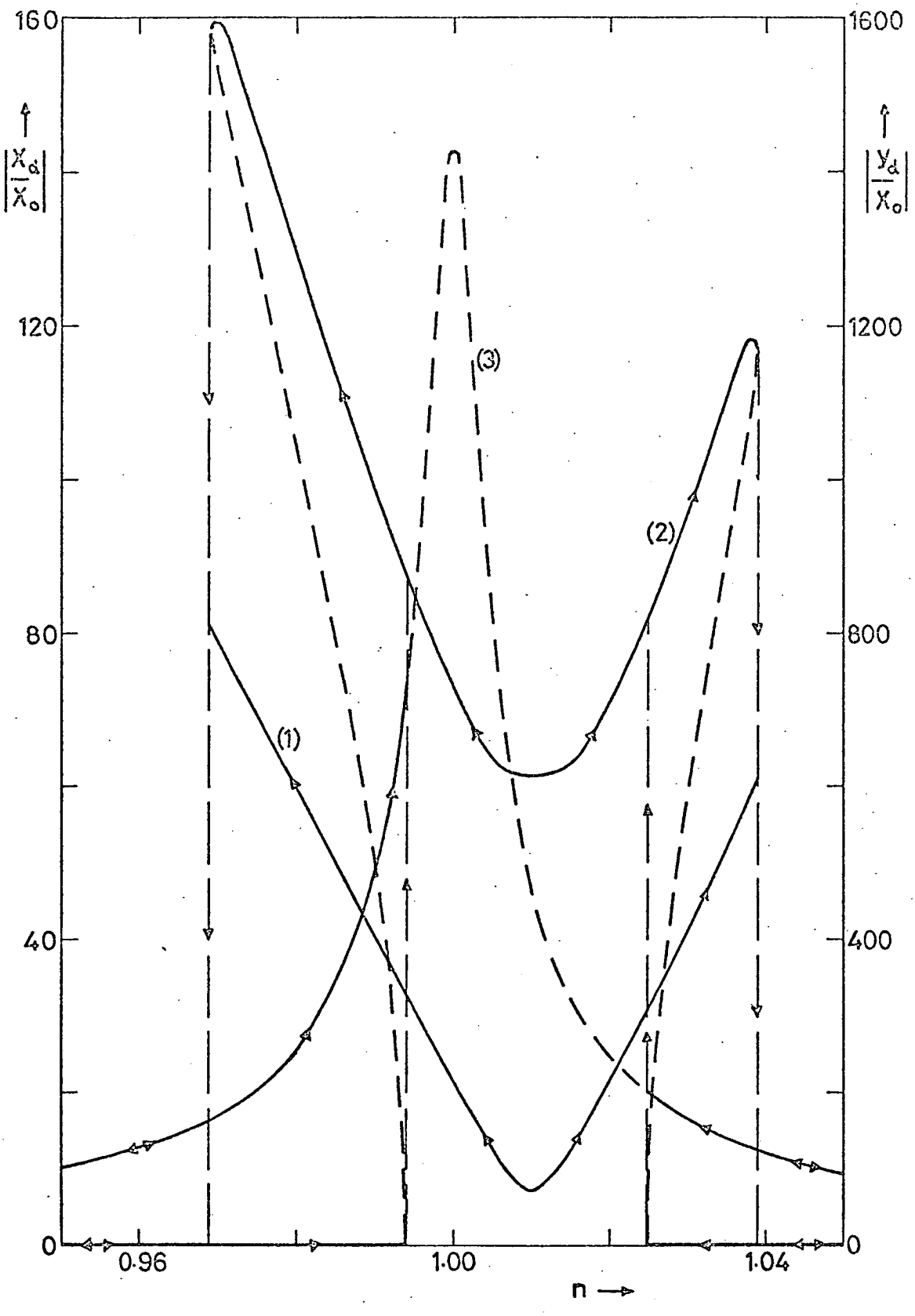

Fig. 3.3.2

Theoretical Amplitude Response Curves
for $\epsilon\eta_1 = 0.0035$, $\epsilon\eta_2 = 0.0035$, $(\rho = 1.01)$.

(1) main mass response,

(2) absorber response,

(3) main mass response (absorber locked).

3.4 Comparison of AVA with LTDA

A glance at equation 3.2.1 shows that a more powerful absorber action is achieved when the value of the parameter ϵ $(= 6X_o/5\ell)$ is increased. This implies an increase in the ratio of axial motion to lateral motion of the absorber end mass. In practice this can be achieved by dimensioning the absorber cantilever beam to provide the same natural frequency (ω_2) with the same mass (m) while decreasing the length (ℓ).

Experimentally it was possible to produce an absorber of small length, giving an ϵ value of 0.0025 (cf. $\epsilon = 0.0005$ used previously). Fig. 3.4.1 shows a set of theoretical main mass responses for such an absorber. Studying Figs. 3.2.1, 3.2.3 and 3.4.1, it can be seen that a general improvement in the performance of the absorber has been obtained by shortening its length but this improvement is obtained at the expense of greater strain amplitudes in the absorber.

To provide a measure of the effectiveness of this improved AVA system it was decided to effect a theoretical comparison with the linear tuned and damped absorber (contracted to LTDA). It is assumed that the theory of the LTDA is known to the reader, if not, it is well documented by J.P. den Hartog in his book "Mechanical Vibrations". The LTDA main mass response is

$$\frac{X_d}{X_o} = \left[\frac{(2\gamma n)^2 + (n^2 - 1)^2}{(2\gamma n)^2(n^2 - 1 + \frac{m}{M} n^2)^2 + [\frac{m}{M} n^2 - (n^2 - 1)^2]^2}\right]^2$$

where m/M is the ratio of absorber mass to main mass, γ is the damping introduced between m and M. The experimental ratio (m/M) = 0.02 is chosen for both AVA and LTDA systems.

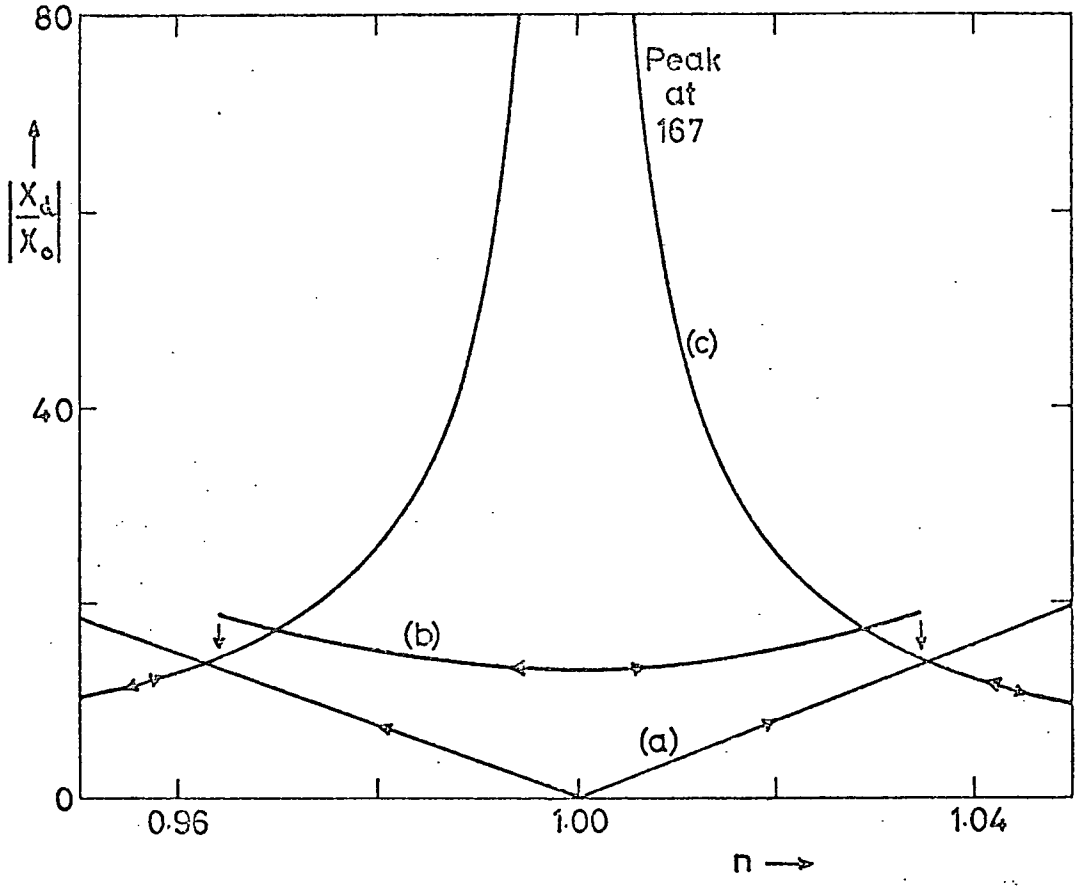

Fig. 3.4.1

Theoretical Main Mass Response Amplitude under the Action of Small Length AVA.

(a) $\epsilon_{\eta_1} = 0$, $\epsilon_{\eta_2} = 0$,

(b) $\epsilon_{\eta_1} = 0.0030$, $\epsilon_{\eta_2} = 0.0338$,

(c) $\epsilon_{\eta_1} = 0.0030$ (absorber locked).

Since this ratio is small compared with unity, the LTDA natural frequency ratio is taken as unity and the optimum damping between its two mass system is found to be 0.09.

Fig. 3.4.2 compares the resulting LTDA main mass response (a) with two AVA response curves (b) and (c). Also shown is the one-degree of freedom response (d) for the absorber locked. The AVA response (c) represents the minimum collapse amplitude attainable for the stated parameters but this $\epsilon\zeta_2$ value does not produce good absorber action near resonance. Response (b) for a smaller $\epsilon\zeta_2$ value compares more favourably with the LTDA near resonance but the consequent widening of the parametric instability zone results in much higher collapse amplitudes.

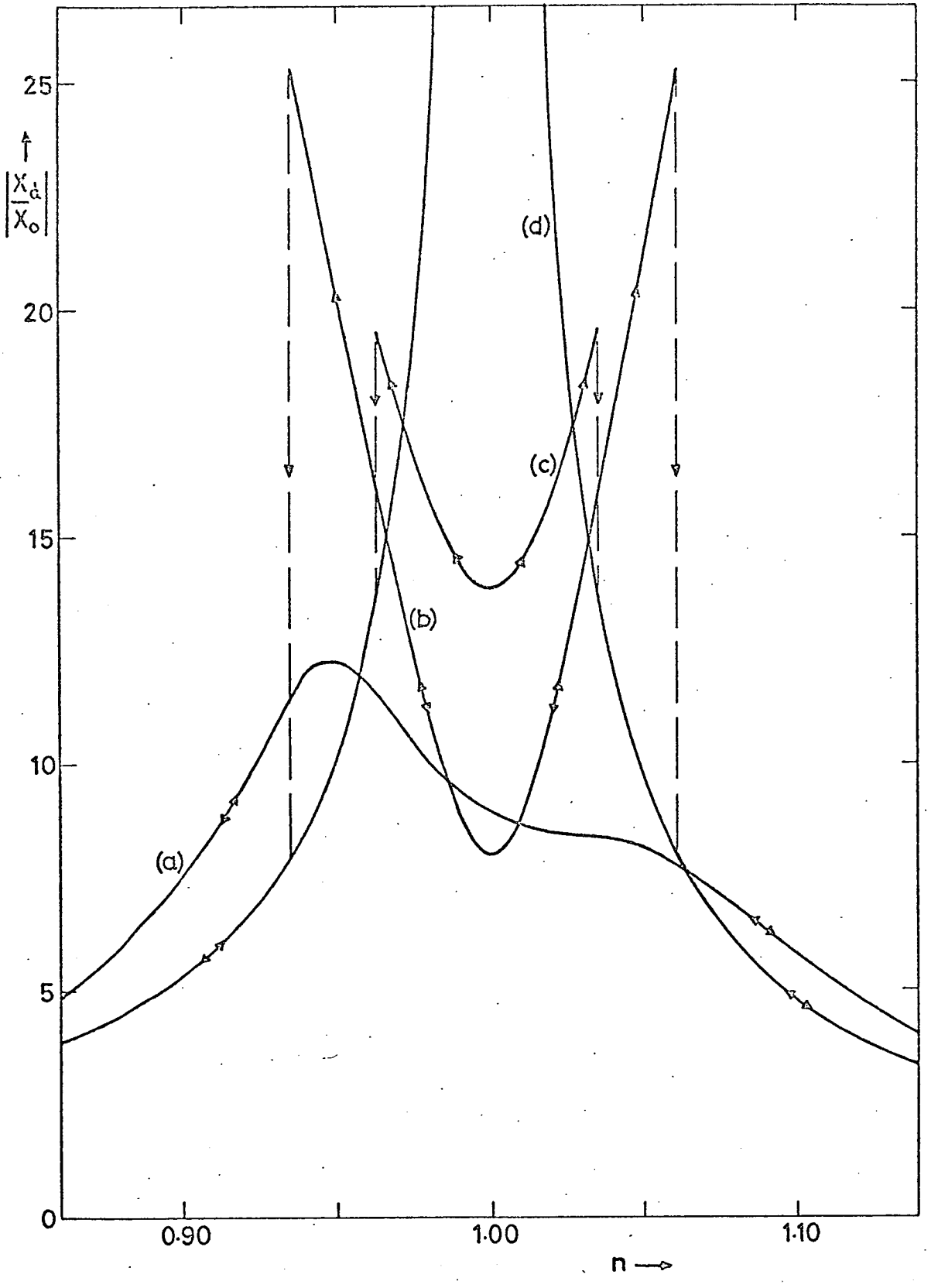

Fig. 3.4.2

Comparison of Main Mass Response Amplitude of a LTDA with that of a Small Length AVA of the same Mass Ratio.

(a) LTDA main mass response,

(b) AVA main mass response, $\epsilon\eta_1 = 0$, $\epsilon\eta_2 = 0.0208$,

(c) AVA main mass response, $\epsilon\eta_1 = 0$, $\epsilon\eta_2 = 0.0360$,

(d) main mass response (absorber locked).

CHAPTER 4

EXPERIMENTAL INVESTIGATION

4.1 Introduction

The theoretical model of Chapter 2 was derived from the experimental apparatus shown in Fig. 4.2.1. This apparatus had been in use for some time to study the phenomenon of autoparametric vibration. During these early experiments it was observed that over a certain frequency range the system exhibited the characteristics of vibration absorption. From this it became apparent that the theoretical model with its nonlinear second order differential equations represented some form of vibration absorber and the idea of the autoparametric vibration absorber was conceived.

After the theoretical solution of the steady-state behaviour of the absorber had been obtained it was necessary to confirm these predictions experimentally. The aim of the experimental investigation described here is to assess the performance of the AVA for various amounts of viscous damping in the X and y motions. The amplitude response curves for the main mass and absorber may then be compared with their theoretical counterparts.

4.2 Experimental Apparatus

A study of the performance of the AVA requires:

1. An appropriate two-degree of freedom spring-mass system with good amplitude response (low damping).
2. A force producing device.
3. Instrumentation to monitor the input to the system and measure its response to such input.

To fulfil the first of these requirements several spring-mass models were tested. The original model is shown in Fig. 4.2.1. It is essentially a two-beam system the two lowest modes of which can be thought of as constituting a two-degree of freedom system.

The main mass system consists of a heavy gauge spring steel beam which deflects in the plane of the figure and is assumed to be effectively rigid in torsion. It supports at its free end a vertical cantilever consisting of a thin spring steel strip carrying an adjustable end mass. This absorber system has its flexible direction normal to that of the beam so that it deflects out of the plane of the figure.

It was found that the most suitable force producing device for this system and subsequent systems was the electromagnetic vibrator. In this case the main beam is excited near to its root by a small Pye-Ling vibrator, type V47.

The response of the main beam is measured by a proximity probe situated near its fixed end. Because the main mass response was the one to which greatest interest was attached at this time, no concerted effort was made to monitor the response of the absorber, although several attempts were made using visual techniques and strain gauge placements at the base of the absorber cantilever.

Although the two beam system exhibited a good amplitude response in that the inherent damping was extremely low, it had several notable disadvantages. The first of these concerned the distribution of the main mass. Clearly the theoretical model of Chapter 2 is based on a concentrated main mass system making it difficult to equate the response of the distributed main mass of the beam system to that of the theoretical model.

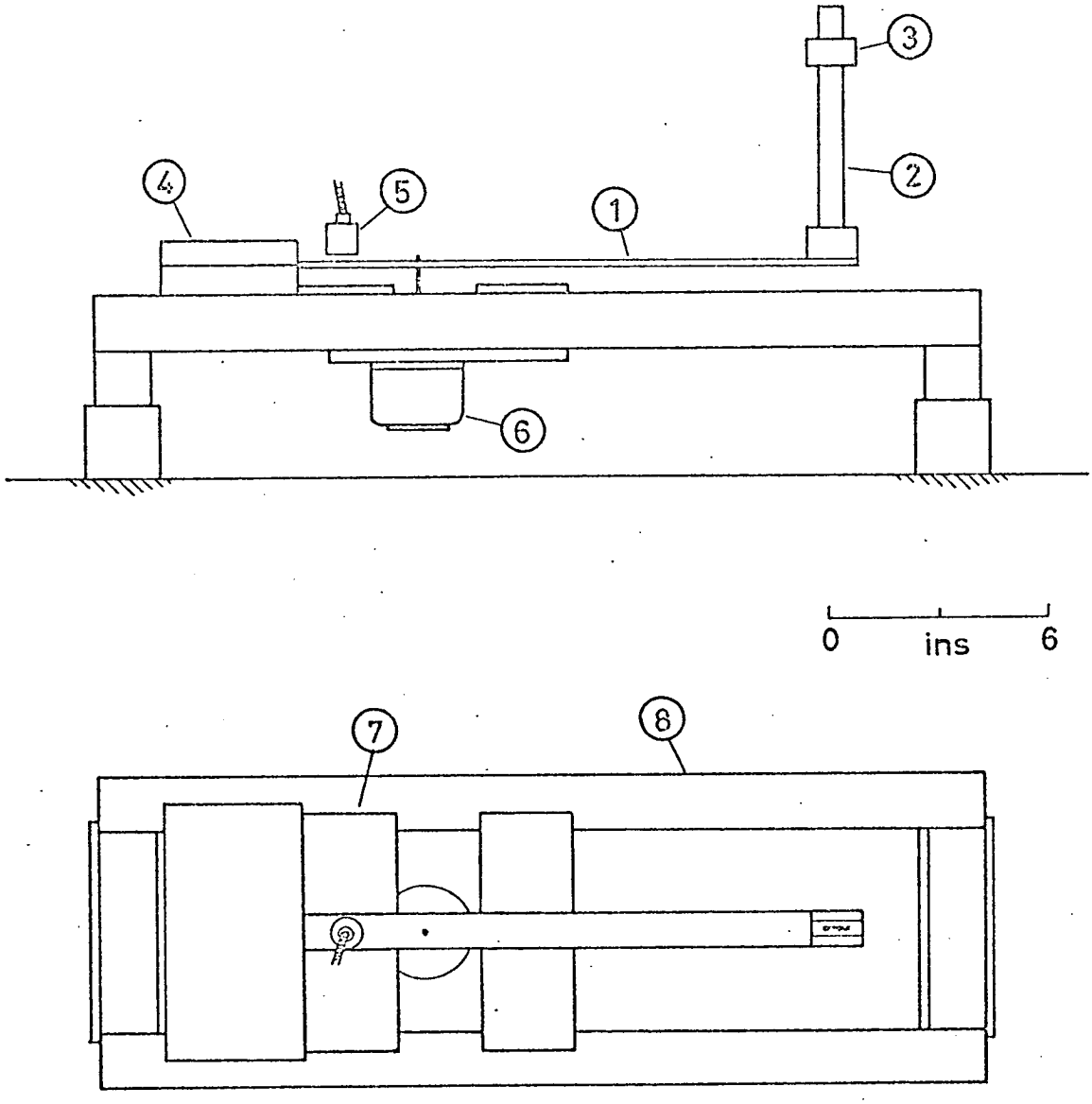

Fig. 4.2.1

Original Experimental Model.

1. main mass, 2. absorber cantilever spring,
2. absorber end mass, 4. main beam clamping block,
5. proximity probe, 6. vibrator,
7. vibrator clamping plates, 8. steel framework.

Further, the response of the main beam was measured near its root (because of amplitude restrictions imposed by the proximity probe) and consequently the response of the tip (where the idealised main mass is assumed to act) had to be assessed assuming a static deflection mode shape for the cantilever. Finally, difficulty was experienced in determining the force input to the system. It was found that the current to the vibrator varied considerably during a response test because of the varying impedance of the system over a given frequency range. Although the vibrator current could be held at a constant level this was no indication that the force input to the system was constant.

These shortcomings in the experimental set-up caused the validity of the experimental findings to be placed in doubt. The only effective way to dispel these doubts was to design a new two-degree of freedom system which more closely approached the theoretical model and which made instrumentation both easier and more effective.

The system which was finally adopted is shown in Figs. 4.2.2 and 4.2.3. Fig. 4.2.2 is a plan and elevation drawing of the essential features while Fig. 4.2.3 shows the model in situ.

The main mass is a solid steel block supported and restrained to horizontal motion by four spring steel legs. A coil spring provides the necessary horizontal stiffness giving a natural frequency of 6.92 Hz. The absorber system consists of a spring steel beam with an adjustable end mass. This system is attached to the main mass by means of a light clamping block. A cantilever beam 0.020 in. thick by 0.75 in. wide giving an absorber of length 7.25 in. was used for most of the investigation (called absorber system 1) although a short length absorber (1.45 in.) was tested (absorber system 2) using a beam 0.005 in. thick by 0.50 in. wide.

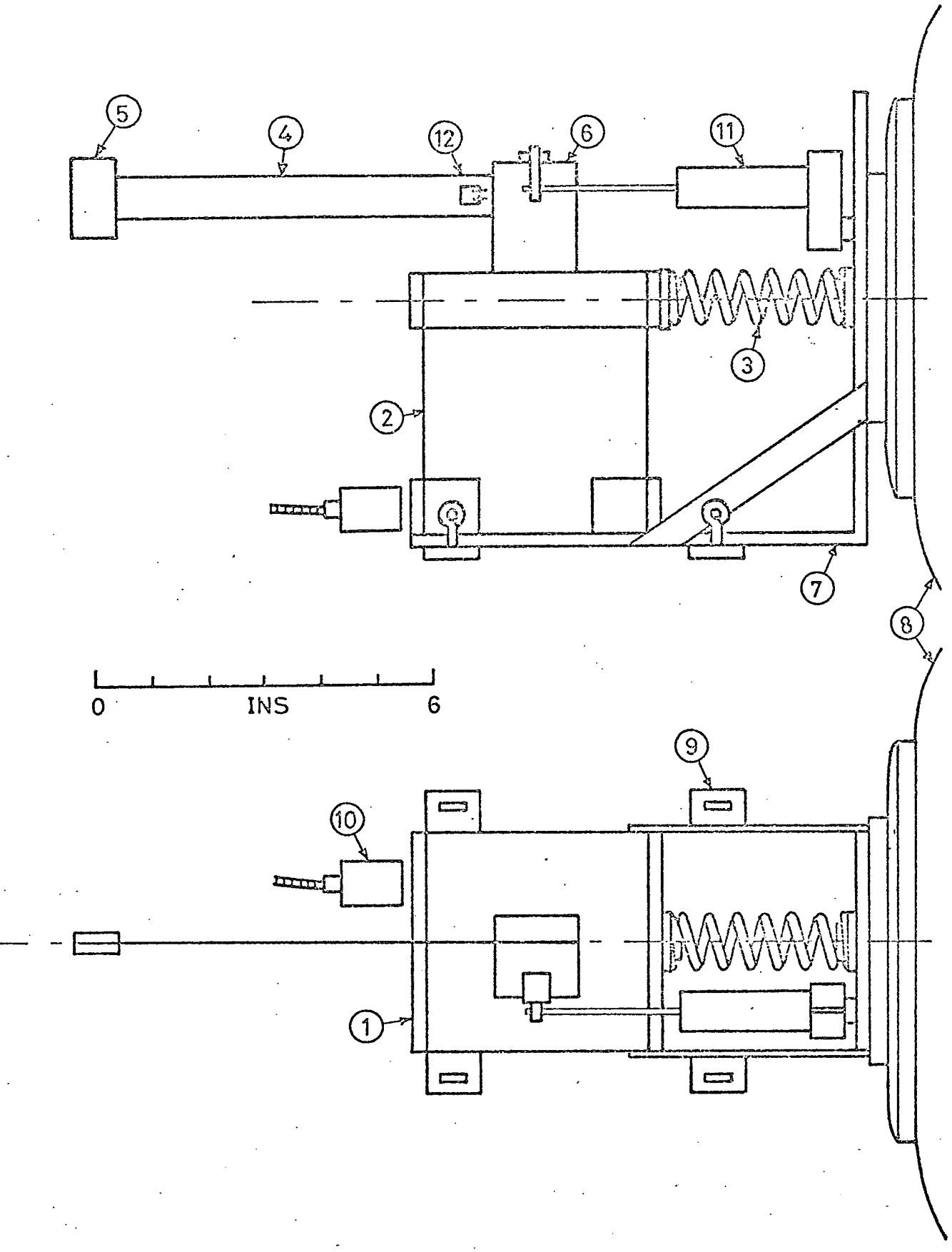

Fig. 4.2.2

Experimental Apparatus.

1. main mass, 2. spring steel legs, 3. coil spring,
4. absorber cantilever spring, 5. absorber end mass,
6. absorber clamping block, 7. angle bracket,
8. vibrator, 9. support points, 10. proximity probe,
11. linear displacement transducer, 12. strain gauges.

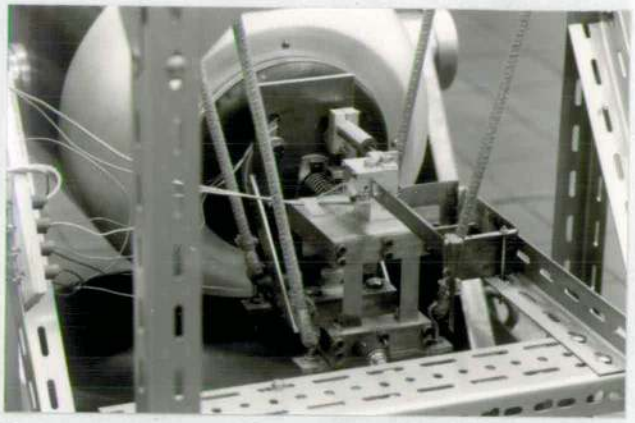

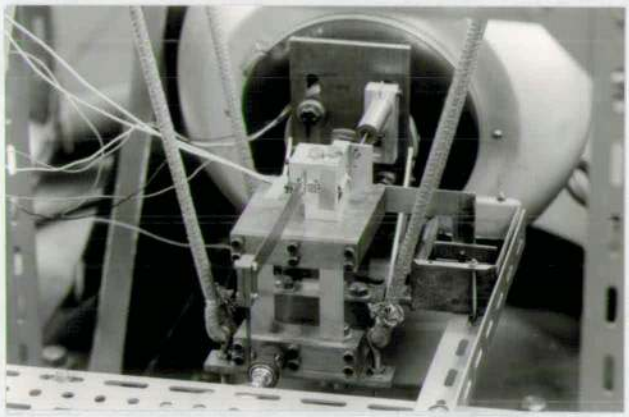

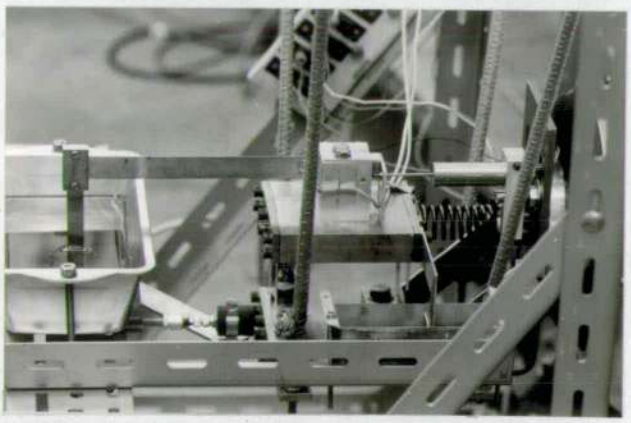

Fig. 4.2.3

Three Views of Experimental Apparatus .

(For the advantages of a short length absorber, see Chapter 3).

The complete system is mounted on an angle bracket which is strapped to the head of a Pye-Ling vibrator, type V1006. To prevent a bending moment on the vibrator head, the deadweight is taken by suspending the whole assembly on elastic ropes connected to four support points on the angle bracket.

Viscous damping is introduced into both main mass and absorber systems by the addition of light vanes operating in oil baths. In this way the damping can be varied by increasing or decreasing the depth to which the vanes are immersed in the oil.

Thus the experimental rig is basically a spring mass system on a moving support (vibrator head). Keeping the amplitude of the support constant ensures a constant exciting force on the system.

With this design the shortcomings of the original system have been eliminated. Now the main mass system has a form which closely resembles the theoretical model and which makes direct amplitude measurement possible. Also, by monitoring the vibrator head amplitude the force input to the system is known.

The basic arrangement of the instrumentation incorporated in the set-up is shown diagrammatically in Fig. 4.2.4 while Fig. 4.2.5 shows the array of equipment in its laboratory setting.

Excitation of the vibrator is through a power amplifier (Pye-Ling PP1/2P) from an accurate Muirhead low frequency decade oscillator (type D-880-A).

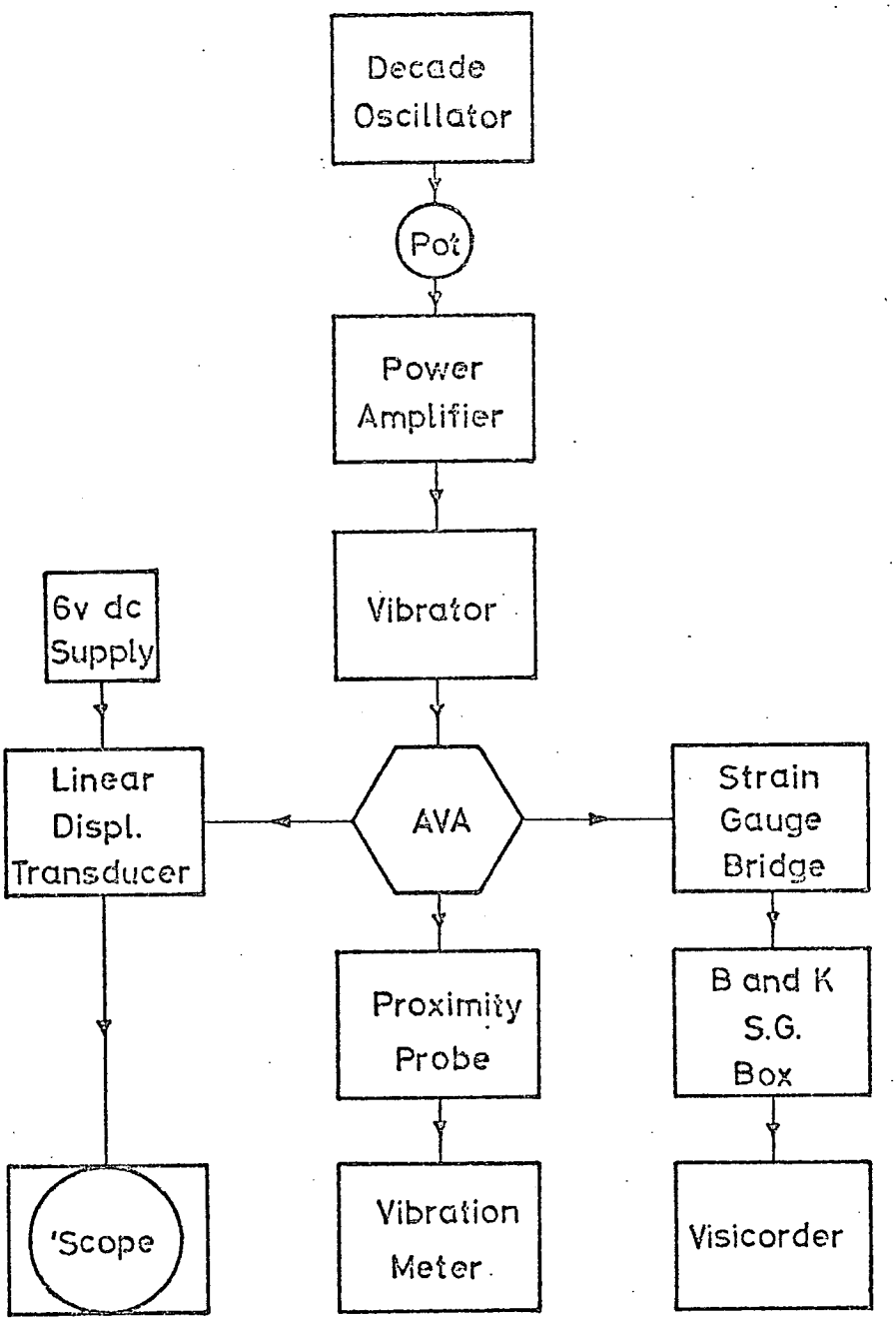

Fig. 4.2.4

Schematic Diagram of Instrumentation.

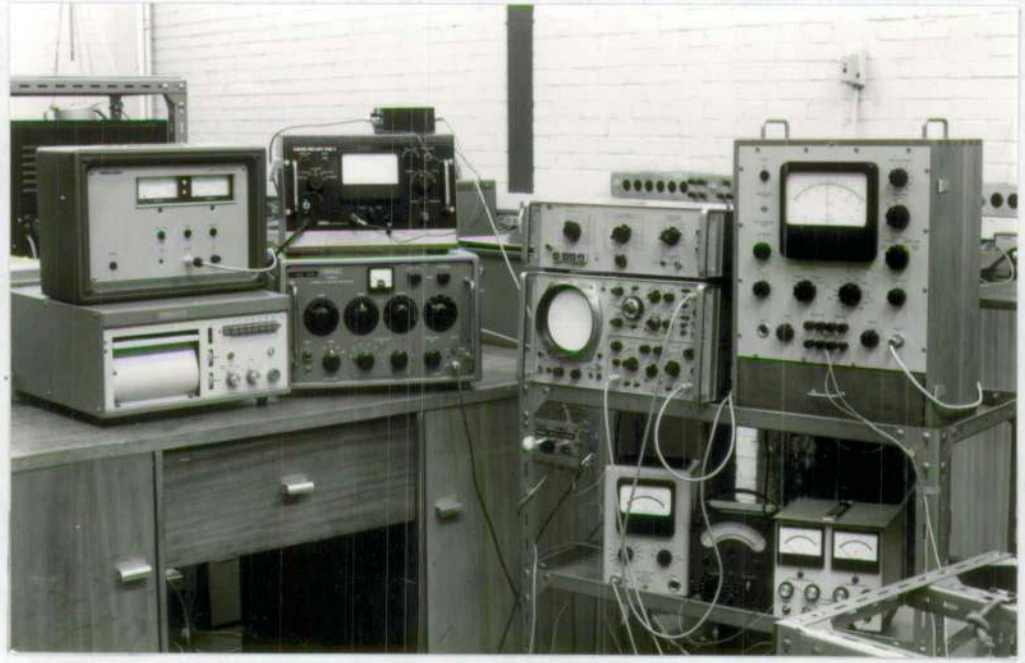

Fig. 4.2.5

Experimental Equipment.

Vibrator field current is stabilised against voltage variations using the Pye-Ling Stab 4 unit which is also interlocked with the vibrator cooling system so that the blower motor operates when the Stab unit is switched on. Potentiometers, in series with the oscillator and amplifier, provide a fine control over the power input to the vibrator.

Vibrator head amplitude is measured by a probe which is brought into proximity with the metallic end-face of the angle bracket. This proximity probe monitors the capacitance so formed and displays it in terms of peak to peak vibration amplitude on the meter of the Wayne Kerr vibration meter B731B.

A Hewlett Packard linear displacement transducer (type 7DCDT-250) measures the displacement of the main mass relative to the vibrator head movement. It is basically a linear variable differential transformer with built-in carrier oscillator and demodulator systems. The coil assembly is fixed to the angle bracket and is energised by a 6 volt d.c. supply. When the core, which is attached to the main mass, is displaced axially within the bore of the coil assembly it produces a voltage change in the output proportional to the displacement.

Because of the slight lowering of the main mass on its legs when performing large vibration amplitudes, adequate clearance between the core and the bore of the coil assembly is essential. The standard core (0.120 in. dia.) supplied with these transducers did not provide enough clearance on the bore diameter of 0.125 in. However it was possible to obtain a core of 0.098 in. dia. which ensured the necessary freedom.

The output from the displacement transducer is displayed on a Hewlett Packard 141A oscilloscope. A particular feature of this 'scope is its variable persistence facility which allowed the measurement of damping rates in the X-mode by the amplitude decay method.

The response of the absorber end mass is monitored using strain gauges placed at the root of the absorber cantilever. Because of the considerable curvature of the beam near its root due to the large deflections of the end mass, it was found desirable to use gauges of small dimensions. Those chosen were Showa foil strain gauges, type SF-1, of gauge length 1.0 mm and width 2.1 mm. Strain gauge terminals were used to protect the fragile lead-out wires of the gauges.

Two active gauges were employed, the bridge circuit being completed by the Brüel and Kjaer strain gauge apparatus, type 1516. This equipment energises the bridge circuit using a 3 kc/s oscillator and monitors the magnitude and sense of the bridge unbalance on a centre zero meter. There is also provision for output to a recording instrument (essential when measuring dynamic strain).

The output from the B and K equipment is in the form of a modulated signal, the carrier frequency being 3 kc/s. This signal was amplified and fed into a Honeywell visicorder, model 2106, (ultraviolet recorder) which provides a permanent record of the magnitude of the dynamic strain at the root of the absorber cantilever from which the amplitude of the end mass is obtained.

4.3 Calibration of Experimental Apparatus

The instrumentation described in the previous section consists of three monitoring systems, two of which require calibration. The three systems may be identified by the quantities which they measure:

System A : Vibrator head amplitude,

System B : Main mass amplitude,

and System C : Absorber end mass amplitude.

System A requires no calibration because only relative measurements of vibrator head amplitude are made. The purpose of this system is to detect any change in the magnitude of the exciting force.

In system B the manufacturers' calibration of the linear displacement transducer was found satisfactory in that the scale factor of 6 volt/in. was linear over $\pm$ full stroke. The vertical sensitivity of the 'scope was adjusted following the procedure outlined in the instruction manual. Thus if the peak to peak amplitude reading on the 'scope is P cm for a sensitivity range of S v/cm then the main mass amplitude is given by (P.S/12)in.

Finally, in System C, the output trace of the ultraviolet recorder is calibrated against direct measurement of the absorber end mass amplitude. A light needle is fixed to the end mass and a smoked glass slide brought up to it until contact is just made. This amplitude measurement is compared with the recorder printout for various steady-state amplitudes of the absorber. The resulting calibration curve was found to be linear over a wide range of amplitude response and so the absorber end mass amplitude is obtained by multiplying the amplitude of the recorder trace by the gradient of this calibration curve.

4.4 Experimental Procedure

At the start of a series of amplitude response tests the absorber is locked (using tape) so that the damping ratio ($\epsilon\zeta_1$) in the X-mode can be measured by the amplitude decay method using the long persistence facility of the oscilloscope. With the absorber still locked a one-degree of freedom test is performed to determine the damped natural frequency and resonant amplitude of the main mass system. Then the absorber is unlocked and tuned as near as possible to half the main mass frequency, after which, the main mass is locked (using clamps) and the y-mode damping ratio ($\epsilon\zeta_2$) measured using the ultraviolet recorder.

Two-degree of freedom amplitude response tests are then performed, each set in a given series having a common damping ratio in the X-mode but differing in the value of the y-mode damping which must be measured before each individual test in the manner described above.

Typical test procedure involves the step-wise increase and decrease of the forcing frequency through the resonance region. At each setting of frequency the vibrator head amplitude is held at a constant predetermined level by means of the potentiometer in the power amplifier output and the steady-state amplitudes of the main mass and absorber systems are recorded.

4.5 Experimental Response Curves

Absorber System 1 : $\epsilon = 0.0005$

As with the theoretical curves, the experimental response curves are plotted in nondimensional form.

Each graph is a plot of (X_d/X_o) and (y_d/X_o) against the forced frequency ratio, n. Interpretation of these experimental curves follows the same pattern as outlined for the theoretical case.

The first series of tests is shown by Figs. 4.5.1 to 4.5.4. In each case the damping ratio in the X-mode is $\epsilon\gamma_1 = 0.0035$ while the y-mode damping ratios $(\epsilon\gamma_2)$ are 0.0017, 0.0035, 0.0110 and 0.0184, respectively.

Figs. 4.5.5 to 4.5.7 present a second series of tests for an X-mode damping ratio of 0.0116 and y-mode damping ratios of 0.0016, 0.0050 and 0.0116, respectively.

In each graph the curves are labelled (1), (2) and (3). Curves (1) are the amplitude responses of the main mass under absorber action. Curves (2) are the corresponding response curves for the absorber system. Finally, curves (3) (shown by broken line) are the system responses with the absorber locked $((y_d/X_o) = 0)$. These are only shown in selected graphs.

Absorber System 2 : $\epsilon = 0.0025$

Fig. 4.5.8 shows a typical main mass response (1) under the action of the short length cantilever absorber for an X-mode damping ratio of 0.0030. Unfortunately the absorber response was unobtainable due to the extreme deflections of the end mass relative to the absorber's length. In fact the end mass doubled back on itself with the end slope of the beam approaching 180^o.

In keeping with the labelling convention, curve (3) is the main mass response with the absorber locked.

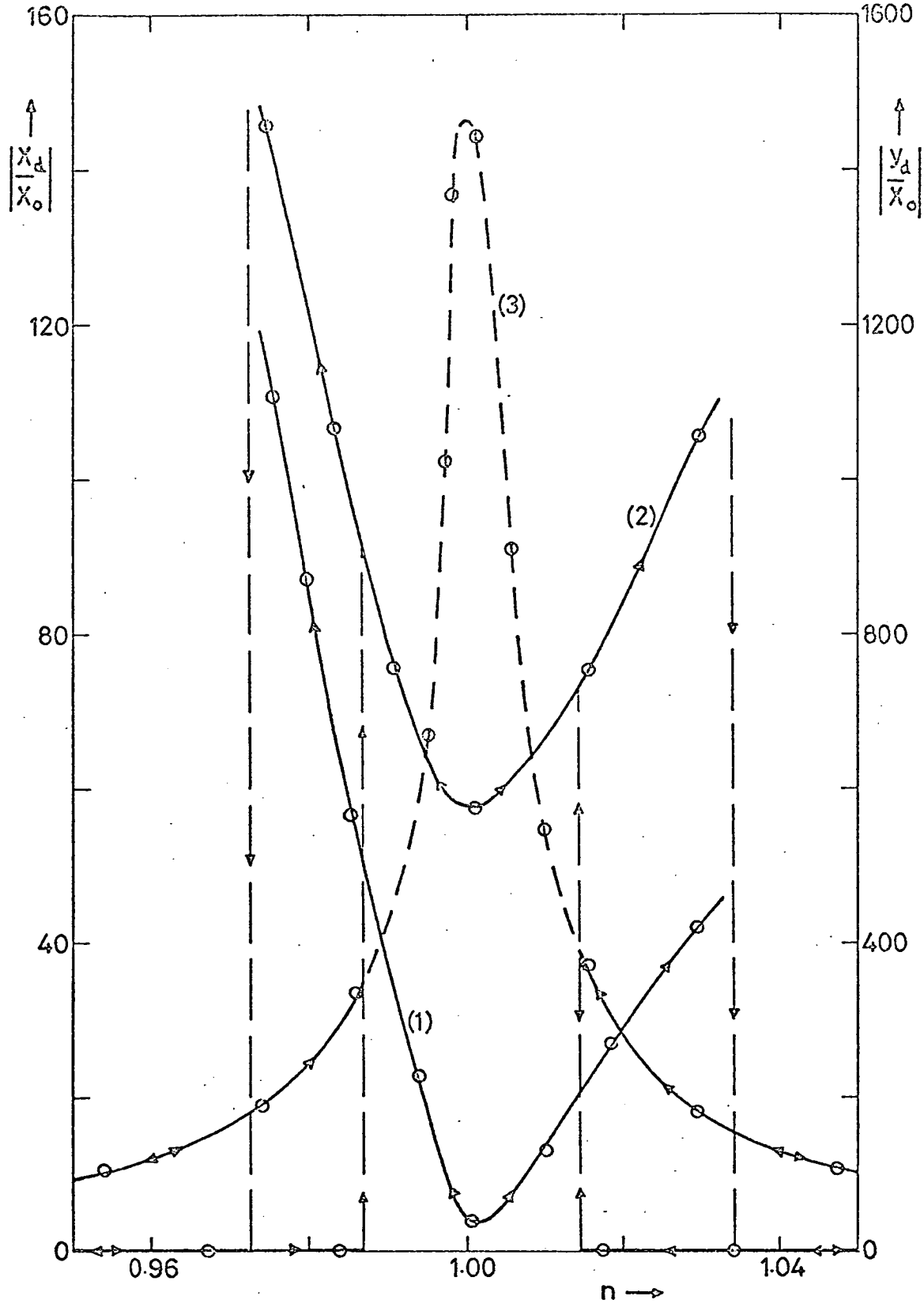

Fig. 4.5.1

Experimental Amplitude Response Curves
for $\epsilon\eta_1 = 0.0035$, $\epsilon\eta_2 = 0.0017$.

(1) main mass response,

(2) absorber response,

(3) main mass response (absorber locked).

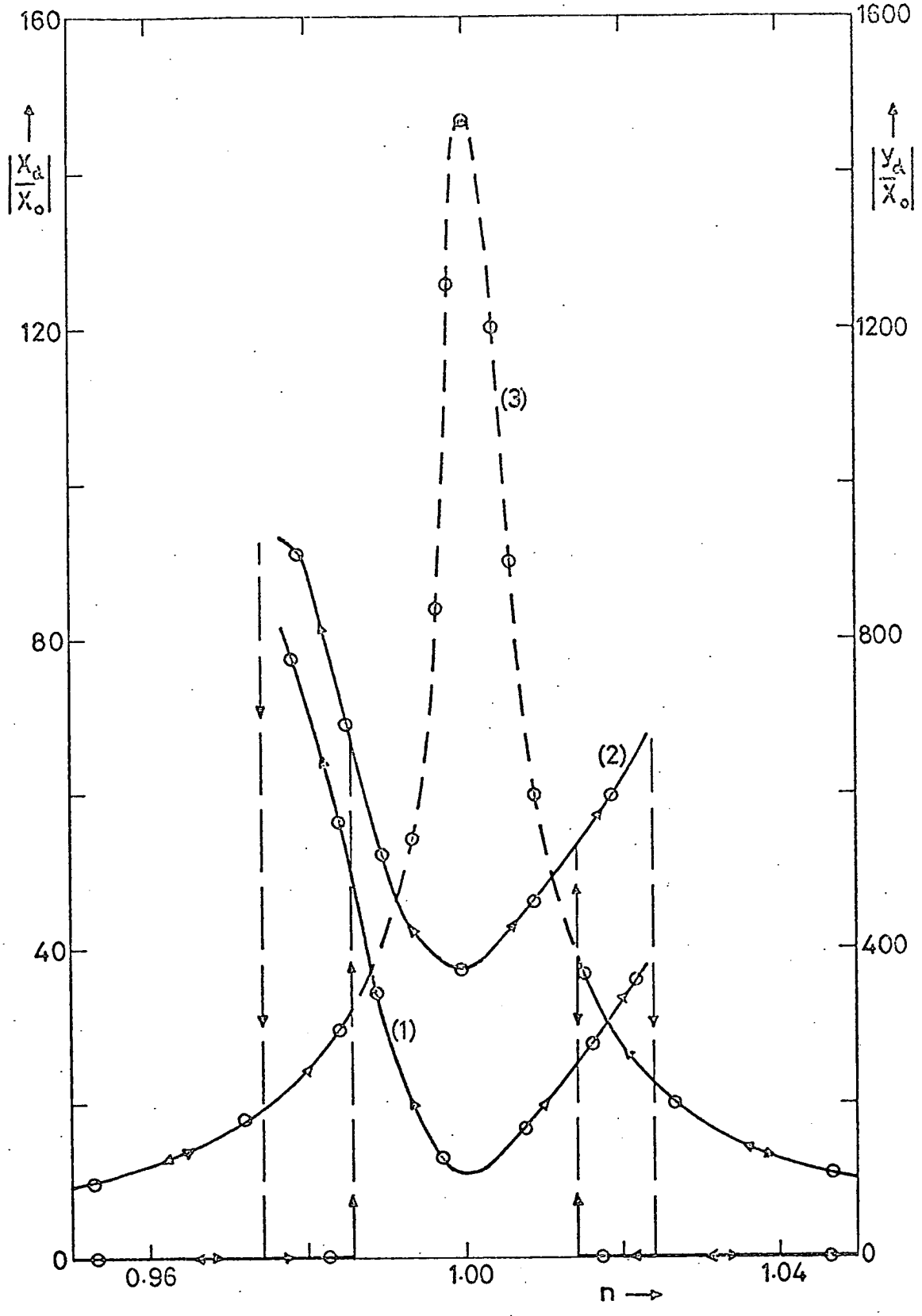

Fig. 4.5.2

Experimental Amplitude Response Curves

for $\epsilon\eta_1 = 0.0035$, $\epsilon\eta_2 = 0.0035$.

(1) main mass response,

(2) absorber response,

(3) main mass response (absorber locked).

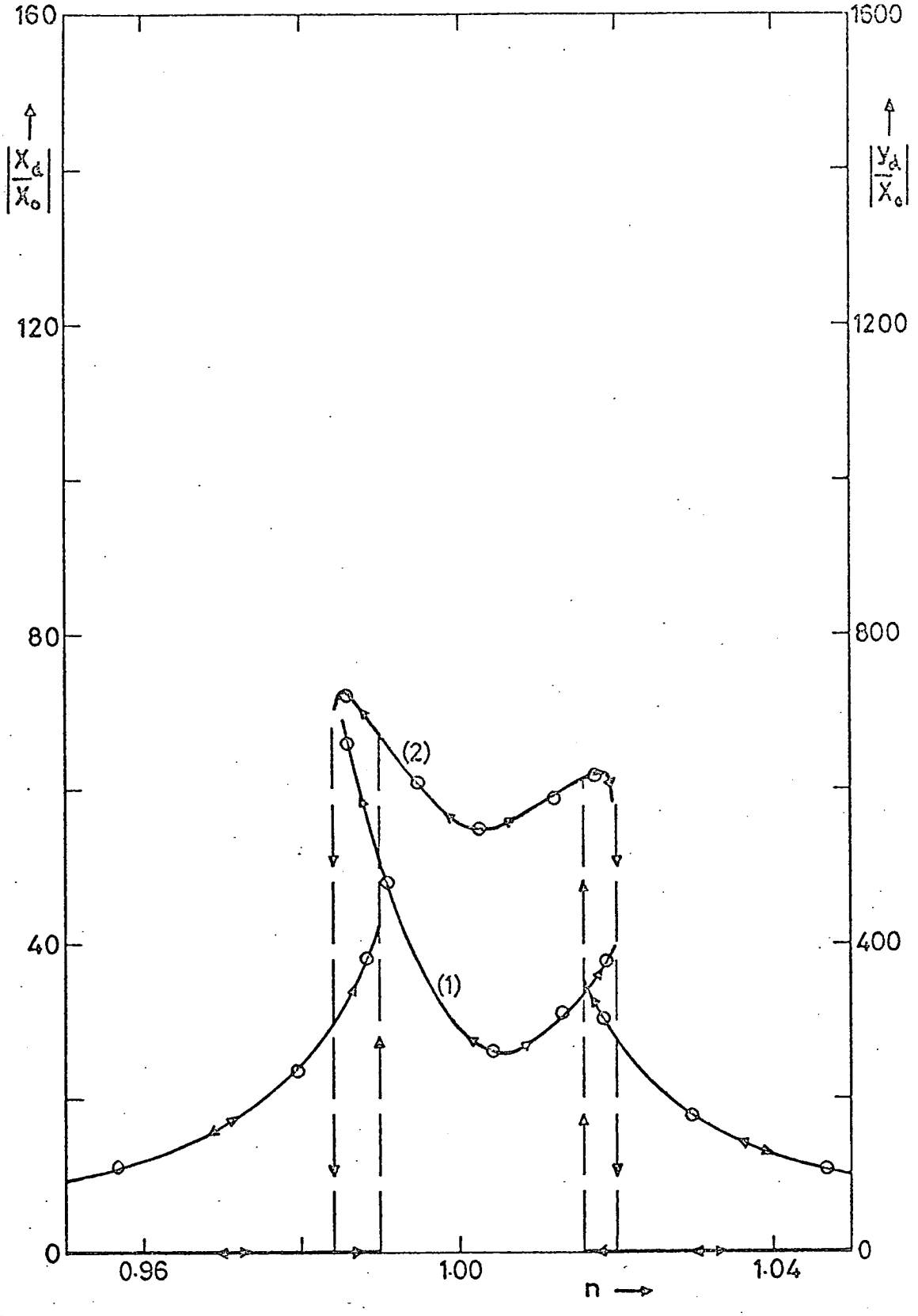

Fig. 4.5.3

Experimental Amplitude Response Curves for $\epsilon\eta_1 = 0.0035$, $\epsilon\eta_2 = 0.0110$.

(1) main mass response,

(2) absorber response.

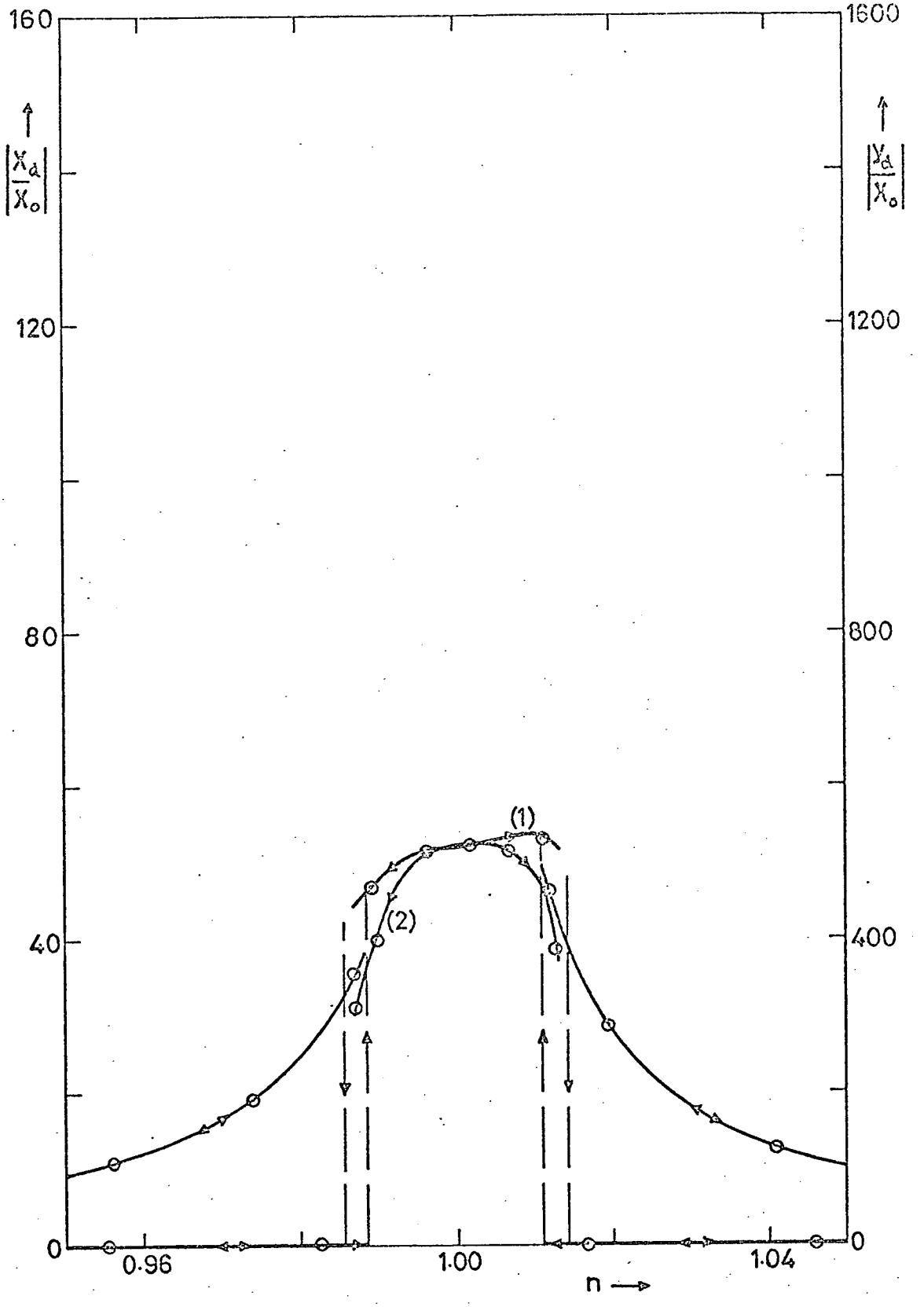

Fig. 4.5.4

Experimental Amplitude Response Curves

for $\epsilon\eta_1 = 0.0035$, $\epsilon\eta_2 = 0.0184$.

(1) main mass response,

(2) absorber response.

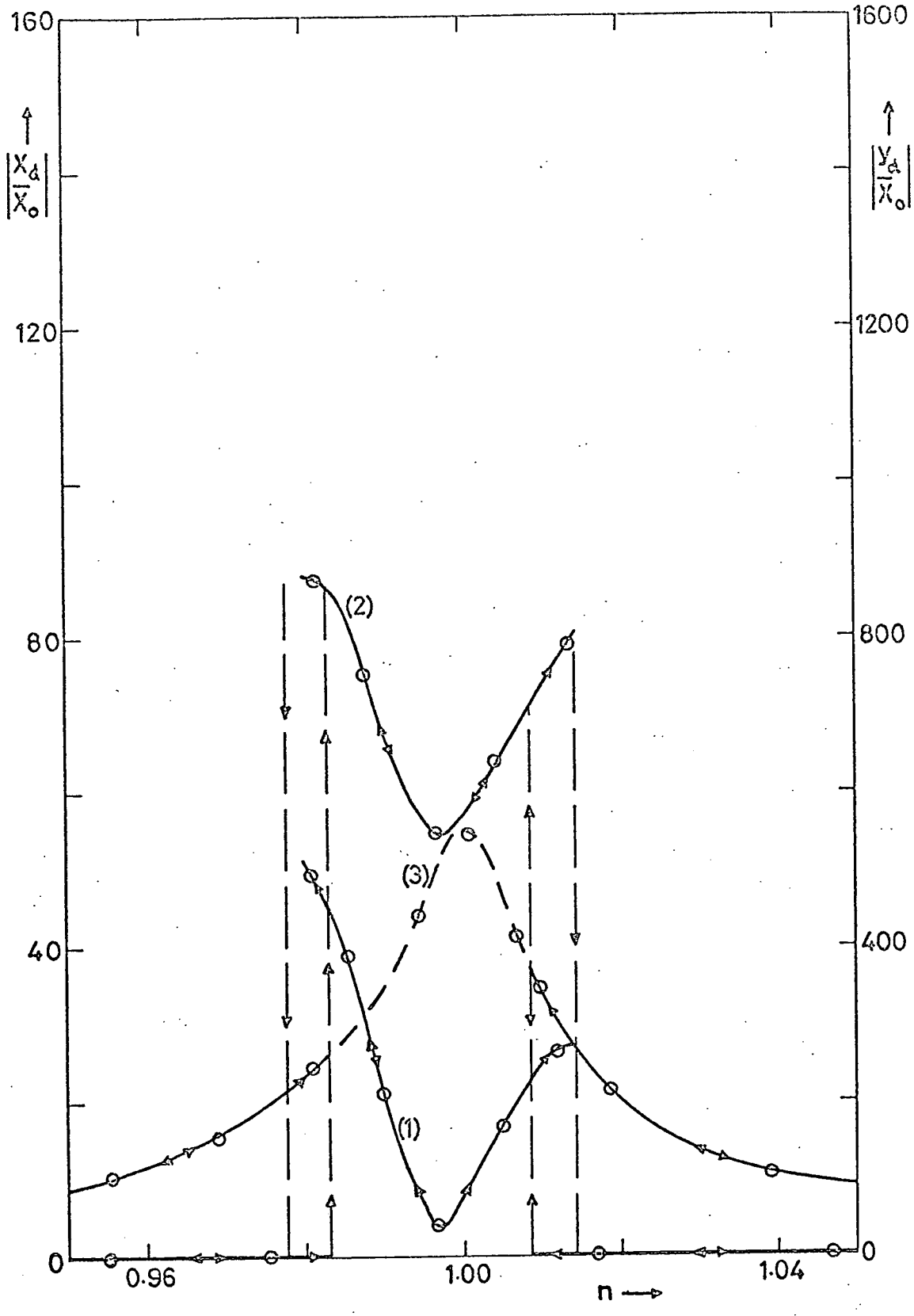

Fig. 4.5.5

Experimental Amplitude Response Curves for $\epsilon\eta_1 = 0.0116$, $\epsilon\eta_2 = 0.0016$.

(1) main mass response,

(2) absorber response,

(3) main mass response (absorber locked).

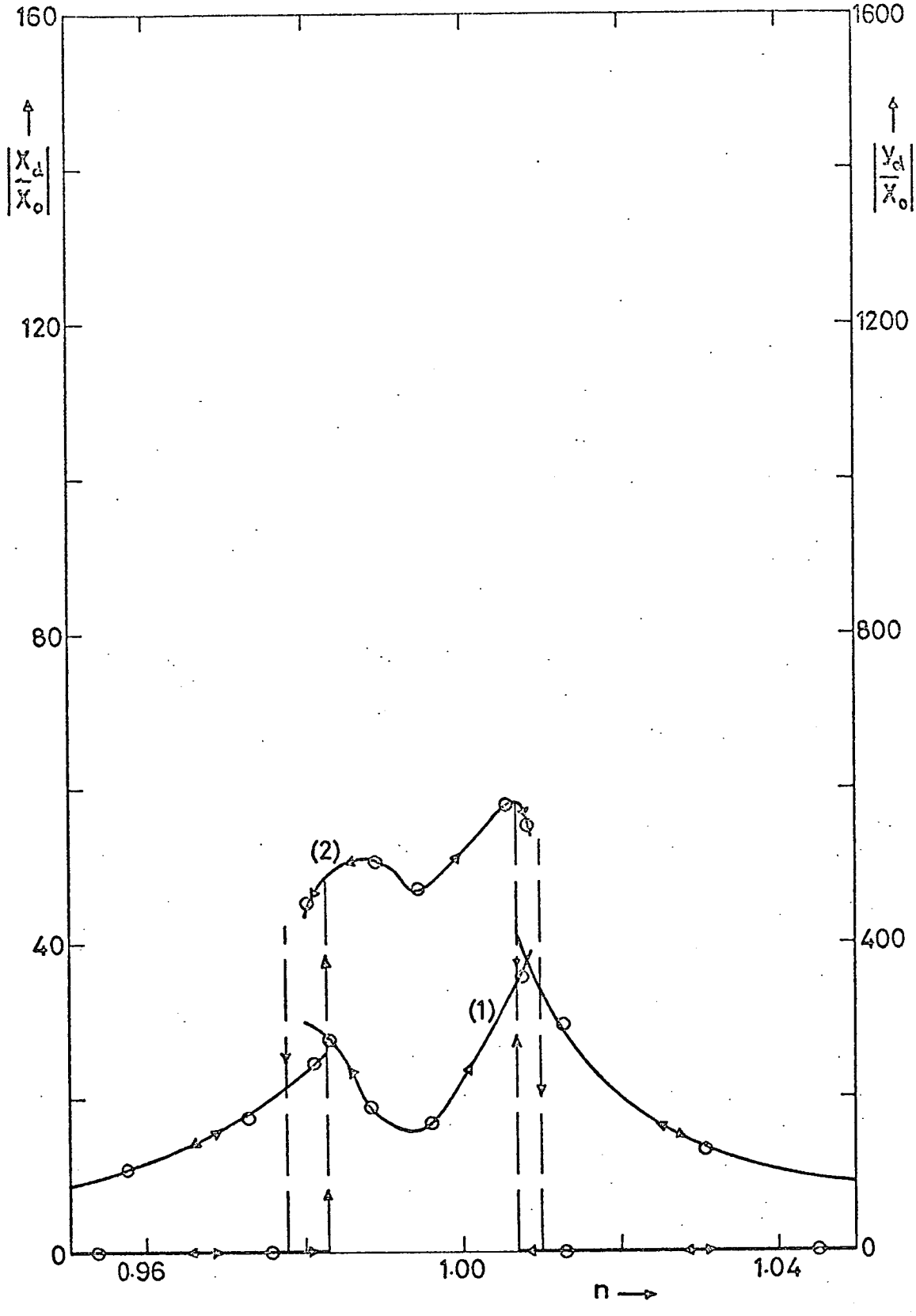

Fig. 4.5.6

Experimental Amplitude Response Curves for $\epsilon\eta_1 = 0.0116$, $\epsilon\eta_2 = 0.0050$.

(1) main mass response,

(2) absorber response.

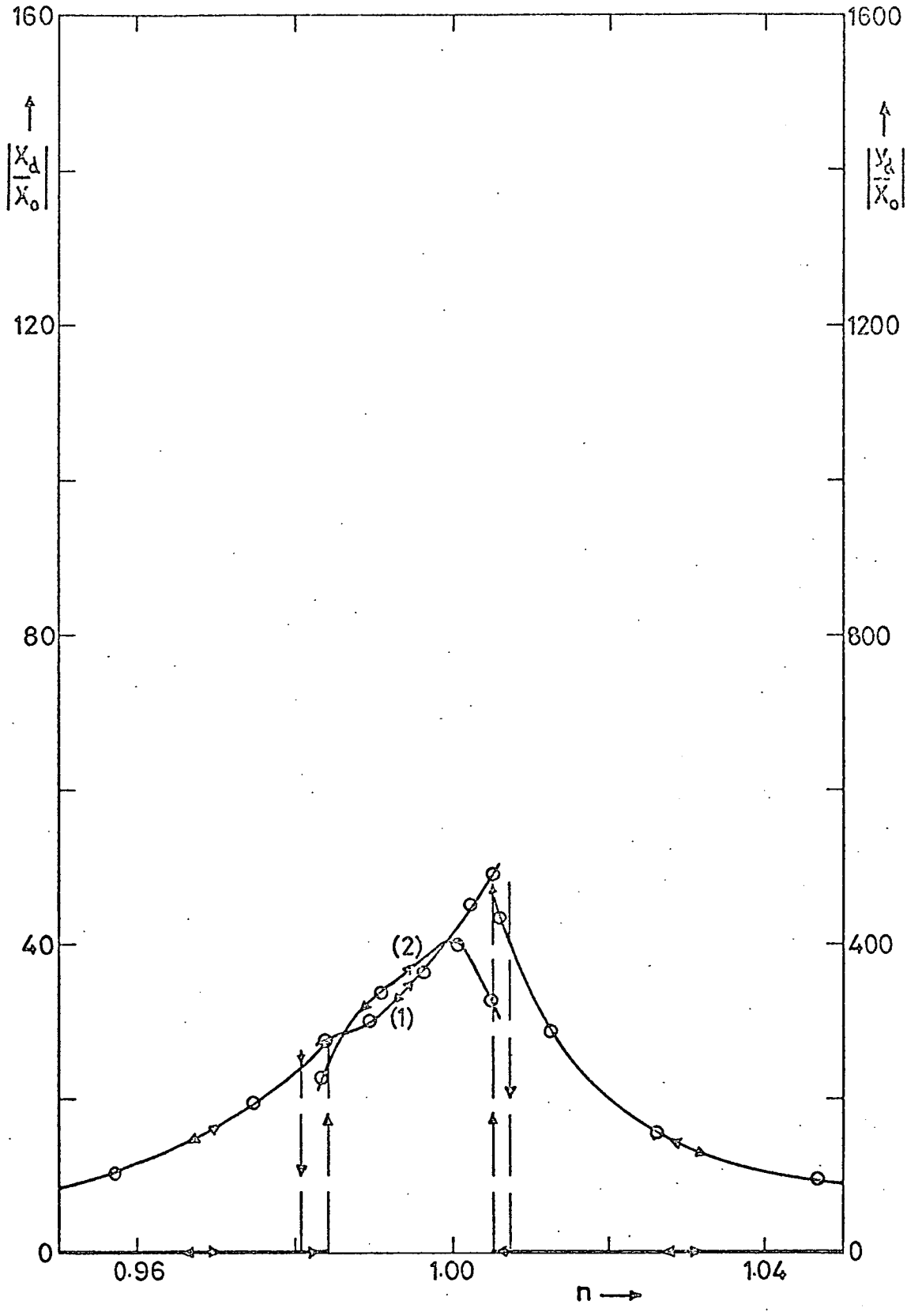

Fig. 4.5.7

Experimental Amplitude Response Curves for $\epsilon\eta_1 = 0.0116$, $\epsilon\eta_2 = 0.0116$.

(1) main mass response,

(2) absorber response.

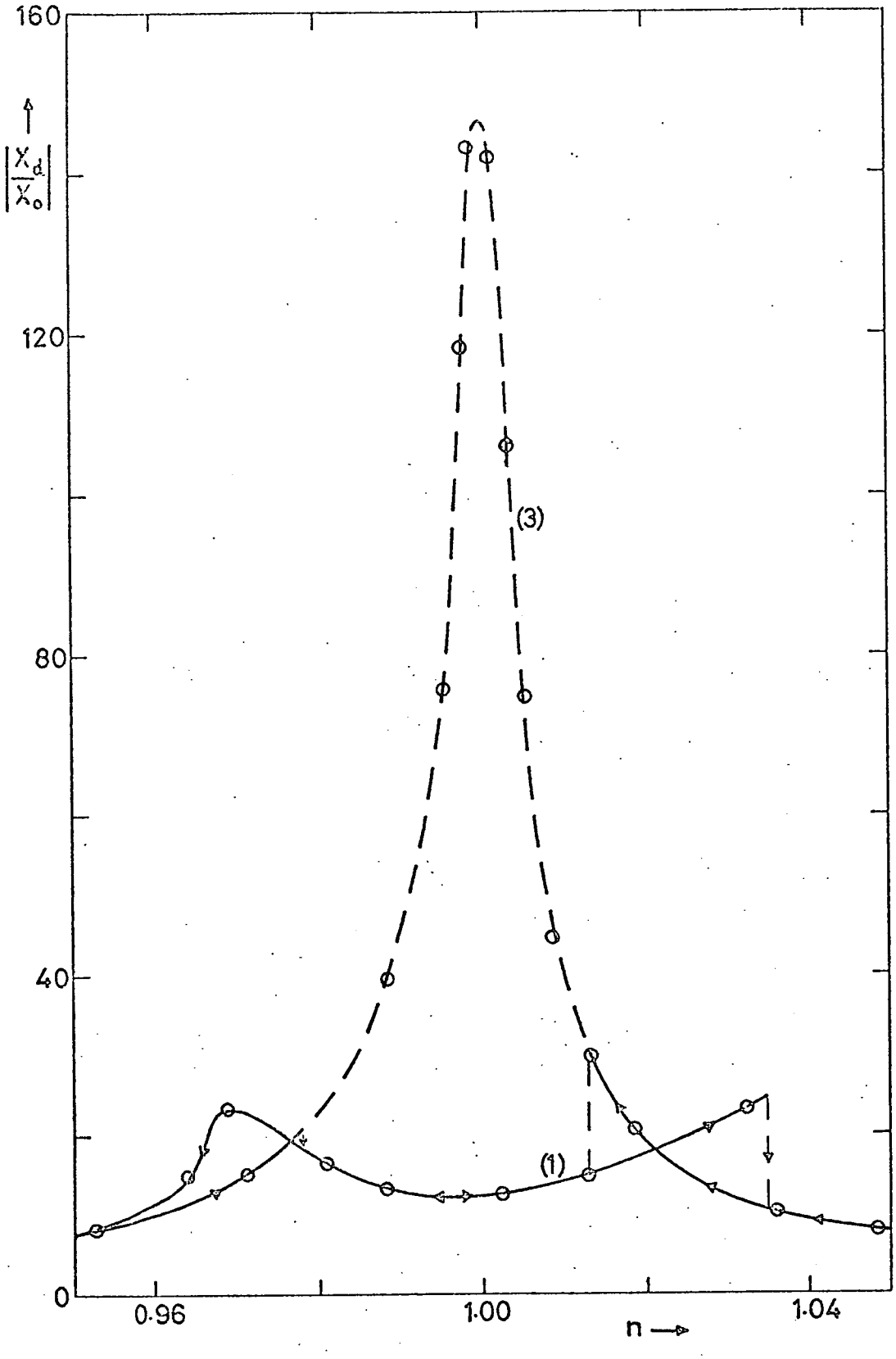

Fig. 4.5.8

Experimental Main Mass Response Amplitude under the Action of Small Length AVA.

(1) ϵ_{η_1} = 0.0030,

(2) ϵ_{η_1} = 0.0030 (absorber locked).

CHAPTER 5

DISCUSSION OF RESULTS

5.1 Comments on the Theoretical Response Curves

The theoretical amplitude response curves of the AVA are presented in Chapter 3. For the most part these curves represent the steady-state response of a perfectly tuned AVA with an ϵ value of 0.0005. The effects of detuning are clearly demonstrated and a comparison is made between the response curves of the perfectly tuned absorber and those of a slightly detuned absorber. This is followed by a brief theoretical comparison of the performance of a short length AVA with that of a linear tuned and damped absorber of the same mass ratio. In this present section a few additional comments are made on the theoretical findings of Chapter 3.

From a study of Figs. 3.2.7 and 3.2.8 it is evident that for low values of the y-mode damping ratio, $\epsilon\eta_2$, (the X-mode damping ratio, $\epsilon\eta_1$, is constant) the absorber action greatly reduces the main mass amplitude in the resonance region and that the steady-state response of both the main mass and absorber systems is characterised by a deep U-shaped trough. However, at these low $\epsilon\eta_2$ values the absorber action also produces very large collapse amplitudes in the main mass response which are obviously undesirable. These can virtually be eliminated by increasing the value of $\epsilon\eta_2$ but this results in decreased absorber efficiency through the resonance region (in the neighbourhood of $n = 1.0$). Although it was shown in Chapter 3 that there exists a value of $\epsilon\eta_2$ (for a given $\epsilon\eta_1$) which produces a minimum value of the collapse amplitude this is not necessarily the best choice of damping parameter because the efficiency of the absorber must be assessed over the complete frequency range.

Clearly a compromise must be reached between the acceptable limits of the collapse amplitude of the main mass and its amplitude at n = 1.0. The difficulty in choosing optimum damping conditions for the AVA is highlighted by the comparison made between the performance of the AVA and that of the LTDA (see Fig. 3.4.2). In this case, however, the difficulty is aggravated by the upper limit placed on the value of ϵ (0.0025) which was based on the best value obtainable in practice with a cantilever absorber system.

5.2 Comments on the Experimental Response Curves

Chapter 4 presents a selection of experimental amplitude response curves for a cantilever absorber system with an ϵ value of 0.0005. In the first series of tests (Figs. 4.5.1 to 4.5.4) the X-mode damping ratio has the constant value of 0.0035 while the y-mode damping ratio is allowed to vary. Although the effect of viscous damping was not considered in Chapter 2 when discussing the causes of detuning in the experimental system, it is obvious that increasing the y-damping ratio reduces the value of the first resonant frequency of the absorber system and results in the detuning of the AVA. Further, because of the nature of the experimental damping system, an increase in y-damping causes an increase in the value of the absorber end mass, m, due to the entrained mass effect of the oil in which the vane operates, with the result that the frequency of the absorber system is lowered and the AVA detuned. Consequently, for each change in y-damping an attempt was made to ensure the best possible tuning, with the minimum amplitude of the main mass system occurring at n = 1.0, by making slight adjustments to the active length of the cantilever beam.

It is noted, however, that no matter how good the tuning, the curves of this first series of tests still exhibit considerable asymmetry. This feature of the experimental curves will be discussed later.

A second series of tests (Figs. 4.5.5 to 4.5.7) were performed for $\epsilon\eta_1 = 0.0116$ to demonstrate the amplitude reducing effect of increased X-damping on the steady-state response of the main mass and absorber. This series also shows the effect of y-damping on the tuning of the absorber because no attempt was made to retune the absorber after a change in y-damping. As expected the curves move bodily to the left when the y-damping ratio is increased.

For both series of tests the behaviour of the system and the trends exhibited by the response curves under increasing y-damping are similar to those described in the previous section for the theoretical response curves.

Experiments conducted with a short length cantilever absorber of ϵ value 0.0025 demonstrate the improved performance of such an AVA. A typical test result is given in Fig. 4.5.8. The reduction in cantilever length increases the ratio of axial to lateral movement of the absorber end mass thereby enhancing the absorbing power of the AVA. The theoretical comparison between the AVA and the LTDA is based on the performance of an AVA having this particular ϵ value.

5.3 Comparison of Theoretical and Experimental Response Curves

Direct comparison between the theoretical and experimental response curves can be made using Figs. 3.2.2 and 4.5.2 for

$\epsilon\eta_1 = 0.0035$, $\epsilon\eta_2 = 0.0035$; Figs. 3.2.4 and 4.5.3 for

$\epsilon\eta_1 = 0.0035$, $\epsilon\eta_2 = 0.0110$; and Figs. 3.2.5 and 4.5.4 for

$\epsilon\eta_1 = 0.0035$, $\epsilon\eta_2 \doteq 0.0186$.

The experimental curves used in this comparison are taken from the first series of tests in which every effort was made to tune the absorber precisely to the condition $\omega_1 = 2\omega_2$, however they lack the symmetry displayed by the theoretical curves about the n = 1.0 axis. This asymmetry is partly attributable to the detuned condition of the experimental absorber system and consequently the detuning characteristics illustrated by the theoretical curves of Figs. 3.3.1 and 3.3.2 must be borne in mind when assessing the merits of this visual comparison. But obviously there must be other factors which contribute to this asymmetry of the experimental results. The theoretical analysis does not take into account, for example, the inherent nonlinearity in the spring force of the absorber cantilever which, with the relatively large amplitudes involved, is quite significant.

Judging by the overall form of the response curves the comparison is seen to be quite reasonable although the experimental amplitudes of the main mass are, in general, greater than those predicted theoretically. The theoretical analysis predicts the degeneration of the AVA response under the action of increasing viscous damping, a trend which is clearly exhibited by the experimental response curves.

More specifically, the experimental curves exhibit such features as entry frequencies (bounds of zero b_2 stability),

jumps in the main mass response on the entry of absorber action, collapse amplitudes, etc., all of which are mirrored in the theoretical response curves. It can be concluded, therefore, that the theoretical response curves of the AVA's steady-state behaviour, derived from the first order theory of Chapter 2, compare favourably with known experimental data.

5.4 Discussion of the Theoretical Analysis

A first order approximation to the steady-state behaviour of the AVA has been obtained using three different techniques. For reasons already stated the asymptotic method presented in Chapter 2 is preferred to the averaging method and the two-variable expansion procedure described in Appendix III.

In each case the equations of motion (2.3.1) are written in what is known as the standard form (2.4.1) in which right-hand side is proportional to a small parameter (ϵ) of the system. As mentioned in Chapter 2, this reduction of the equations to the standard form permits the study of the solution close to external resonance because of the association of the forcing term with the small parameter. The alternative would be the 'hard' forcing case where the equations of motion are written as

$$\ddot{X} + 4\Omega^2 X = \epsilon[\epsilon^{-1}(4\Omega^2 - \omega_1^2)X - 2\eta_1\omega_1\dot{X} + R(\dot{y}^2 + y\ddot{y})] + \omega_1^2\cos 2\Omega t$$

$$\ddot{y} + \Omega^2 y = \epsilon[\epsilon^{-1}(\Omega^2 - \omega_2^2)y - 2\eta_2\omega_2\dot{y} + \ddot{X}y - \epsilon y(\dot{y}^2 + y\ddot{y})]$$

and the solution taken in the form

$$X = A(t)\cos[\omega_1 t + \phi(t)] + \frac{\omega_1^2}{\omega_1^2 - 4\Omega^2}\cos 2\Omega t + \epsilon X_1(t) + \ldots$$

$$y = B(t)\cos[\omega_2 t + \theta(t)] + \epsilon y_1(t) + \ldots \qquad 5.4.1$$

Applying the asymptotic method leads to the following set of first order variational equations

$$-A\dot{\phi} = (\epsilon/2\omega_2)\left[2\epsilon^{-1}(\Omega^2 - \omega_2^2)A - \tfrac{1}{2}RB^2\omega_2^2\cos(2\theta - \phi) - \frac{4\eta_1\Omega\omega_2^3}{\omega_2^2 - \Omega^2}\sin\phi\right]$$

$$-\dot{A} = (\epsilon/2\omega_2)\left[4\eta_1\omega_2^2 A + \tfrac{1}{2}RB^2\omega_2^2\sin(2\theta - \phi) + \frac{4\eta_1\Omega\omega_2^3}{\omega_2^2 - \Omega^2}\cos\phi\right]$$

$$-B\dot{\theta} = (\epsilon/2\omega_2)\left[\epsilon^{-1}(\Omega^2 - \omega_2^2)B - 2AB\omega_2^2\cos(2\theta - \phi) - \frac{2\Omega^2\omega_2^2}{\omega_2^2 - \Omega^2}B\cos 2\theta\right]$$

and

$$-\dot{B} = (\epsilon/2\omega_2)\left[2\eta_2\omega_2^2 B - 2AB\omega_2^2\sin(2\theta - \phi) - \frac{2\Omega^2\omega_2^2}{\omega_2^2 - \Omega^2}B\sin 2\theta\right]$$

... 5.4.2

where equations 5.4.2 are formulated assuming the exact internal resonance condition, $\omega_1 = 2\omega_2$, and the external resonance condition, $\Omega = \omega_2 + 0(\epsilon)$.

From the form of 5.4.1 the solution is seen to consist of a forced and 'natural' response superimposed as though the system were linear. Both portions of the response exist when the forcing frequency 2Ω is well away from the natural frequency ω_1. However, it is noted that as the forcing frequency approaches ω_1, the natural response becomes entrained by the forced response. In fact, as pointed out by Struble in his book 'Nonlinear Differential Equations', when discussing hard forcing of the van der Pol equation, the rapidity with which the natural response portion fades out is increased by

(a) increases in the hardness of the forcing function,

and (b) decreases in the separation of the natural and impressed frequencies.

It can be concluded, then, that the soft forcing case is to be preferred when considering the nature of the solution in the neighbourhood of external resonance.

In Chapter 2 the asymptotic method was used to obtain the variational equations of the second order of approximation, however, as results have shown, there seems little to be gained (in this particular problem at least) by working to an order of ϵ greater than unity. The variational equations of the first order of approximation give an adequate representation of the steady-state performance of the AVA.

The comparison of the theoretical and experimental steady-state amplitude response curves, discussed in section 5.3, not only shows the merits of the first order theory but serves to highlight the advantages which the more general detuning theory has over the rather restrictive theory of the perfectly tuned absorber. Although the exact internal resonance case provides many of the essential features of the steady-state behaviour, it requires a detuning theory to predict the asymmetry exhibited by the experimental curves which is characterised by such features as jumps in the main mass response on the entry of absorber action and collapse amplitude differences on either side of the $n = 1.0$ axis.

A study of the transient behaviour of the AVA was made in Appendix I, but unfortunately, difficulty was found in formulating a plausible theoretical solution. The analysis of the transient solution of an autonomous system is a relatively simple matter. Struble and Heinbockel, for example, were able to analyse the transient behaviour of a beam-pendulum system. However the AVA is a nonautonomous system which does not yield easily to analysis.

The results of a computer simulation of the AVA equations of motion suggest that a rather sophisticated theoretical analysis is required to reproduce anything resembling the actual transient response of the system.

While investigating the validity of the transient solution derived in Appendix I, it was thought necessary to check the transient response properties of the first order variational equations. A computer simulation verified that the transient response of these equations was similar to that of the full equations of motion derived from the theoretical model. Although this result did not improve the standing of the theoretical transient solution it at least served to strengthen the opinion that the first order variational equations are a good representation of the AVA's response.

5.5 Comments on the Experimental Investigation

The aim of the experimental investigation described in Chapter 4 was to provide a quick and reliable means of assessing the merits of the theoretical steady-state analysis. However, a more extensive experimental investigation would have been interesting. For example, to supplement the theoretical comparison between the AVA and the linear tuned and damped absorber, it would have been interesting to perform an experimental comparison of these two absorbers, both for deterministic and stochastic excitation of the main mass system. Future experimental work might also include a study of the performance of the combined AVA-LTDA system discussed in Appendix II (System 3).

The response of the AVA to random excitation of the main mass is discussed in Appendix IV.

The experimental measurements of the response spectral densities of the main mass with and without absorber action, demonstrate the AVA's ability to reduce the power density level. However, such a brief look at such a vast topic leaves many questions unanswered. The experimental and theoretical study of the performance of the AVA, (and similar systems) under stochastic excitation would seem to be a fruitful area for future research.

5.6 Future Areas of Study

Apart from the study of the AVA's performance under stochastic excitation there are several other areas of study which stem from the present research. One such area of interest concerns the design of the AVA itself.

Because of the unfavourable comparison between the AVA and the linear tuned and damped absorber (unfavourable to the former) it was decided to design a more efficient AVA system. The results of this work are detailed in Appendix II. However a more rigorous study of these alternative systems is required with a view to obtaining an optimum design for the AVA. Of the three systems discussed in Apppendix II, the combination AVA-LTDA (System 3) seems the best prospect and certainly more work is required on the theoretical and experimental study of this system.

The application of the AVA to systems exhibiting torsional oscillations is another aspect which is worth considering. For example, by placing one or more AVAs on the end of a rotating shaft which has torsional oscillations at frequencies ω and 2ω, the axis of the AVA being normal to the shaft axis and displaced from it, it is possible to envisage the absorption of both frequencies simultaneously by suitable alignment of the absorber axis relative to the radius line from the shaft axis to the root fixing of the AVA (see Fig. 5.6.1).

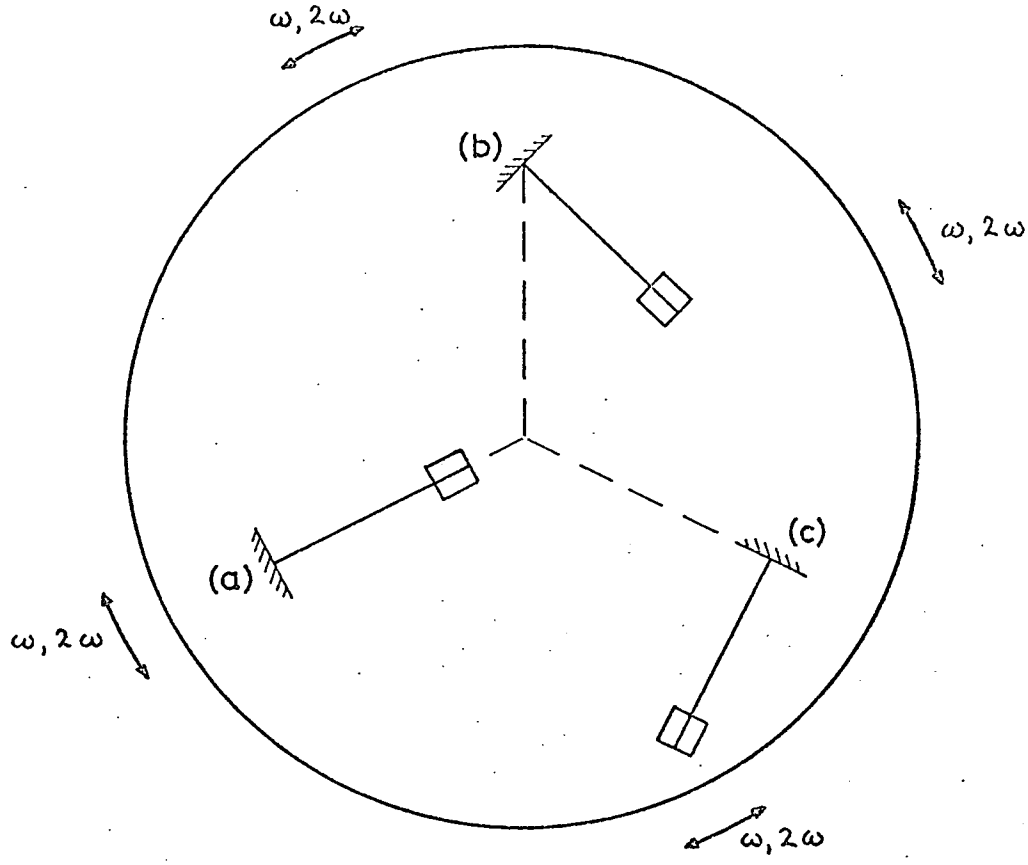

Fig. 5.6.1

Application of the AVA to Systems Exhibiting Torsional Oscillations.

(A) AVA axis along radius line, acts as a LTDA, absorbing frequency ω,

(b) AVA axis at arbitrary angle to radius line, acts as a combination LTDA-AVA, absorbing both ω and 2ω frequencies,

(c) AVA axis at right angles to radius line, acts as an AVA, absorbing frequency 2ω.

Situations in which the AVA is subjected to harmonic forcing frequencies which are linear combinations of the natural frequencies (ω_1 and ω_2) of the system, for example ($\omega_1 + \omega_2$), are also of interest. In this case a study of the first order perturbational equations is required to find which terms become resonant under this new input condition.

CHAPTER 6

CONCLUSIONS

6.1 Review of Principal Results

This investigation has studied the basic absorbing action of an autoparametric system. Although this absorbing action was first observed in the laboratory, it may well have been anticipated from existing theory. The device described in this thesis, which is known as the autoparametric vibration absorber or simply as the AVA, depends for its operation on the timewise variation of its spring stiffness, arising from the motion of the main mass to which it is attached. This time-variation of one of the parameters of the absorber leads to the growth of large lateral amplitudes of the end mass which eventually reach a limiting value due to the inherent nonlinearities of the system, while the associated axial motion of the absorber end mass produces nonlinear inertial feedback terms which influence the main mass response.

In summary, the principal results are as follows. The absorbing action of the cantilever AVA has been shown experimentally and the first order asymptotic theory developed in Chapter 2 has effectively predicted the essential features of the steady-state response. Further, the good agreement, both qualitatively and quantitatively, between the amplitude response curves of the detuned absorber and those obtained experimentally suggests that there is no advantage to be gained in taking the theoretical analysis beyond the first order of approximation.

With regard to the mathematical analysis of the AVA under harmonic excitation, it has been shown that the same results for the steady-state solution of the AVA system equations can be obtained by three distinct, but not unrelated, techniques. Of these, the asymptotic method of Struble is to be preferred as it is the easiest to apply and is the most physically meaningful. (The other two methods are discussed in Appendix III).

Although the comparison described between an autoparametric absorber and a linear tuned and damped absorber of the same mass ratio is not favourable towards the former, it does serve to highlight the important role played by the ratio of axial to lateral motion of the end mass in determining the absorbing efficiency of the AVA. Of course, this feature of the absorber action can be reasoned intuitively from the theoretical model when it is realised that the efficiency of the absorber depends on the magnitude of the axial inertia force which it exerts on the main mass.

With regard to the transient response of the AVA, clearly more thought must be given to the theoretical analysis of this problem. The computer simulation of the full equations of motion revealed a complicated amplitude response pattern which would be difficult to predict by analytical means. Two additional factors emerge from the digital computer simulation of the AVA system. Firstly, the simulation of the first order variational equations produces a transient response pattern similar in nature to that of the full equations of motion. This is a further indication that the first order theory is sufficient to predict the response performance of the AVA.

Secondly, a comparison of the simulated transient response of an AVA and a linear tuned and damped absorber of the same mass ratio was not favourable towards the former, in that the LTDA passed through the transition zone from the given starting conditions to steady-state operation without the violent interaction of the main mass and absorber modes, so clearly illustrated in Fig. I.2.1, Appendix I. Also the LTDA has a better transient response time in that it settles more quickly into its steady-state mode of operation.

6.2 Concluding Remarks

It can be concluded from this study of the absorbing capabilities of the AVA that it is unlikely that it will replace the well-established absorbers such as the linear tuned and damped or the gyrostatic absorber in their present industrial role. However there is still a great deal of development of the autoparametric device which might still be carried out and it may prove advantageous in some applications. For example, it is possible to design an absorber which will act simultaneously as an autoparametric and a tuned and damped absorber (see Appendix II).

In the search for a practicable form of AVA it is necessary to consider parameters such as the ratio of absorber end mass to main mass, which remained invariable at approximately 1/50 in this particular study. Increasing this ratio to 1/10, or more, must improve the efficiency of the absorber, however, the mechanical constraints of the cantilever-type absorber system would probably restrict its use to small mass ratios, in which case, System 3 of Appendix II would appear to be the most likely choice for a possible commercial prototype.

Finally, the whole question of the stochastic excitation of the AVA and other similar systems presents a wide area for future research.

PRINCIPAL NOTATION

The principal usage of the symbols is given here, other meanings are made clear in the relevant portions of the text.

$A(t)$	Varying amplitude of main mass.
$b_1(t)$	$= [R/P]^{\frac{1}{2}}\omega_2 A(t)$.
$b_2(t)$	$= [R/P]^{\frac{1}{2}}\omega_2 B(t)$.
$B(t)$	Varying lateral amplitude of absorber end mass.
c_1, c_2	Viscous damping.
EI	Flexural rigidity.
$F(t)$	External harmonic forcing.
F_o	Force amplitude.
g	Acceleration due to gravity.
J_o, .., J_4	Coefficients of characteristic equation.
k	Spring stiffness of main mass.
k'	Spring stiffness.
ℓ	Active length of cantilever absorber.
m	Absorber end mass.
M	Main mass.
$\underset{t}{M}\{Q\}$	Averaging operator $= \underset{T\to\infty}{\text{Lim}} \frac{1}{T}\int_o^T Q\, dt$.
n	Forced frequency ratio $= 2\Omega/\omega_1$.
P	Forcing function $= \omega_1^{\,2}/\epsilon$.
$p_{1,2}$	Principal co-ordinates.
Q	$= 1/n$.
$q_{1,2}$	Generalised co-ordinates.
R	Mass ratio $= m/(M + m)$.
t	Real time.

t^* $= 2\Omega t.$

t_1 $= t^*(1 + \epsilon^2\omega + \ldots).$

t_2 $= \epsilon t^*.$

T Kinetic energy function.

V Potential energy function.

$X(t)$ Motion of main mass $= X_d/X_o.$

$X_d(t)$ Motion of main mass (dimensional).

X_o Static deflection of main mass $= F_o/k.$

$X_1, X_2, \ldots$ Perturbational parameters.

$y(t)$ Lateral motion of absorber end mass $= y_d/X_o.$

$y_d(t)$ Lateral motion of absorber end mass (dimensional).

$y_1, y_2, \ldots$ Perturbational parameters.

$z(t), Z(t)$ Axial motion of absorber end mass.

$\alpha(t)$ Phase angle.

$\beta(t)$ Phase angle.

γ Frequency function $= (\omega_2^2 - \Omega^2)/\epsilon\omega_2\sqrt{PR}.$

δ Detuning factor $= 2\omega_2 - \omega_1.$

ϵ Small natural parameter of system.

$\eta_{1,2}$ Viscous damping parameters.

$\theta(t)$ Phase angle.

λ Spring stiffness of absorber; eigenvalue.

$\mu(t)$ Phase angle.

ρ Detuning factor $= 2\omega_2/\omega_1.$

τ Slow time $= (\epsilon/4)\sqrt{PR}\ t.$

$\phi(t)$ Phase angle.

$\psi_{1,2}(t)$, $\bar{\psi}_{1,2}(t)$	Phase angles.
ω	Circular frequency.
ω_1	Undamped natural frequency of entire system $= [k/(M + m)]^{\frac{1}{2}}$.
ω_2	Undamped natural frequency of absorber $= [\lambda/m]^{\frac{1}{2}}$.
2Ω	External forcing frequency.

BIBLIOGRAPHY

ANDRONOV, A.A. and LEONTOVICH, M.A. — On the Vibrations of Systems with Periodically Varying Parameters. Zh. Russk. Fiz.-Khim. Obshch., 59, 429-443, 1927.

ARIARATNAM, S.T. and GRAEFE, P.W.U. — Linear Systems with Stochastic Coefficients. Int. J. Contr., 1, 239-250, 1965; Ibid., 2, 161-169, 1965; Ibid., 2, 205-210, 1965.

ARNOLD, F.R. — Steady-State Behaviour of Systems Provided with Nonlinear Dynamic Vibration Absorbers. J. Appl. Mech., 22, 487-492, 1955.

ARNOLD, R.N. — The Tuned and Damped Gyrostatic Vibration Absorber. Proc. I. Mech. E., 157, 1-19, 1947.

ARTEM'EV, N.A. — Une méthode pour déterminer les exposants caractéristiques et son application à deux problemes de la méchanique céleste. Izv. Akad. Nauk SSSR, Ser. Mat.8, 61-100, 1944.

BARR, A.D.S. — Dynamic Instabilities in Moving Beams and Beam Systems. Proc. 2nd Int. Congr. Theory of Machines and Mechanisms, Zakopane, Poland, 1, 365-374, 1969.

BARR, A.D.S. and McWHANNEL, D.C. — Parametric Instability in Structures Under Support Motion. J. Sound Vib., 14(4), 491-509, 1971.

BELIAEV, N.M. — Stability of Prismatic Rods Subjected to Variable Longitudinal Forces. Collection of Papers: Engineering Constructions and Structural Mechanics, Put', Leningrad, 149-167, 1924.

BLAQUIÈRE, A. — Nonlinear System Analysis. Academic Press Inc., 1966.

BOLOTIN, V.V. — The Dynamic Stability of Elastic Systems. Holden-Day, Inc., 1964.

BOGOLYUBOV, N.N. and MITROPOL'SKII, Yu.A. — Asymptotic Methods in the Theory of Nonlinear Oscillations. Hindustan Publishing Corpn., 1961.

CHELOMEI, V.N. — The Vibrations of Rods Subjected to the Action of Periodically Varying Longitudinal Forces. Trudy KAI, 8, 1937.

CHHATPAR, C.K. and DUGUNDJI, J. — Dynamic Stability of a Pendulum Under Coexistence of Parametric and Forced Excitation. AFOSR Report 68-0001, M.I.T. ASRL-TR-134-5, 1967.

COLE, J.D. — Perturbation Methods in Applied Mathematics. Blaisdell Pub. Co., 1968.

COLE, J.D. and KEVORKIAN, J. — Uniformly Valid Asymptotic Approximations for Certain Non-Linear Differential Equations. Int. Symposium on Nonlinear Differential Equations and Nonlinear Mechanics, Edited by J.P. La Salle and S. Lefschetz, Academic Press, 1963.

DEN HARTOG, J.P. — Mechanical Vibrations. McGraw-Hill Book Co., Fourth edition, 1956.

DWIGHT, H.B. — Tables of Integrals and Other Mathematical Data. The Macmillan Co., 1961.

FARADAY, M. — On a Peculiar Class of Acoustical Figures; and On Certain Forms Assumed by a Group of Particles Upon Vibrating Elastic Surfaces. Phil. Trans., Roy. Soc. London, 121, 229-318, 1831.

FRAZER, R.A., DUNCAN, W.J. and COLLAR, A.R. — Elementary Matrices. Cambridge University Press, 1950.

HSU, C.S. — On the Parametric Excitation of a Dynamic System having Multiple Degrees of Freedom. J. Appl. Mech., 30, 367-372, 1963.

HSU, C.S. — Further Results on Parametric Excitation of a Dynamic System. J. Appl. Mech., 32, 373-377, 1965.

JAEGER, L.G. and BARR, A.D.S. — Parametric Instabilities in Structures Subjected to Prescribed Periodic Support Motion. Proc. Sympos. on Design for Earthquake Loadings, VII-I McGill Univ. Canada, 1966.

KRYLOV, N.M. and BOGOLYUBOV, N.N. — Introduction to Nonlinear Mechanics. Princeton University Press, 1947.

MELDE, F. — Über Erregung stehender Wellen eines fadenförmigen Körpers. Ann. Physik u. Chemie, 109, 193-215, 1859.

METTLER, E. — Nichtlineare Schwingungen und Kinetische Instabilitäten bei Saiten und Stäben. Ing.-Arch., 23, 354-364, 1955; AMR, 9, Rev. 1369, 1956.

METTLER, E. — Stability and Vibration Problems of Mechanical Systems Under Harmonic Excitation. Proc. Int. Conf. Dynamic Stability of Structures (1965), 169-188, Pergamon Press, 1967.

METTLER, E. and WEIDENHAMMER, F. — Der axial pulsierend belastete Stab mit Endmasse. ZAMM, 36, 284-287, 1956.

MINORSKY, N. — Nonlinear Oscillations. D. Van Nostrand Co., 1962.

SETHNA, P.R. — Transients in Certain Autonomous Multiple-Degree-of-Freedom Nonlinear Vibrating Systems. J. Appl. Mech., 30, 44-50, 1963.

SETHNA, P.R. — Vibrations of Dynamical Systems With Quadratic Nonlinearities. J.Appl. Mech., 32, 576-582, 1965.

SEVIN, E. — On the Parametric Excitation of a Pendulum-Type Vibration Absorber. J. Appl. Mech., 28, 330-334, 1961.

STRUBLE, R.A. — Nonlinear Differential Equations. McGraw-Hill Book Co., 1962.

STRUBLE, R.A. and HEINBOCKEL, J.H. — Energy Transfer in a Beam-Pendulum System. J. Appl. Mech., 29, 590-592, 1962.

STRUBLE, R.A. and HEINBOCKEL, J.H. — Resonant Oscillations of a Beam-Pendulum System. J. Appl. Mech., 30, 181-188, 1963.

STRUTT, J.W. (Lord Rayleigh) — On the Crispations of Fluid Resting Upon a Vibrating Support. Phil. Mag., 16, 50-53, 1883.

TIMOSHENKO, S. — Strength of Materials, Part II. D. Van Nostrand Co., Third edition, 1956.

APPENDIX I

TRANSIENT RESPONSE OF AVA SYSTEM UNDER EXTERNAL EXCITATION

I.1 Theoretical Approach

In this section a possible analytical solution of the transient behaviour of a perfectly tuned AVA is discussed. The starting point for this analysis is the set of four first order variational equations obtained by the asymptotic method of Chapter 2. Before transformation the equations have the form

$$-\dot{A} = (\epsilon/2\omega_2)[4\gamma_1\omega_2^2 A + \tfrac{1}{2}RB^2\omega_2^2\sin(2\theta - \phi) + \tfrac{1}{2}P\sin\phi]$$

$$-A\dot{\phi} = (\epsilon/2\omega_2)[2\epsilon^{-1}(\Omega^2 - \omega_2^2)A - \tfrac{1}{2}RB^2\omega_2^2\cos(2\theta - \phi) + \tfrac{1}{2}P\cos\phi]$$

$$-\dot{B} = (\epsilon/2\omega_2)[2\gamma_2\omega_2^2 B - 2AB\omega_2^2\sin(2\theta - \phi)]$$

$$-B\dot{\theta} = (\epsilon/2\omega_2)[\epsilon^{-1}(\Omega^2 - \omega_2^2)B - 2AB\omega_2^2\cos(2\theta - \phi)]$$

... I.1.1

Now choose a solution for A, B, ϕ and θ in the form of a perturbation series

$$A = A_o + \epsilon A_1 + \epsilon^2 A_2 + \epsilon^3 A_3 + \ldots$$

$$B = B_o + \epsilon B_1 + \epsilon^2 B_2 + \epsilon^3 B_3 + \ldots$$

$$\phi = \phi_o + \epsilon\phi_1 + \epsilon^2\phi_2 + \epsilon^3\phi_3 + \ldots$$

$$\theta = \theta_o + \epsilon\theta_1 + \epsilon^2\theta_2 + \epsilon^3\theta_3 + \ldots$$

... I.1.2

Solution I.1.2 is substituted into equations I.1.1 to order ϵ^3. Terms in sine and cosine are expanded thus,

$$\sin(2\theta - \phi) = \sin(2\theta_o - \phi_o) + \epsilon(2\theta_1 - \phi_1)\cos(2\theta_o - \phi_o)$$
$$+ \epsilon^2(2\theta_2 - \phi_2)\cos(2\theta_o - \phi_o) + \ldots$$

The resulting four equations are

$$\dot{(A_o + \epsilon A_1 + \epsilon^2 A_2 + \epsilon^3 A_3)}$$
$$= -(\epsilon/2\omega_2)[4\zeta_1\omega_2^2(A_o + \epsilon A_1 + \epsilon^2 A_2) +$$
$$+ \tfrac{1}{2} P(\sin\phi_o + \epsilon\phi_1\cos\phi_o + \epsilon^2\phi_2\cos\phi_o) +$$
$$+ \tfrac{1}{2} R\omega_2^2(B_o + \epsilon B_1 + \epsilon^2 B_2)^2 \{\sin(2\theta_o - \phi_o) +$$
$$+ \epsilon(2\theta_1 - \phi_1)\cos(2\theta_o - \phi_o) + \epsilon^2(2\theta_2 - \phi_2)\cos(2\theta_o - \phi_o)\}]$$

$$\dot{(A_o + \epsilon A_1 + \epsilon^2 A_2 + \epsilon^3 A_3)}\dot{(\phi_o + \epsilon\phi_1 + \epsilon^2\phi_2 + \epsilon^3\phi_3)}$$
$$= -(\epsilon/2\omega_2)[2\epsilon^{-1}(\Omega^2 - \omega_2^2)(A_o + \epsilon A_1 + \epsilon^2 A_2) +$$
$$+ \tfrac{1}{2} P(\cos\phi_o - \epsilon\phi_1\sin\phi_o - \epsilon^2\phi_2\sin\phi_o) -$$
$$- \tfrac{1}{2} R\omega_2^2(B_o + \epsilon B_1 + \epsilon^2 B_2)^2 \{\cos(2\theta_o - \phi_o) -$$
$$- \epsilon(2\theta_1 - \phi_1)\sin(2\theta_o - \phi_o) - \epsilon^2(2\theta_2 - \phi_2)\sin(2\theta_o - \phi_o)\}]$$

$$\dot{(B_o + \epsilon B_1 + \epsilon^2 B_2 + \epsilon^3 B_3)}$$
$$= -(\epsilon/2\omega_2)[2\zeta_2\omega_2^2(B_o + \epsilon B_1 + \epsilon^2 B_2) - 2\omega_2^2(A_o + \epsilon A_1 + \epsilon^2 A_2).$$
$$.(B_o + \epsilon B_1 + \epsilon^2 B_2)\{\sin(2\theta_o - \phi_o) + \epsilon(2\theta_1 - \phi_1)\cos(2\theta_o - \phi_o) +$$
$$+ \epsilon^2(2\theta_2 - \phi_2)\cos(2\theta_o - \phi_o)\}]$$

and

$$(B_o + \epsilon B_1 + \epsilon^2 B_2 + \epsilon^3 B_3)\overline{(\theta_o + \epsilon\theta_1 + \epsilon^2\theta_2 + \epsilon^3\theta_3)}$$

$$= -(\epsilon/2\omega_2)[\epsilon^{-1}(\Omega^2 - \omega_2^2)(B_o + \epsilon B_1 + \epsilon^2 B_2) - 2\omega_2(A_o + \epsilon A_1 + \epsilon^2 A_2).$$

$$.(B_o + \epsilon B_1 + \epsilon^2 B_2)\{\cos(2\theta_o - \phi_o) - \epsilon(2\theta_1 - \phi_1)\sin(2\theta_o - \phi_o) -$$

$$- \epsilon^2(2\theta_2 - \phi_2)\sin(2\theta_o - \phi_o)\}]$$

... I.1.3

From equations I.1.3, equating terms of zero order in ϵ gives

$$\dot{A}_o = 0 \ , \ \dot{B}_o = 0 \ , \ A_o\dot{\phi}_o = 0 \text{ and } B_o\dot{\theta}_o = 0 \qquad \text{I.1.4}$$

A possible solution is

$$A_o = B_o = 1 \text{ and } \phi_o = \theta_o = 0 \qquad \text{I.1.5}$$

Equating terms of the first order in ϵ gives

$$\dot{A}_1 = -(1/2\omega_2)[4\eta_1\omega_2^2 A_o + \tfrac{1}{2}R\omega_2^2 B_o^2\sin(2\theta_o - \phi_o) + \tfrac{1}{2}P\sin\phi_o]$$

$$\dot{B}_1 = -(1/2\omega_2)[2\eta_2\omega_2^2 B_o - 2\omega_2^2 A_o B_o\sin(2\theta_o - \phi_o)]$$

$$A_o\dot{\phi}_1 + A_1\dot{\phi}_o = -(1/2\omega_2)[2\epsilon^{-1}(\Omega^2 - \omega_2^2)A_o - \tfrac{1}{2}R\omega_2^2 B_o^2\cos(2\theta_o - \phi_o) +$$

$$+ \tfrac{1}{2}P\cos\phi_o]$$

$$B_o\dot{\theta}_1 + B_1\dot{\theta}_o = -(1/2\omega_2)[\epsilon^{-1}(\Omega^2 - \omega_2^2)B_o - 2\omega_2^2 A_o B_o\cos(2\theta_o - \phi_o)]$$

... I.1.6

Substituting I.1.5 into I.1.6 and integrating produces

$$A_1 = -2\eta_1\omega_2 t \ , \ B_1 = -\eta_2\omega_2 t$$

$$\phi_1 = [-\epsilon^{-1}\left(\frac{\Omega^2 - \omega_2^2}{\omega_2}\right) + \tfrac{1}{4}R\omega_2 - (P/4\omega_2)]t$$

$$\theta_1 = [-\tfrac{1}{2}\epsilon^{-1}\left(\frac{\Omega^2 - \omega_2^2}{\omega_2}\right) + \omega_2]t$$

... I.1.7

Note that in formulating I.1.7, the constants of integration are chosen to be zero.

Equating terms of the second order in ϵ yields

$$\dot{A}_2 = -(1/2\omega_2)[4\gamma_1\omega_2^2 A_1 + \tfrac{1}{2}R\omega_2^2 B_o^2(2\theta_1 - \phi_1)\cos(2\theta_o - \phi_o) +$$

$$+ R\omega_2^2 B_o B_1 \sin(2\theta_o - \phi_o) + \tfrac{1}{2} P \phi_1 \cos\phi_o]$$

$$\dot{B}_2 = -(1/2\omega_2)[2\gamma_2\omega_2^2 B_1 - 2\omega_2^2 A_o B_o(2\theta_1 - \phi_1)\cos(2\theta_o - \phi_o) -$$

$$- 2\omega_2^2(A_o B_1 + A_1 B_o)\sin(2\theta_o - \phi_o)]$$

$$A_o\dot{\phi}_2 + A_1\dot{\phi}_1 + A_2\dot{\phi}_o = -(1/2\omega_2)[2\epsilon^{-1}(\Omega^2 - \omega_2^2)A_1 + \tfrac{1}{2}R\omega_2^2 B_o^2(2\theta_1 - \phi_1).$$

$$.\sin(2\theta_o - \phi_o) - R\omega_2^2 B_o B_1 \cos(2\theta_o - \phi_o) - \tfrac{1}{2} P\phi_1 \sin\phi_o]$$

$$B_o\dot{\theta}_2 + B_1\dot{\theta}_1 + B_2\dot{\theta}_o = -(1/2\omega_2)[\epsilon^{-1}(\Omega^2 - \omega_2^2)B_1 + 2\omega_2^2 A_o B_o(2\theta_1 - \phi_1).$$

$$.\sin(2\theta_o - \phi_o) - 2\omega_2^2(A_o B_1 + A_1 B_o)\cos(2\theta_o - \phi_o)]$$

... I.1.8

Using I.1.5 and I.1.7, equations I.1.8 produce on integration

$$A_2 = [(P/8)\epsilon^{-1}\left(\frac{\Omega^2 - \omega_2^2}{\omega_2^2}\right) + 2\gamma_1^2\omega_2^2 - (PR/16) - \tfrac{1}{4}R\omega_2^2 + (R\omega_2)^2/32 +$$

$$+ (P^2/32\omega_2^2)]t^2$$

$$B_2 = [\tfrac{1}{2}\gamma_2^2\omega_2^2 + \omega_2^2 - (R\omega_2^2/8) + P/8]t^2$$

$$\phi_2 = [\tfrac{1}{4}R\omega_2^2(\gamma_1 - \gamma_2) - \tfrac{1}{4} P\gamma_1]\, t^2$$

$$\theta_2 = -\gamma_1\omega_2^2\, t^2$$

... I.1.9

Finally, equating terms of order ϵ^3 gives,

$$\dot{A}_3 = -(1/2\omega_2)[4\eta_1\omega_2^2 A_2 + \tfrac{1}{2}R\omega_2^2 B_o^2(2\theta_2 - \phi_2)\cos(2\theta_o - \phi_o) +$$

$$+ R\omega_2^2 B_o B_1(2\theta_1 - \phi_1)\cos(2\theta_o - \phi_o) +$$

$$+ \tfrac{1}{2}R\omega_2^2(B_1^2 + 2B_oB_2)\sin(2\theta_o - \phi)_o + \tfrac{1}{2}P\phi_2\cos\phi_o]$$

$$\dot{B}_3 = -(1/2\omega_2)[2\eta_2\omega_2^2 B_2 - 2\omega_2^2 A_o B_o(2\theta_2 - \phi_2)\cos(2\theta_o - \phi_o) -$$

$$- 2\omega_2^2(A_oB_1 + A_1B_o)(2\theta_1 - \phi_1)\cos(2\theta_o - \phi_o) -$$

$$- 2\omega_2^2(A_oB_2 + A_1B_1 + A_2B_o)\sin(2\theta_o - \phi_o)]$$

$$A_o\dot{\phi}_3 + A_1\dot{\phi}_2 + A_2\dot{\phi}_1 + A_3\dot{\phi}_o$$

$$= -(1/2\omega_2)[2\epsilon^{-1}(\Omega^2 - \omega_2^2)A_2 + \tfrac{1}{2}R\omega_2^2 B_o^2(2\theta_2 - \phi_2)\sin(2\theta_o - \phi_o) +$$

$$+ R\omega_2^2 B_o B_1(2\theta_1 - \phi_1)\sin(2\theta_o - \phi_o) -$$

$$- \tfrac{1}{2}R\omega_2^2(B_1^2 + 2B_oB_2)\cos(2\theta_o - \phi_o) - \tfrac{1}{2}P\phi_2\sin\phi_o]$$

$$B_o\dot{\theta}_3 + B_1\dot{\theta}_2 + B_2\dot{\theta}_1 + B_3\dot{\theta}_o$$

$$= -(1/2\omega_2)[\epsilon^{-1}(\Omega^2 - \omega_2^2)B_2 + 2\omega_2^2 A_oB_o(2\theta_2 - \phi_2)\sin(2\theta_o - \phi_o) +$$

$$+ 2\omega_2^2(A_oB_1 + A_1B_o)(2\theta_1 - \phi_1)\sin(2\theta_o - \phi_o) -$$

$$- 2\omega_2^2(A_oB_2 + A_1B_1 + A_2B_o)\cos(2\theta_o - \phi_o)]$$

... I.1.10

Once again the substitutions I.1.5, I.1.7 and I.1.9 are made in equations I.1.10 which yield on integration,

$$A_3 = [-(P/12)\epsilon^{-1}(\frac{\Omega^2 - \omega_2^2}{\omega_2})\gamma_1 - (4\gamma_1^2\omega_2^3/3) + (PR/16)\gamma_2\omega_2 +$$

$$+ (R/3)\omega_2^3(\gamma_1 + \gamma_2) - (R/4)^2\gamma_2\omega_2^3]t^3$$

$$B_3 = [-(\gamma_2^3\omega_2^3/6) - \omega_2^3(2\gamma_1 + \gamma_2) + (R/24)\omega_2^3(2\gamma_1 + 5\gamma_2) -$$

$$- (P/24)\omega_2(2\gamma_1 + 3\gamma_2)]t^3$$

$$\phi_3 = [(P^2/96)\epsilon^{-1}(\frac{\Omega^2 - \omega_2^2}{\omega_2^3}) - (PR/96)\epsilon^{-1}(\frac{\Omega^2 - \omega_2^2}{\omega_2}) - (P/6)\gamma_1^2\omega_2 -$$

$$- (P^2R/128\omega_2) + (R/6)\omega_2^3(\gamma_1 - \gamma_2)^2 + (R/6)\omega_2^3 - (R^3/384)\omega_2^3 +$$

$$+ (PR^2/128)\omega_2 + (P^3/384)\omega_2^3]t^3$$

$$\theta_3 = [(P/24)\epsilon^{-1}(\frac{\Omega^2 - \omega_2^2}{\omega_2}) + (2\gamma_1^2\omega_2^3/3) - (R/12)\omega_2^3 + (R^2/96)\omega_2^3 -$$

$$- (PR/48)\omega_2 + P^2/96\omega_2]t^3$$

... I.1.11

The solutions for A, B, ϕ and θ may now be written to order ϵ^3. Thus

$$A = 1 - \epsilon[2\gamma_1\omega_2]t + \epsilon^2[(P/8)\epsilon^{-1}(\frac{\Omega^2 - \omega_2^2}{\omega_2^2}) + 2\gamma_1^2\omega_2^2 - (PR/16) -$$

$$- \tfrac{1}{4}R\omega_2^2 + (R^2/32)\omega_2^2 + P^2/32\omega_2^2]t^2 - \epsilon^3[(P/12)\epsilon^{-1}(\frac{\Omega^2 - \omega_2^2}{\omega_2})\gamma_1 +$$

$$+ (4\gamma_1^2\omega_2^3/3) - (PR/16)\gamma_2\omega_2 - (R/3)\omega_2^3(\gamma_1 + \gamma_2) + (R/4)^2\gamma_2\omega_2^3]t^3 +$$

$$+ O(t^4)$$

$$B = 1 - \epsilon[\gamma_2\omega_2]t + \epsilon^2[\tfrac{1}{2}\gamma_2^2\omega_2^2 + \omega_2^2 - (R/8)\omega_2^2 + P/8]t^2$$

$$- \epsilon^3[(\gamma_2^3\omega_2^3/6) + \omega_2^3(2\gamma_1 + \gamma_2) - (R/24)\omega_2^3(2\gamma_1 + 5\gamma_2) +$$

$$+ (P/24)\omega_2(2\gamma_1 + 3\gamma_2)]t^3 + O(t^4)$$

$$\phi = -\epsilon[\epsilon^{-1}(\frac{\Omega^2 - \omega_2^2}{\omega_2}) - \tfrac{1}{4}R\omega_2 + P/4\omega_2]t + \epsilon^2[\tfrac{1}{4}R\omega_2^2(\gamma_1 - \gamma_2) - \tfrac{1}{4}P\gamma_1]\,t^2$$

$$+ \epsilon^3[(P^2/96)\epsilon^{-1}(\frac{\Omega^2 - \omega_2^2}{\omega_2^3}) - (PR/96)\epsilon^{-1}(\frac{\Omega^2 - \omega_2^2}{\omega_2}) - (P/6)\gamma_1^2\omega_2 -$$

$$- (P^2R/128\omega_2) + (R/6)\omega_2^3(\gamma_1 - \gamma_2)^2 + (R/6)\omega_2^3 - (R^3/384)\omega_2^3 +$$

$$+ (PR^2/128)\omega_2 + (P^3/384)\omega_2^3]t^3 + O(t^4)$$

$$\theta = -\epsilon[\tfrac{1}{2}\epsilon^{-1}(\frac{\Omega^2 - \omega_2^2}{\omega_2}) - \omega_2]t - \epsilon^2[\gamma_1\omega_2^2]t^2 + \epsilon^3[(P/24)\epsilon^{-1}(\frac{\Omega^2 - \omega_2^2}{\omega_2}) +$$

$$+ (2\gamma_1^2\omega_2^3/3) - (R/12)\omega_2^3 + (R^2/96)\omega_2^3 - (PR/48)\omega_2 + P^2/96\omega_2]t^3$$

$$+ O(t^4)$$

... I.1.12

The results of the theoretical approach to the transient solution are given by equations I.1.12. Comments on the validity of these results are made after the next section which discusses computer simulation of the AVA system.

I.2 Computer Simulation of Transient Behaviour of the AVA

The transient behaviour of the AVA can be simulated using a digital computer. An IBM computing package known as CSMP (continuous system modelling program) allowed the direct programming of the AVA system equations on the System/360 computer.

The equations of motion 2.3.1 are rewritten to give two uncoupled equations in $\ddot{X}$ and $\ddot{y}$ of the form

$$\ddot{X} = (-4AX - E\dot{X} - ABy^2 - BDy\dot{y} + B\dot{y}^2 + 4A\sin 2\Omega t)/(1 - BCy^2)$$

$$\ddot{y} = (-Ay - D\dot{y} - 4ACXy - CE\dot{X}y + BCy\dot{y}^2 + 4ACy\sin 2\Omega t)/(1 - BCy^2) \qquad \text{I.2.1}$$

These equations were written in Fortran into the program deck together with initial conditions for X and y, and the computer instructed to perform a double integration of the quantities $\ddot{X}$ and $\ddot{y}$. When the equations are written in the above form the implicit loop situation of the original equations, in which $\ddot{X}$ depends on $\ddot{y}$, is eliminated and the computer finds no difficulty in performing the integrations.

The package provided a choice of integration routines of varying degrees of sophistication. For this work, a fourth order Runge-Kutta integration with fixed step length was found to be adequate.

Finally the computer is instructed to provide a print-plot of the dependent variables X and y against the independent variable t (time). It is necessary to choose a print-plot step length which is small enough to provide adequate resolution of the X and y response frequencies.

A typical print-plot is shown in Fig. I.2.1. For this particular simulation the parameter values were

$$\epsilon = 0.0010 \ , \ \epsilon\gamma_1 = 0.0020 \ , \ \epsilon\gamma_2 = 0.0200 \ ,$$

$$R = 0.0196 \ , \ n = 0.995 \ , \ X_o = 0 \ , \ y_o = 0.001 \ ,$$

where n is the forced frequency ratio and X_o, y_o are the initial conditions imposed on the system. Thus Fig. I.2.1 shows the behaviour of the system, under the action of a forcing frequency near the resonance of the main mass, when it is suddenly released at t = 0 with the above starting conditions.

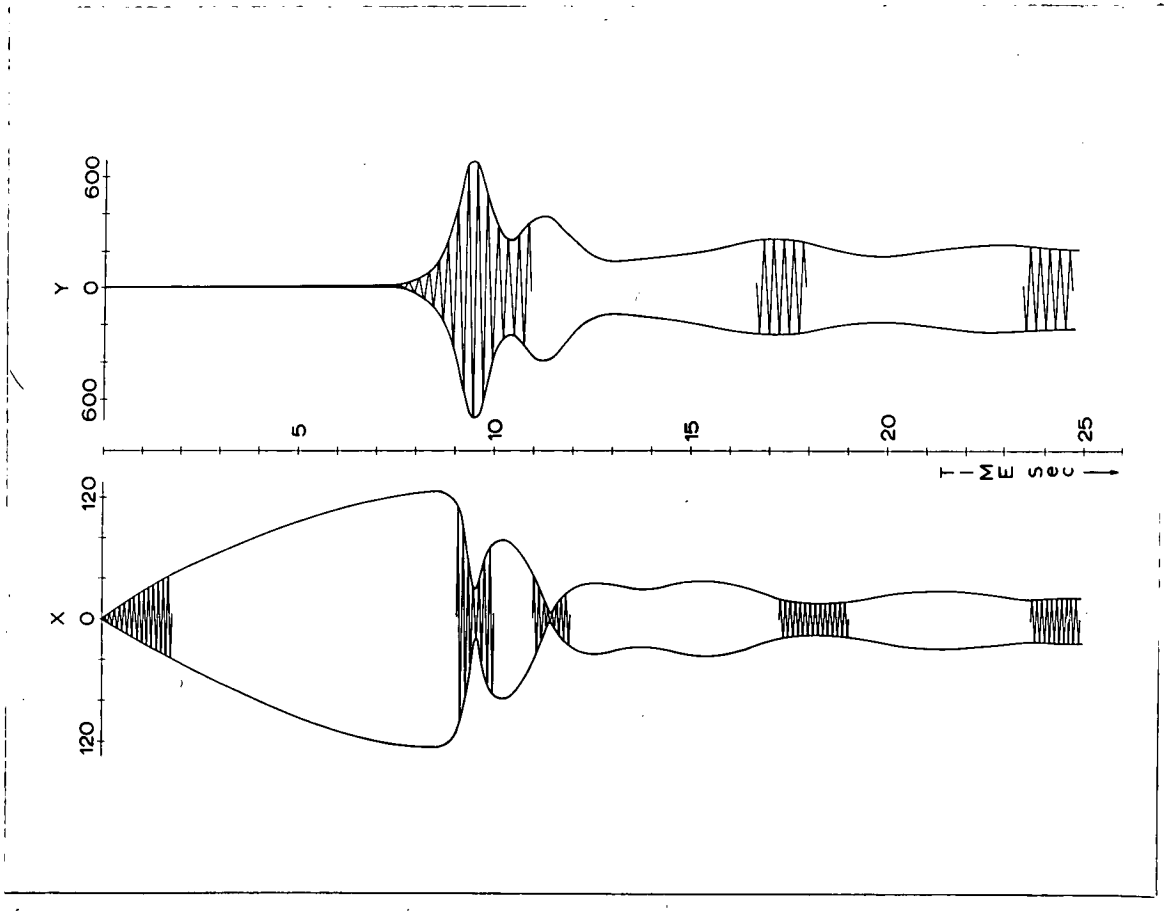

Fig. I.2.1

Digital Computer Print-Plot of Transient Response
of Main Mass (X) and Absorber (Y).

The interaction of the two modes can be clearly seen. At $t = 10$ this interplay is quite violent but gradually the responses settle down to their steady-state amplitudes at $t = 25$. It is interesting to note that the amplitude ratio X/y at $t = 25$ is approximately 1/9 which is in good agreement with the ratios found theoretically (see theoretical response curves, Chapter 2).

In a similar manner the response of the linear tuned and damped absorber, described in Chapter 3, was also simulated to compare its transient behaviour with that of the AVA. It was found that the interaction between the absorber and main mass systems of the LTDA was minimal and that a smooth transition to the steady-state situation had been achieved by $t = 5$. On this count the AVA system emerges as a poor second.

I.3 Validity of the Theoretical Solution

To assess the merits of the theoretical solution of the transient behaviour of the AVA system the equations I.1.12 were programmed using the CSMP package described in the preceding section. The computer was instructed to evaluate the functions of time A, B, ϕ and θ and then print-plot $X(= A\cos(\omega_1 t + \phi))$ and $y\ (= B\cos(\omega_2 t + \theta))$ against time, t.

In the resulting print-plot both the X and y modes exhibited continuous exponential growth. This inconclusive result was disappointing although not entirely unexpected (it was realised that a very sophisticated theoretical solution would be required to predict the type of motion illustrated in Fig. I.2.1). Certainly there are terms in equations I.1.12 (e.g. the term $(\epsilon^2 P^2/32\omega_2^2)t^2$ in the expression for A, which is of zero order in ϵ, P is of order ϵ^{-1}),

which tend to dominate the solution and may be the cause of the positive growth of the amplitudes but it would appear that the remedy to the problem is almost certainly of a more fundamental nature.

It is possible of course, that the theoretical solution of the transient behaviour of the AVA is based on variational equations (I.1.1) which in themselves do not produce the transient response of the full equations of motion (I.2.1). Accordingly the variational equations I.1.1 were also programmed using CSMP. In this case the computer print-plot of X and y showed the type of transient response depicted in Fig. I.2.1. Consequently the variational equations retain the transient response properties of the original equations of motion and are not the cause of the poor theoretical results.

APPENDIX II

ALTERNATIVE FORMS OF CONSTRUCTION FOR THE AVA

II.1 Introduction

The effectiveness of the AVA was shown to depend on the ratio of axial to lateral motion of the absorber end mass (see Chapter 3). To improve this ratio it was found that the length, ℓ, of the cantilever AVA had to be small. However there were mechanical limitations to the length reduction of such an absorber and in an attempt to overcome these limitations three other systems were considered.

This Appendix details three alternative theoretical models which may provide a more satisfactory (higher) value for the ϵ parameter. For each model the equations of motion are derived and compared with those of the cantilever model, namely

$$(1 + \frac{m}{M})\ddot{X}_d + \frac{k}{M} X_d + (1 + \frac{m}{M})g - \frac{m}{M}\frac{\epsilon}{X_o}(\dot{y}_d^2 + y_d\ddot{y}_d) = \frac{F(t)}{M}$$

$$\ddot{y}_d + (\frac{\lambda}{m} - \frac{\epsilon}{X_o} g - \frac{\epsilon}{X_o}\ddot{X}_d)y_d + (\frac{\epsilon}{X_o})^2(\dot{y}_d^2 + y_d\ddot{y}_d)y_d = 0 \qquad \text{II.1.1}$$

where $\epsilon = \frac{6X_o}{5\ell}$ and $\lambda = 3EI/\ell^3$.

II.2 System 1

The first of these models is shown in Fig. II.2.1 in which the usual notation is adopted. Here the absorber is a cylinder of radius r free to roll in a circular slot of radius R. Positive contact between the cylinder and main mass is maintained by means of the spring k'.

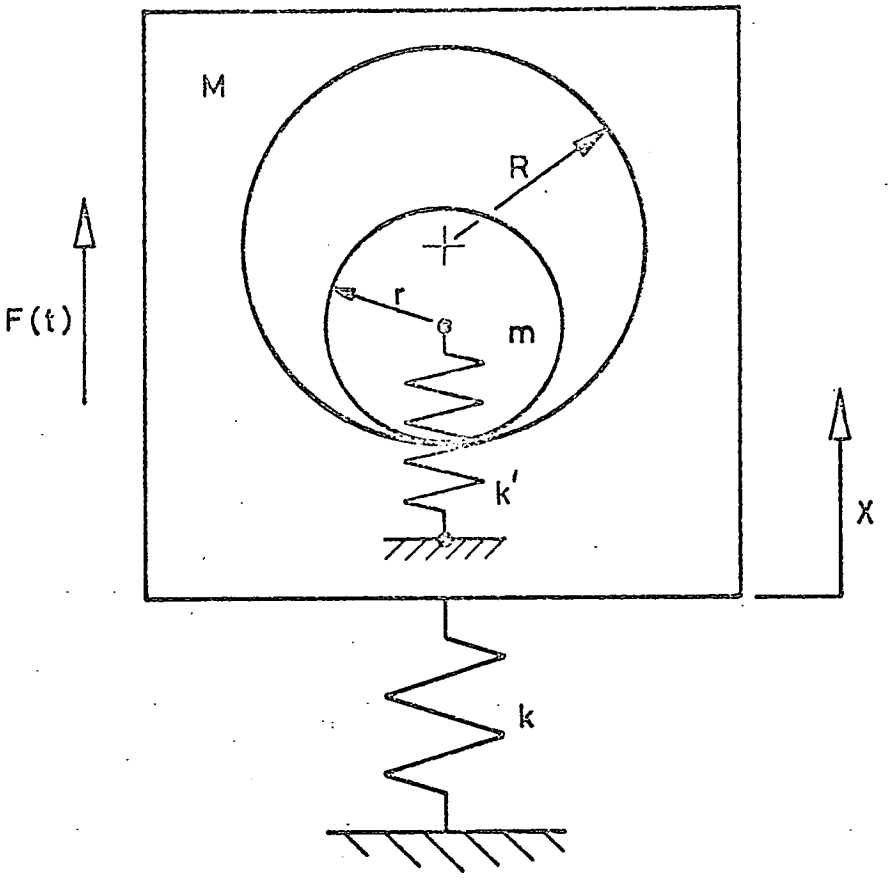

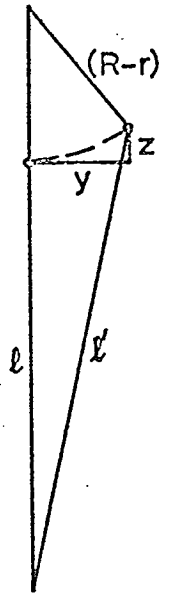

Fig. II.2.1

System 1.

The kinetic energy function is

$$T = \tfrac{1}{2} M\dot{X}^2 + \tfrac{1}{2} m(\dot{X} + \dot{z}) + \tfrac{1}{2} m\dot{y}^2 + \tfrac{1}{2} I\omega^2$$

where $I = \tfrac{1}{2} mr^2$.

Let the absolute rotation of the cylinder be $(\phi - \theta)$ where $R\theta = r\phi$, then $\omega = (R - r)\dot{\theta}/r$. From the geometry, $z = (R - r) - [(R - r)^2 - y^2]^{\frac{1}{2}}$ and on the elimination of θ, the kinetic energy function becomes

$$T = \tfrac{1}{2} M\dot{X}^2 + \tfrac{1}{2} m\dot{X}^2 + \frac{\tfrac{1}{2} m\dot{y}^2 y^2}{[(R - r)^2 - y^2]} + \frac{m\dot{X}\dot{y}y}{[(R - r)^2 - y^2]^{\frac{1}{2}}}$$

$$+ \tfrac{1}{2} m\dot{y}^2 + \frac{\tfrac{1}{4} m(R - r)^2\dot{y}^2}{[(R - r)^2 - y^2]}$$

The potential energy function is

$$V = \tfrac{1}{2} kX^2 + MgX + mg(X + z) + V_{k'}$$

From the geometry of Fig. II.2.1,

$$V_{k'} = \tfrac{1}{2} k'(\ell' - \ell)^2 \text{ where } \ell' = [(\ell + z) + y^2]^{\frac{1}{2}}$$

$$\therefore V_{k'} = k'[\ell^2 + (R - r)^2 + \ell\{(R - r) - [(R - r)^2 - y^2]^{\frac{1}{2}}\} -$$

$$- (R - r)[(R - r)^2 - y^2]^{\frac{1}{2}}] - k'\ell[\ell^2 + 2(R - r)^2 + 2\ell\{(R - r) -$$

$$- [(R - r)^2 - y^2]^{\frac{1}{2}}\} - 2(R - r)[(R - r)^2 - y^2]^{\frac{1}{2}}]^{\frac{1}{2}}$$

Using the Lagrangian formulation, the equations of motion are

$$(1 + \frac{m}{M})\ddot{X} + \frac{k}{M} X + (1 + \frac{m}{M})g + \frac{m}{M}\frac{\epsilon}{X_o}\left(\frac{(R - r)^2\dot{y}^2}{[(R - r)^2 - y^2]} + y\ddot{y}\right) = \frac{F(t)}{M} \qquad \text{II.2.1}$$

and

$$\ddot{y} + \frac{2}{3}\left(\frac{\lambda}{m} + \frac{\epsilon}{X_o} g + \frac{\epsilon}{X_o}\ddot{X}\right)y + \left(\frac{\epsilon}{X_o}\right)^2\left(\frac{(R - r)^2\dot{y}^2}{[(R - r)^2 - y^2]} + y\ddot{y}\right)y = 0$$

where $\epsilon = \dfrac{X_o}{[(R - r)^2 - y^2]^{\frac{1}{2}}}$ and $\lambda = k' \dfrac{\{(R - r) - [(R - r)^2 - y^2]^{\frac{1}{2}}\}}{[(R - r)^2 - y^2]^{\frac{1}{2}}}$

II.3 System 2

Fig. II.3.1 shows the second of the AVA models. In this case the absorber is a simple pendulum supported by a pivot point on the main mass and given a prescribed natural frequency by the linear springs k'. (Note, the stiffness of the absorber system could be provided by a torsional spring at the pivot thereby providing greater freedom of angular oscillation).

Using the notation of Fig. II.3.1, the energy functions are

$$T = \tfrac{1}{2} M\dot{X}^2 + \tfrac{1}{2} m[\dot{y}^2 + (\dot{X} - \dot{z})^2]$$

and $$V = \tfrac{1}{2} kX^2 + \tfrac{1}{2}\lambda y^2 + MgX + mg(X - z)$$

where λ has yet to be defined.

From the geometry,

$$z = \ell - [\ell^2 - y^2]^{\frac{1}{2}} \quad , \quad \dot{z} = \frac{y\dot{y}}{[\ell^2 - y^2]^{\frac{1}{2}}}$$

and the absorber spring potential $\tfrac{1}{2}\lambda y^2 = \dfrac{r^2}{\ell^2} k' y^2$

i.e. $\lambda = 2\dfrac{r^2}{\ell^2} k'$.

Thus the kinetic and potential energy functions become

$$T = \tfrac{1}{2} M\dot{X}^2 + \tfrac{1}{2} m \left\{ \dot{y}^2 + \left(\dot{X} - \frac{y\dot{y}}{[\ell^2 - y^2]^{\frac{1}{2}}}\right)^2 \right\}$$

and $$V = \tfrac{1}{2} kX^2 + \frac{r^2}{\ell^2} k' y^2 + MgX + mg(X - \ell + [\ell^2 - y^2]^{\frac{1}{2}})$$

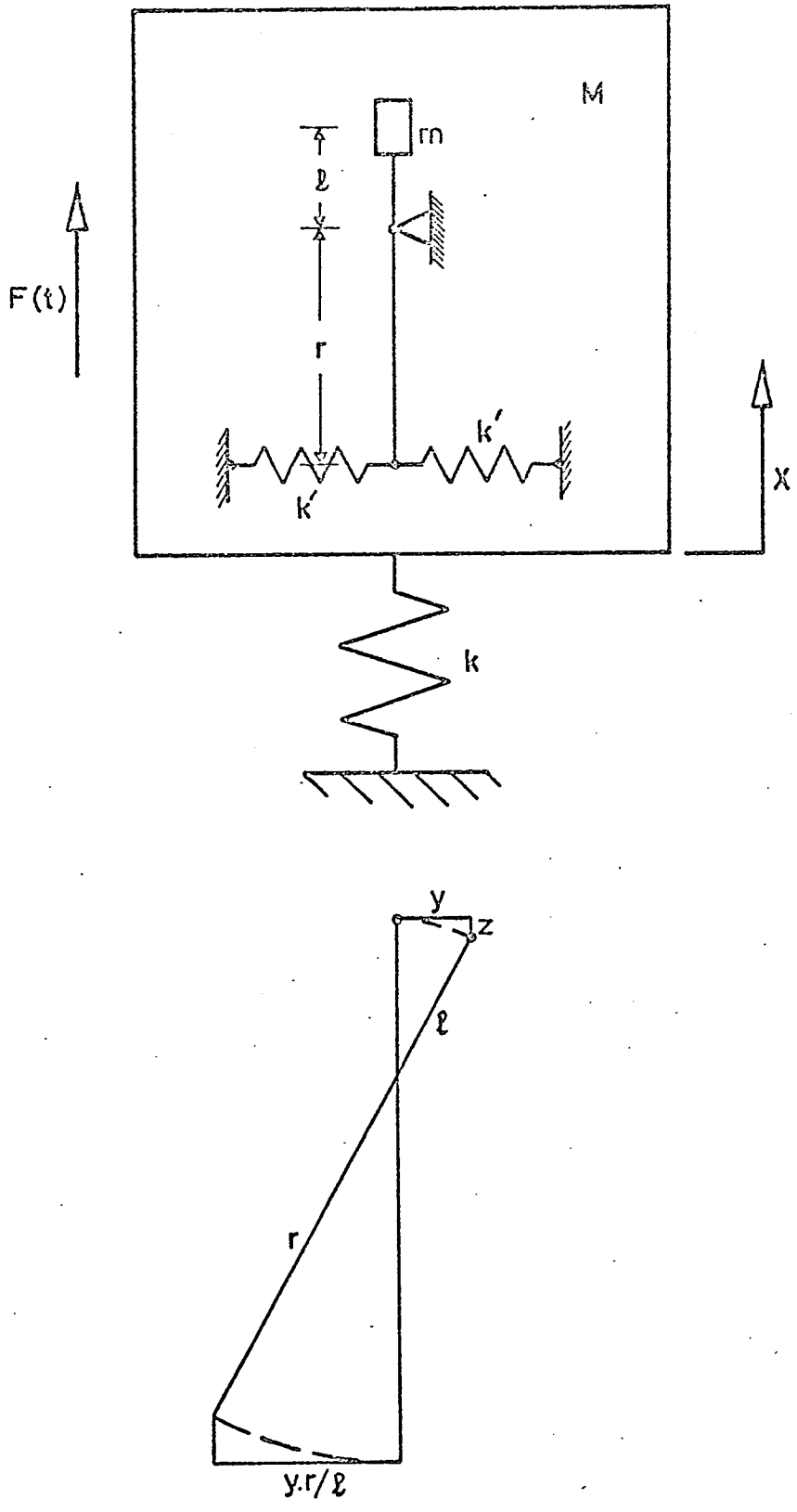

Fig. II.3.1

System 2.

Applying the Lagrangian formulation, the equations of motion are

$$(1 + \frac{m}{M})\ddot{X} + \frac{k}{M} X + (1 + \frac{m}{M})g - \frac{m}{M}\frac{\epsilon}{X_o}\left(\frac{\ell^2\dot{y}^2}{[\ell^2 - y^2]} + y\ddot{y}\right) = \frac{F(t)}{M} \qquad \text{II.3.1}$$

and $$\ddot{y} + \left(\frac{\lambda}{m} - \frac{\epsilon}{X_o} g - \frac{\epsilon}{X_o}\ddot{X}\right)y + \left(\frac{\epsilon}{X_o}\right)^2\left(\frac{\ell^2\dot{y}^2}{[\ell^2 - y^2]} + y\ddot{y}\right)y = 0$$

where $\epsilon = \dfrac{X_o}{[\ell^2 - y^2]^{\frac{1}{2}}}$ and $\lambda = 2\dfrac{r^2}{\ell^2} k'$

II.4 System 3

The final scheme for an improved AVA introduces an additional degree of freedom. Fig. II.4.1 shows the basic features in which the absorber end mass is now free to slide along the massless rigid arm of the pendulum. The three degrees of freedom are X, r (dynamic length of pendulum), and ϕ (angular displacement of arm).

The kinetic and potential energy functions are

$$T = \tfrac{1}{2} M\dot{X}^2 + \tfrac{1}{2} m[(\dot{r} + \dot{X}\cos\phi)^2 + (r\dot{\phi} - \dot{X}\sin\phi)^2]$$

and $$V = \tfrac{1}{2}\lambda_1 X^2 + \tfrac{1}{2}\lambda_2\phi^2 + \tfrac{1}{2}\lambda_3(r - \ell)^2$$

where λ_1, λ_2 and λ_3 are system stiffnesses and ℓ is the static length of the pendulum. (Note, gravitational effects have been ignored).

Applying the Lagrangian formulation once more, produces the following equations of motion,

$$(1 + \frac{m}{M})\ddot{X} + \frac{\lambda_1}{M} X + \frac{m}{M}[\ddot{r} - 2\dot{r}\phi\dot{\phi} - r(\dot{\phi}^2 + \phi\ddot{\phi})] = \frac{F(t)}{M}$$

$$\ddot{\phi} + \left(\frac{\lambda_2}{mr^2} - \frac{1}{r}\ddot{X}\right) + 2\frac{\dot{r}}{r}\dot{\phi} = 0$$

$$\ddot{r} + \frac{\lambda_3}{m}(r - \ell) + \ddot{X} - r\dot{\phi}^2 = 0$$

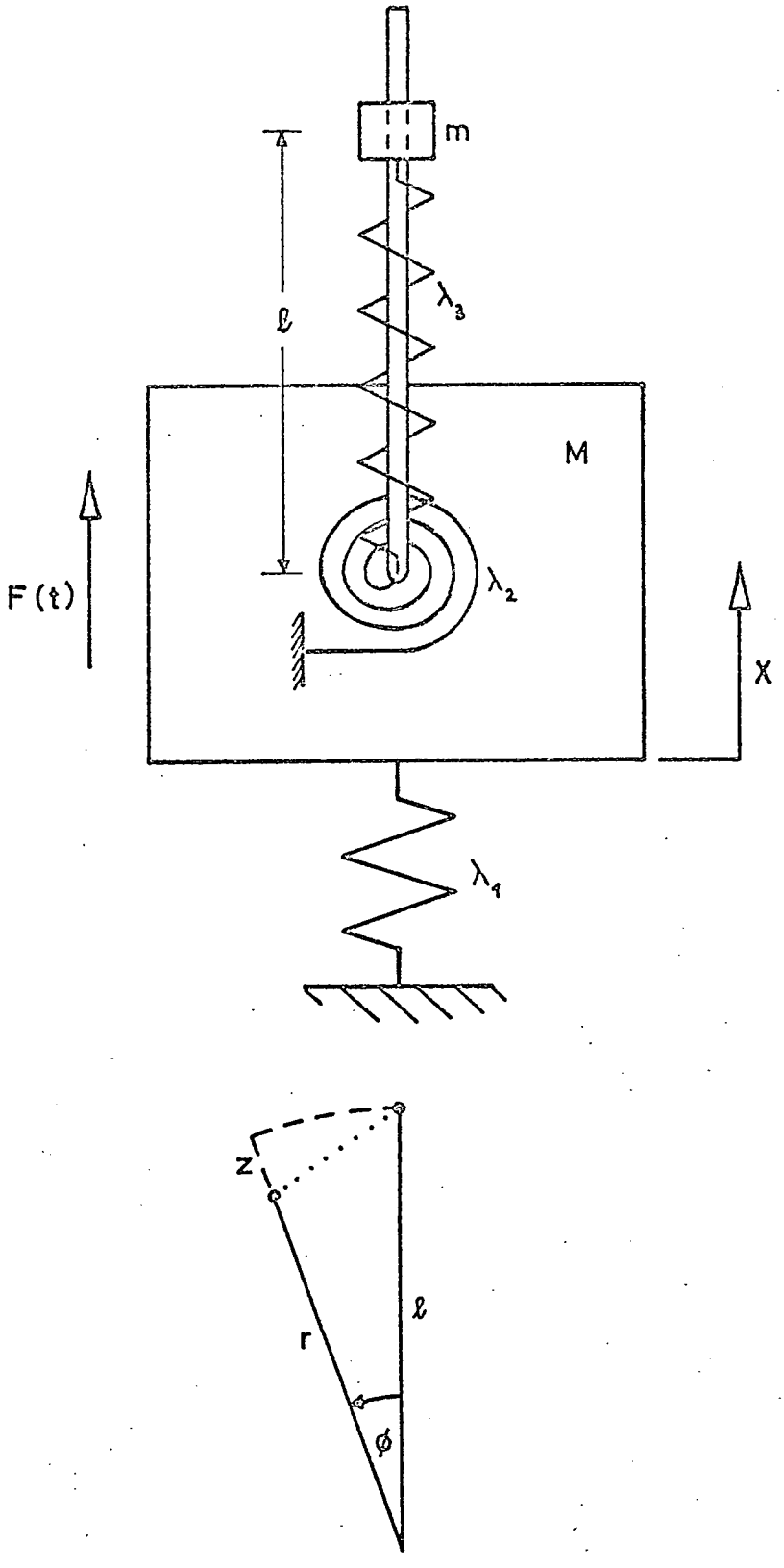

Fig. II.4.1

System 3.

On introducing a new variable $z = r - \ell$, the equations become

$$(1 + \frac{m}{M})\ddot{X} + \frac{\lambda_1}{M} X + \frac{m}{M}[\ddot{z} - 2\dot{z}\phi\dot{\phi} - (z + \ell)(\dot{\phi}^2 + \phi\ddot{\phi})] = \frac{F(t)}{M}$$

$$\ddot{\phi} + [\frac{\lambda_2}{m(z + \ell)^2} - \frac{\ddot{X}}{(z + \ell)}]\phi + \frac{2\dot{z}\dot{\phi}}{(z + \ell)} = 0$$

$$\ddot{z} + (\frac{\lambda_3}{m} - \dot{\phi}^2)z + \ddot{X} - \ell\dot{\phi}^2 = 0$$

... II.4.1

II.5 Comparison of the Theoretical Models

Systems 1 and 2 have equations of motion (II.2.1 and II.3.1) whose form is very similar to those of the cantilever model of Chapter 2 (II.1.1), and consequently it is expected that their solutions will also take the same form. It is only necessary then to consider the form taken by the ϵ parameters.

In System 1 it is seen that ϵ is large (here 'large' is a comparative term, ϵ remains small compared to unity) if the ratio $y/(R - r)$ approaches unity. Similarly in System 2, ϵ is large if the ratio y/ℓ tends to unity. Since there appears to be no mechanical constraints to designing these systems with the necessary geometry, an AVA system with absorbing capabilities comparable to any other type of absorber seems plausible.

The form of equations II.4.1 for System 3 makes any comparison between itself and the other systems very difficult. It is necessary to solve these equations using the technique of Chapter 2 and compare the form of its theoretical solution with that of the cantilever model. In the final section of this Appendix a possible means of solution is considered.

II.6 A Solution to System 3 Equations

The first step is to nondimensionalise the equations II.4.1 giving

$$\ddot{X} + R\ddot{z} + \omega_1^2 X - \epsilon R(\dot{\phi}^2 + \phi\ddot{\phi}) - \epsilon^2 R[2\dot{z}\dot{\phi}\dot{\phi} + z(\dot{\phi}^2 + \phi\ddot{\phi})] = \omega_1^2 \cos 2\Omega t$$

$$\ddot{\phi} + \omega_2^2 \phi + \epsilon(2z\ddot{\phi} + 2\dot{z}\dot{\phi} - \phi\ddot{X}) + \epsilon^2(z^2\ddot{\phi} + 2z\dot{z}\dot{\phi} - z\phi\ddot{X}) = 0$$

$$\ddot{z} + \ddot{X} + \omega_3^2 z - \epsilon\dot{\phi}^2 - \epsilon^2 z\dot{\phi}^2 = 0$$

... II.6.1

where $F(t) = F_o \cos 2\Omega t$, $X_o = F_o/\lambda_1$ and the above X, ϕ, z are the nondimensional quantities X/X_o, $\ell\phi/X_o$ and z/X_o.

The other quantities are defined thus,

$$R = m/(m + M) \ , \ \omega_1^2 = \lambda_1/(m + M) \ , \ \omega_2^2 = \lambda_2/m\ell^2,$$

$$\omega_2^3 = \lambda_3/m \ , \text{ and } \epsilon = X_o/\ell \ .$$

A glance at equations II.6.1 reveals the inertia coupling in the X and z modes, so the next step is to uncouple these modes replacing them with normal modes p_1 and p_2.

Consider the set of equations

$$\ddot{X} + R\ddot{z} + \omega_1^2 X = 0$$

$$\ddot{z} + \ddot{X} + \omega_3^2 z = 0 \qquad \text{II.6.2}$$

These equations have the form

$$A\ddot{q} + Cq = 0$$

where A is an inertia matrix, C a stiffness matrix and q a modal column vector.

By solving the characteristic equation $|A - \lambda I| = 0$ the eigenvalues (λ's) are obtained which, when substituted into the characteristic matrix, provide the eigenvectors of the system. These eigenvectors form a modal matrix, T, which is used in the transformation to normal co-ordinates thus

$$q = T\,p \qquad \text{II.6.3}$$

where p is a column vector of the normal co-ordinates.

Consequently the X and z equations in II.6.1 are replaced by equations of the form

$$\ddot{p} + T^{-1}\,A^{-1}\,C\,T\,p = T^{-1}\,A^{-1}\,f$$

where $T^{-1}\,A^{-1}\,C\,T$ is a diagonal matrix, Ω^2, of the eigenvalues and f is a column vector of the forcing functions.

Returing to equations II.6.2, their characteristic equation yields the eigenvalues

$$2\lambda_{1,2} = [(\omega_1^2 + \omega_3^2)/(1 - R)] \pm [\{(\omega_1^2 + \omega_3^2)^2/(1 - R)^2\} - 4\omega_1^2\omega_3^2/(1 - R)]^{\frac{1}{2}}$$

$$\text{or} \quad \lambda_{1,2} = \alpha \pm \beta \qquad \text{II.6.4}$$

where α, β are self-evident.

At this stage the question of system tuning must be discussed. In an attempt to 'marry' the potentialities of the AVA and LTDA systems it should be possible to tune the frequency of the absorber axial motion to that of the main mass and adjust the absorber's lateral frequency to half this amount.

In other words the desired internal resonance condition is

$$\lambda_1 = \lambda_2 = 4\omega_2^2 \quad \text{or} \quad \Omega_1 = \Omega_2 = 2\omega_2 \qquad \text{II.6.5}$$

where Ω_1 and Ω_2 are the frequencies of the normal modes p_1 and p_2 which replace X and z respectively.

This exact internal resonance condition (II.6.5) presents a problem however, in that the eigenvalues $\lambda_{1,2}$ become identical. From II.6.4,

$$\lambda_{1,2} = \alpha \; ; \quad \beta = 0$$

$$\text{i.e.} \quad \lambda_{1,2} = \tfrac{1}{2}(\omega_1^2 + \omega_3^2)/(1 - R) = \omega_1\omega_3/(1 - R)^{\frac{1}{2}} \qquad \text{II.6.6}$$

If the repeated eigenvalue II.6.6 is substituted into the characteristic matrix there emerges only one eigenvector,

$$\begin{bmatrix} \omega_3^2(1 - R)^{\frac{1}{2}} - \omega_1\omega_3 \\ \\ \omega_1 \;\; \omega_3 \end{bmatrix} \qquad \text{II.6.7}$$

In order to perform the transformation $q = T\,p$ it is necessary to have a modal matrix which is nonsingular, that is, which possesses an ~~adjoint~~ inverse, T^{-1} ($|T| \neq 0$). However a nonsingular modal matrix must have column vectors which are linearly independent of one another and so it is necessary to find another eigenvector, linearly independent of II.6.7, to form the modal matrix, T.

Although time did not permit a detailed study of this particular aspect, a brief survey of the literature did suggest that a generalised eigenvector was not easily obtained, especially when the characteristic matrix, $f(\lambda)$, is nonsymmetric, as in this case where,

$$f(\lambda) = \begin{bmatrix} \omega_1^2 - \lambda & -R\lambda \\ -\lambda & \omega_3^2 - \lambda \end{bmatrix} \qquad \text{II.6.8}$$

A method of avoiding this problem would be to assume a near resonance condition between modes p_1 and p_2 such that

$$\Omega_1 = \Omega_2 + O(\epsilon) \qquad \text{II.6.9}$$

This means that there are now two distinct eigenvalues

$$\lambda_1 = \alpha - \beta \quad \text{and} \quad \lambda_2 = \alpha + \beta \qquad \text{II.6.10}$$

where β is of the first order in ϵ.

Substituting II.6.10 into the characteristic matrix II.6.8 determines the two linearly independent eigenvectors,

$$\begin{bmatrix} \omega_3^2 - \alpha + \beta \\ \alpha - \beta \end{bmatrix} \text{ for } \lambda_1 \text{ and } \begin{bmatrix} \omega_3^2 - \alpha - \beta \\ \alpha + \beta \end{bmatrix} \text{ for } \lambda_2,$$

and thus the modal matrix is

$$T = \begin{bmatrix} \omega_3^2 - \alpha + \beta & \omega_3^2 - \alpha - \beta \\ \alpha - \beta & \alpha + \beta \end{bmatrix} = \begin{bmatrix} t_{11} & t_{21} \\ t_{12} & t_{22} \end{bmatrix} \qquad \text{II.6.11}$$

Performing the transformation II.6.3, yields

$$\begin{aligned} X &= t_{11}\, p_1 + t_{21}\, p_2 \\ z &= t_{12}\, p_1 + t_{22}\, p_2 \end{aligned} \qquad \text{II.6.12}$$

If the equations are considered to the first order in ϵ then the force vector, f, in the matrix equation,

$$\ddot{p} + \Omega^2 p = T^{-1} A^{-1} f$$

is $$\begin{bmatrix} \omega_1^2 \cos 2\Omega t + \epsilon R(\dot{\phi}^2 + \phi\ddot{\phi}) \\ \epsilon\dot{\phi}^2 \end{bmatrix}$$

and

$$T^{-1}A^{-1}f = \frac{1}{|T||A|} \begin{bmatrix} (t_{22} + Rt_{12})\{\omega_1^2 \cos 2\Omega t + \epsilon R(\dot{\phi}^2 + \phi\ddot{\phi})\} - (t_{22} + t_{12})\epsilon\dot{\phi}^2 \\ (t_{11} + t_{21})\epsilon\dot{\phi}^2 - (t_{21} + Rt_{11})\{\omega_1^2 \cos 2\Omega t + \epsilon R(\dot{\phi}^2 + \phi\ddot{\phi})\} \end{bmatrix}$$

where $|T|$ and $|A|$ are the determinants of the modal and inertia matrices respectively.

Therefore the equations of motion II.6.1 are uncoupled to give the following three equations in p_1, p_2 and ϕ,

$$\ddot{p}_1 + \Omega_1^2 p_1 = \frac{1}{|T|\,|A|}[(t_{22} + Rt_{12})\{\omega_1^2 \cos 2\Omega t + \epsilon R(\dot{\phi}^2 + \phi\ddot{\phi})\} - (t_{22} + t_{12})\epsilon\dot{\phi}^2]$$

$$\ddot{\phi} + \omega_2^2 \phi = -\epsilon[2\ddot{\phi}(t_{12}p_1 + t_{22}p_2) + 2\dot{\phi}(t_{12}\dot{p}_1 + t_{22}\dot{p}_2) - \phi(t_{11}\ddot{p}_1 + t_{21}\ddot{p}_2)]$$

$$\ddot{p}_2 + \Omega_2^2 p_2 = \frac{1}{|T|\,|A|}[(t_{21} + t_{11})\epsilon\dot{\phi}^2 - (t_{21} + Rt_{11})\{\omega_1^2 \cos 2\Omega t + \epsilon R(\dot{\phi}^2 + \phi\ddot{\phi})\}]$$

... II.6.13

Applying the asymptotic method of Chapter 2, equations II.6.13 are rewritten

$$\ddot{p}_1 + 4\Omega^2 p_1 = \epsilon[\epsilon^{-1}(4\Omega^2 - \Omega_1^2)p_1 + c_1 R(\dot{\phi}^2 + \phi\ddot{\phi}) - c_2\dot{\phi}^2 + c_1 P \cos 2\Omega t]$$

$$\ddot{\phi} + \Omega^2 \phi = \epsilon[\epsilon^{-1}(\Omega^2 - \omega_2^2)\phi + (t_{11}\ddot{p}_1 + t_{21}\ddot{p}_2)\phi - 2(t_{12}\dot{p}_1 + t_{22}\dot{p}_2)\dot{\phi} -$$

$$- 2(t_{12}p_1 + t_{22}p_2)\ddot{\phi}]$$

$$\ddot{p}_2 + 4\Omega^2 p_2 = \epsilon[\epsilon^{-1}(4\Omega^2 - \Omega_2^2)p_2 - c_3 R(\dot{\phi}^2 + \phi\ddot{\phi}) + c_4\dot{\phi}^2 - c_3 P \cos 2\Omega t]$$

... II.6.14

where $\epsilon P = \omega_1^2$, $c_1 = (t_{22} + Rt_{12})/|T|\,|A|$, $c_2 = (t_{22} + t_{12})/|T|\,|A|$, $c_3 = (t_{21} + Rt_{11})/|T|\,|A|$, $c_4 = (t_{21} + t_{11})/|T|\,|A|$,

and a solution taken in the form

$$p_1 = A\cos(\Omega_1 t + \alpha) + \epsilon p_{11} + \epsilon^2 p_{12} + \ldots$$

$$\phi = B\cos(\omega_2 t + \beta) + \epsilon\phi_1 + \epsilon^2\phi_2 + \ldots$$

$$p_2 = C\cos(\Omega_2 t + \mu) + \epsilon p_{21} + \epsilon^2 p_{22} + \ldots$$

... II.6.15

where each of A, B, C, α, β and μ is, in general, a function of time.

Substituting the solution II.6.15, to the first order in ϵ, into the equations of motion II.6.14 yields the following three equations

$$[\ddot{A} - A(\Omega_1 + \dot{\alpha})^2]\cos(\Omega_1 t + \alpha) - [A\ddot{\alpha} + 2\dot{A}(\Omega_1 + \dot{\alpha})]\sin(\Omega_1 t + \alpha)$$

$$+ \epsilon\ddot{p}_{11} + 4\Omega^2 A\cos(\Omega_1 t + \alpha) + 4\Omega^2\epsilon p_{11}$$

$$= \epsilon[\epsilon^{-1}(4\Omega^2 - \Omega_1^2)A\cos(\Omega_1 t + \alpha)] + \epsilon c_1 R[(B\ddot{B} + \dot{B}^2)\cos^2(\omega_2 t + \beta) -$$

$$- B^2(\omega_2 + \dot{\beta})^2\{\cos^2(\omega_2 t + \beta) - \sin^2(\omega_2 t + \beta)\} -$$

$$- \{B^2\ddot{\beta} + 4B\dot{B}(\omega_2 + \dot{\beta})\}\sin(\omega_2 t + \beta)\cos(\omega_2 t + \beta)]$$

$$- \epsilon c_2[\dot{B}^2\cos^2(\omega_2 t + \beta) + B^2(\omega_2 + \dot{\beta})^2\sin^2(\omega_2 t + \beta) - 2B\dot{B}(\omega_2 + \dot{\beta}).$$

$$.\sin(\omega_2 t + \beta)\cos(\omega_2 t + \beta)] + \epsilon c_1 P\cos 2\Omega t \qquad \text{II.6.16}$$

$$[\ddot{B} - B(\omega_2 + \dot{\beta})^2]\cos(\omega_2 t + \beta) - [B\ddot{\beta} + 2\dot{B}(\omega_2 + \dot{\beta})]\sin(\omega_2 t + \beta)$$

$$+ \epsilon\ddot{\phi}_1 + \Omega^2 B\cos(\omega_2 t + \beta) + \Omega^2\epsilon\phi_1$$

$$= \epsilon[\epsilon^{-1}(\Omega^2 - \omega_2^2)B\cos(\omega_2 t + \beta)] + \epsilon t_{11}[\{B\ddot{A} - AB(\Omega_1 + \dot{\alpha})^2\}\cos(\Omega_1 t + \alpha).$$

$$.\cos(\omega_2 t + \beta) - \{AB\ddot{\alpha} + 2B\dot{A}(\Omega_1 + \dot{\alpha})\}\sin(\Omega_1 t + \alpha)\cos(\omega_2 t + \beta)]$$

$$+ \epsilon t_{21}[\{B\ddot{C} - BC(\Omega_2 + \dot{\mu})^2\}\cos(\Omega_2 t + \mu)\cos(\omega_2 t + \beta) -$$

$$- \{BC\ddot{\mu} + 2B\dot{C}(\Omega_2 + \dot{\mu})\}\sin(\Omega_2 t + \mu)\cos(\omega_2 t + \beta)]$$

$$- 2\epsilon t_{12}[\dot{A}\dot{B}\cos(\Omega_1 t + \alpha)\cos(\omega_2 t + \beta) - B\dot{A}(\omega_2 + \dot{\beta})\cos(\Omega_1 t + \alpha)\sin(\omega_2 t + \beta) -$$

$$- A\dot{B}(\Omega_1 + \dot{\alpha})\sin(\Omega_1 t + \alpha)\cos(\omega_2 t + \beta) +$$

$$+ AB(\Omega_1 + \dot{\alpha})(\omega_2 + \dot{\beta})\sin(\Omega_1 t + \alpha)\sin(\omega_2 t + \beta)]$$

$$- 2\epsilon t_{22}[\dot{B}\dot{C}\cos(\Omega_2 t + \mu)\cos(\omega_2 t + \beta) - B\dot{C}(\omega_2 + \dot{\beta})\cos(\Omega_2 t + \mu).$$

$$.\sin(\omega_2 t + \beta) - C\dot{B}(\Omega_2 + \dot{\mu})\sin(\Omega_2 t + \mu)\cos(\omega_2 t + \beta) +$$

$$+ BC(\Omega_2 + \dot{\mu})(\omega_2 + \dot{\beta})\sin(\Omega_2 t + \mu)\sin(\omega_2 t + \beta)]$$

$$- 2\epsilon t_{12}[\{A\ddot{B} - AB(\omega_2 + \dot{\beta})^2\}\cos(\Omega_1 t + \alpha)\cos(\omega_2 t + \beta) -$$

$$- \{AB\ddot{\beta} + 2A\dot{B}(\omega_2 + \dot{\beta})\}\cos(\Omega_1 t + \alpha)\sin(\omega_2 t + \beta)]$$

$$- 2\epsilon t_{22}[\{C\ddot{B} - BC(\omega_2 + \dot{\beta})^2\}\cos(\Omega_2 t + \mu)\cos(\omega_2 t + \beta) -$$

$$- \{BC\ddot{\beta} + 2C\dot{B}(\omega_2 + \dot{\beta})\}\cos(\Omega_2 t + \mu)\sin(\omega_2 t + \beta)]$$

II.6.17

and

$$[\ddot{C} - C(\Omega_2 + \dot{\mu})^2\cos(\Omega_2 t + \mu) - [C\ddot{\mu} + 2\dot{C}(\Omega_2 + \dot{\mu})]\sin(\Omega_2 t + \mu)$$

$$+\epsilon\ddot{p}_{21} + 4\,\Omega^2 C\cos(\Omega_2 t + \mu) + 4\Omega^2\epsilon p_{21}$$

$$= \epsilon[\epsilon^{-1}(4\Omega^2 - \Omega_2{}^2)C\cos(\Omega_2 t + \mu)] - \epsilon c_3 R[(B\ddot{B} + \dot{B}^2)\cos^2(\omega_2 t + \beta) -$$

$$- B^2(\omega_2 + \dot{\beta})^2\{\cos^2(\omega_2 t + \beta) - \sin^2(\omega_2 t + \beta)\} -$$

$$- \{B^2\ddot{\beta} + 4B\dot{B}(\omega_2 + \dot{\beta})\}\sin(\omega_2 t + \beta)\cos(\omega_2 t + \beta)]$$

$$+\epsilon c_4[\dot{B}^2\cos^2(\omega_2 t + \beta) + B^2(\omega_2 + \dot{\beta})^2\sin^2(\omega_2 t + \beta) -$$

$$- 2B\dot{B}(\omega_2 + \dot{\beta})\sin(\omega_2 t + \beta)\cos(\omega_2 t + \beta)] - \epsilon c_3 P\cos 2\Omega t$$

II.6.18

Equations II.6.16 to II.6.18 provide a set of six first order variational equations, they include the resonant terms from the first order perturbation equations (not given here), and after simplification they may be written as

$$-2A\Omega_1\dot{\alpha} = \epsilon[\epsilon^{-1}(4\Omega^2 - \Omega_1{}^2)A - c_1 RB^2\omega_2{}^2\cos(2\beta - \alpha) + \tfrac{1}{2}c_2 B^2\omega_2{}^2.$$

$$.\cos(2\beta - \alpha) + c_1 P\cos\alpha]$$

$$-2\dot{A}\Omega_1 = \epsilon[c_1 RB^2\omega_2{}^2\sin(2\beta - \alpha) - \tfrac{1}{2}c_2 B^2\omega_2{}^2\sin(2\beta - \alpha) + c_1 P\sin\alpha]$$

$$-2B\omega_2\dot{\beta} = \epsilon[\epsilon^{-1}(\Omega^2 - \omega_2{}^2)B - \tfrac{1}{2}t_{11}AB\Omega_1{}^2\cos(2\beta - \alpha) -$$

$$- \tfrac{1}{2}t_{21}BC\Omega_2{}^2\cos(2\beta - \mu) + t_{12}AB\omega_2{}^2\cos(2\beta - \alpha) -$$

$$- t_{12}AB\Omega_1\omega_2\cos(2\beta - \alpha) + t_{22}BC\omega_2{}^2\cos(2\beta - \mu) - t_{22}BC\Omega_2\omega_2\cos(2\beta - \mu)]$$

$$-2\dot{B}\omega_2 = \epsilon[\ -\tfrac{1}{2}t_{11}AB\Omega_1{}^2\sin(2\beta - \alpha) - \tfrac{1}{2}t_{21}BC\Omega_2{}^2\sin(2\beta - \mu) +$$

$$+ t_{12}AB\omega_2{}^2\sin(2\beta - \alpha) - t_{12}AB\Omega_1\omega_2\cos(2\beta - \alpha) +$$

$$+ t_{22}BC\omega_2{}^2\sin(2\beta - \mu) - t_{22}BC\Omega_2\omega_2\cos(2\beta - \mu)]$$

$$-2\dot{B}\omega_2 = \epsilon[-\tfrac{1}{2}t_{11}AB\Omega_1{}^2\sin(2\beta-\alpha) - \tfrac{1}{2}t_{21}BC\Omega_2{}^2\sin(2\beta-\mu) +$$

$$+ t_{12}AB\omega_2{}^2\sin(2\beta-\alpha) - t_{12}AB\Omega_1\omega_2\cos(2\beta-\alpha) +$$

$$+ t_{22}BC\omega_2{}^2\sin(2\beta-\mu) - t_{22}BC\Omega_2\omega_2\cos(2\beta-\mu)]$$

$$-2C\Omega_2\dot{\mu} = \epsilon[\epsilon^{-1}(4\Omega^2 - \Omega_2{}^2)C + c_3RB^2\omega_2{}^2\cos(2\beta-\mu) -$$

$$-\tfrac{1}{2}c_4B^2\omega_2{}^2\cos(2\beta-\mu) - c_3P\cos\mu]$$

$$-2\dot{C}\Omega_2 = \epsilon[-c_3RB^2\omega_2{}^2\sin(2\beta-\mu) + \tfrac{1}{2}c_4B^2\omega_2{}^2\sin(2\beta-\mu) - c_3P\sin\mu]$$

Equations II.6.19 represent the first order variational equations of this combined AVA-LTDA system where the resonance conditions are chosen to be

$$\Omega_1 = \Omega_2 + O(\epsilon) = 2\omega_2 \quad \text{(internal)}$$

and

$$2\Omega = \Omega_1 + O(\epsilon) \qquad \text{(external)} \qquad \text{II.6.20}$$

Once again it is convenient to transform the variables thus

$$t = 4\tau/\epsilon\sqrt{PR} \;\; ; \;\; \gamma = (\omega_2{}^2 - \Omega^2)/\epsilon\omega_2\sqrt{PR} \;\; ;$$

$$A = b_1\sqrt{P}/\omega_2\sqrt{R} \;\; ; \;\; B = b_2\sqrt{P}/\omega_2\sqrt{R} \;\; ; \;\; C = b_3\sqrt{P}/\omega_2\sqrt{R} \;\; ;$$

$$\alpha = \psi_1 \;\; ; \;\; \beta = \psi_2 \;\; ; \;\; \mu = \psi_3 \qquad \text{II.6.21}$$

The resulting variational equations are

$$b_1\psi_1' = 4\gamma b_1 + c_1 b_2^2\cos(2\psi_2 - \psi_1) - (c_2/2R)b_2^2\cos(2\psi_2 - \psi_1) - c_1\cos\psi_1$$

$$b_1' = -c_1 b_2^2\sin(2\psi_2 - \psi_1) + (c_2/2R)b_2^2\sin(2\psi_2 - \psi_1) - c_1\sin\psi_1$$

$$b_2\psi_2' = 2\gamma b_2 + (2/R)(2t_{11} + t_{12})b_1 b_2\cos(2\psi_2 - \psi_1) + (2/R)(2t_{21} + t_{22}).$$

$$\cdot\ b_2 b_3\cos(2\psi_2 - \psi_3)$$

$$b_2' = (2/R)(2t_{11} + t_{12})b_1 b_2\sin(2\psi_2 - \psi_1) + (2/R)(2t_{21} + t_{22}).$$

$$\cdot\ b_2 b_3\sin(2\psi_2 - \psi_3)$$

$$b_3\psi_3' = 4\gamma b_3 - c_3 b_2^2\cos(2\psi_2 - \psi_3) + (c_4/2R)b_2^2\cos(2\psi_2 - \psi_3) + c_3\cos\psi_3$$

$$b_3' = c_3 b_2^2\sin(2\psi_2 - \psi_3) - (c_4/2R)b_2^2\sin(2\psi_2 - \psi_3) + c_3\sin\psi_3$$

... II.6.22

where primes denote differentiation with respect to slow time, τ.

The steady-state solution is found by equating the right-hand sides of II.6.22 to zero. After some algebra a solution for b_1 can be obtained in the form

$$b_1 = \frac{\gamma R}{(c_3/c_1)(2t_{21} + t_{22})\sin(2\psi_2 - \psi_1)\operatorname{ctn}(2\psi_2 - \psi_3) - (2t_{11} + t_{12})\cos(2\psi_2 - \psi}$$

II.6.23

Unfortunately b_1 is not independent of the phase angles, perhaps more algebraic manipulation might remedy this, however at present, time does not allow a more detailed study.

Note, the form of II.6.23 may be compared with the corresponding result for the cantilever AVA,

$$b_1 = \pm \tfrac{1}{2}\gamma R$$

APPENDIX III

THE METHOD OF AVERAGING AND THE TWO - VARIABLE EXPANSION PROCEDURE

It was mentioned in Chapter 2 that three methods of solution of the AVA system equations had proved successful. The asymptotic method presented in Chapter 2 was considered the most effective but a study of the other procedures is not without interest. This Appendix presents the method of averaging and the two-variable expansion procedure.

III.1 Method of Averaging

The system equations are written in the form

$$\ddot{X} + 4\Omega^2 X = \epsilon[\epsilon^{-1}(4\Omega^2 - \omega_1{}^2)X + R(\dot{y}^2 + y\ddot{y}) + P\cos 2\Omega t]$$

$$\ddot{y} + \Omega^2 y = \epsilon[\epsilon^{-1}(\Omega^2 - \omega_2{}^2)y + \ddot{X}y] \qquad \text{III.1.1}$$

Note, damping terms have been omitted together with the ϵ^2 term in the y equation.

Once again the sinusoidal exciting force is assumed to be of the same order in ϵ as the nonlinear terms, permitting the study of the physically interesting solutions that occur when the frequency of the exciting force is in the neighbourhood of either of the linear natural frequencies of the system.

It is assumed that

$$|4\Omega^2 - \omega_1{}^2| < \epsilon \; ; \quad |\Omega^2 - \omega_2{}^2| < \epsilon \qquad \text{III.1.2}$$

Choose solutions of the form

$$X = A_1(t)\cos(2\Omega t + \Psi_1(t)) \; ; \; \dot{X} = -2\Omega A_1(t)\sin(2\Omega t + \Psi_1(t))$$

$$y = A_2(t)\cos(\Omega t + \Psi_2(t)) \; ; \; \dot{y} = -\Omega A_2(t)\sin(\Omega t + \Psi_2(t)) \qquad \text{III.1.3}$$

The form of III.1.3 requires that

$$-A_1\dot{\Psi}_1\sin\theta_1 + \dot{A}_1\cos\theta_1 = 0$$

$$-A_2\dot{\Psi}_2\sin\theta_2 + \dot{A}_2\cos\theta_2 = 0 \qquad \text{III.1.4}$$

where $\theta_1 = (2\Omega t + \Psi_1)$, $\theta_2 = (\Omega t + \Psi_2)$ III.1.5

From III.1.3

$$\ddot{X} = -2\Omega\dot{A}_1\sin\theta_1 - 2\Omega A_1(2\Omega + \dot{\Psi}_1)\cos\theta_1$$

$$\ddot{y} = -\Omega\dot{A}_2\sin\theta_2 - \Omega A_2(\Omega + \dot{\Psi}_2)\cos\theta_2 \qquad \text{III.1.6}$$

Using III.1.3, III.1.5 and III.1.6, equations III.1.1 become

$$-2\Omega\dot{A}_1\sin\theta_1 - 2\Omega A_1\dot{\Psi}_1\cos\theta_1 = \epsilon[\epsilon^{-1}(4\Omega^2 - \omega_1^2)A_1\cos\theta_1 - R\Omega^2B^2\cos2\theta_2 + P\cos2\Omega t]$$

$$-\Omega\dot{A}_2\sin\theta_2 - \Omega A_2\dot{\Psi}_2\cos\theta_2 = \epsilon[\epsilon^{-1}(\Omega^2 - \omega_2^2)A_2\cos\theta_2 - 4\Omega^2A_1A_2\cos\theta_1\cos\theta_2]$$

... III.1.7

where terms on the right such as $\epsilon A_2\dot{A}_2$, $\epsilon A_2\dot{A}_1$ and $\epsilon A_2^2\dot{\Psi}_2$ have been dropped because they are of the second order in ϵ.

Combining III.1.4 and III.1.7 leads to four variational equations,

$$\dot{A}_1 = -(\epsilon/2\Omega)[\epsilon^{-1}(4\Omega^2 - \omega_1^2)A_1\cos\theta_1\sin\theta_1 - R\Omega^2A_2^2\cos2\theta_2\sin\theta_1 +$$

$$+ P\cos2\Omega t\sin\theta_1]$$

$$A_1\dot{\Psi}_1 = -(\epsilon/2\Omega)[\epsilon^{-1}(4\Omega^2 - \omega_1^2)A_1\cos^2\theta_1 - R\Omega^2A_2^2\cos2\theta_2\cos\theta_1 + P\cos2\Omega t\cos\theta_1]$$

$$\dot{A}_2 = -(\epsilon/\Omega)[\epsilon^{-1}(\Omega^2 - \omega_2^2)A_2\cos\theta_2\sin\theta_2 - 4\Omega^2 A_1 A_2\cos\theta_1\cos\theta_2\sin\theta_2]$$

$$A_2\dot{\Psi}_2 = -(\epsilon/\Omega)[\epsilon^{-1}(\Omega^2 - \omega_2^2)A_2\cos^2\theta_2 - 4\Omega^2 A_1 A_2\cos\theta_1\cos^2\theta_2]$$

... III.1.8

Equations III.1.8 can now be written in complex form, suitable for the application of the method of averaging, thus

$$\dot{A}_1 = -(\epsilon/4i\Omega)[\tfrac{1}{2}\epsilon^{-1}(4\Omega^2 - \omega_1^2)A_1(e^{i2\theta_1} - e^{-i2\theta_1}) -$$

$$- \tfrac{1}{2}R\,\Omega^2 A_2^2(e^{i(2\theta_2 + \theta_1)} - e^{-i(2\theta_2 + \theta_1)} - e^{i(2\theta_2 - \theta_1)} + e^{-i(2\theta_2 - \theta_1)}) +$$

$$+ \tfrac{1}{2}P(e^{i(2\Omega t + \theta_1)} - e^{-i(2\Omega t + \theta_1)} - e^{i(2\Omega t - \theta_1)} + e^{-i(2\Omega t - \theta_1)})]$$

$$A_1\dot{\Psi}_1 = -(\epsilon/4\Omega)[\tfrac{1}{2}\epsilon^{-1}(4\Omega^2 - \omega_1^2)A_1(2 + e^{i2\theta_1} + e^{-i2\theta_1}) -$$

$$- \tfrac{1}{2}R\Omega^2 A_2^2(e^{i(2\theta_2 + \theta_1)} + e^{-i(2\theta_2 + \theta_1)} + e^{i(2\theta_2 - \theta_1)} + e^{-i(2\theta_2 - \theta_1)}) -$$

$$+ \tfrac{1}{2}P(e^{i(2\Omega t + \theta_1)} + e^{-i(2\Omega t + \theta_1)} + e^{i(2\Omega t - \theta_1)} + e^{-i(2\Omega t - \theta_1)})]$$

$$\dot{A}_2 = -(\epsilon/2i\Omega)[\tfrac{1}{2}\epsilon^{-1}(\Omega^2 - \omega_2^2)A_2(e^{i2\theta_2} - e^{-i2\theta_2}) -$$

$$- \Omega^2 A_1 A_2(e^{i(2\theta_2 + \theta_1)} - e^{-i(2\theta_2 + \theta_1)} + e^{i(2\theta_2 - \theta_1)} - e^{-i(2\theta_2 - \theta_1)})]$$

$$A_2\dot{\Psi}_2 = -(\epsilon/2\Omega)[\tfrac{1}{2}\epsilon^{-1}(\Omega^2 - \omega_2^2)A_2(2 + e^{i2\theta_2} + e^{-i2\theta_2}) -$$

$$- \Omega^2 A_1 A_2(2e^{i\theta_1} + 2e^{-i\theta_1} + e^{i(2\theta_2 + \theta_1)} + e^{-i(2\theta_2 + \theta_1)} +$$

$$+ e^{i(2\theta_2 - \theta_1)} + e^{-i(2\theta_2 - \theta_1)})]$$

... III.1.9

III.1.9 are relationships of the form

$$\dot{A}_n = \epsilon F_n(A_1, A_2, \Psi_1, \Psi_2, t)$$

$$\dot{\Psi}_n = \epsilon G_n(A_1, A_2, \Psi_1, \Psi_2, t) \qquad \text{III.1.10}$$

The method of averaging introduces new variables $a_n(t)$ and $\psi_n(t)$ such that

$$A_n = a_n + \epsilon\tilde{F}_n(a_1, a_2, \psi_1, \psi_2, t)$$
$$\Psi_n = \psi_n + \epsilon\tilde{G}_n(a_1, a_2, \psi_1, \psi_2, t) \qquad \text{III.1.11}$$

where $\tilde{F}_n$ and $\tilde{G}_n$ are the indefinite integrals of F_n and G_n, excluding those terms in F_n and G_n that are independent of t. ($\tilde{F}_n$ and $\tilde{G}_n$ are functions of zero order in ϵ). The functions a_n and ψ_n satisfy the following averaged equations,

$$\dot{a}_n = \epsilon M_t\{F_n\}$$
$$\dot{\psi}_n = \epsilon M_t\{G_n\} \qquad \text{III.1.12}$$

where the operator M_t is defined thus

$$M_t\{Q\} = \lim_{T\to\infty} \frac{1}{T}\int_o^T Q\, dt \qquad \text{III.1.13}$$

The integration III.1.3 is performed with respect to explicitly occurring t in Q.

Consider terms like $e^{i2\theta_1}$, $e^{i(2\theta_2 - \theta_1)}$ and $e^{i(2\Omega t - \theta_1)}$ in equations III.1.9, remembering that now $\theta_1 = (2\Omega t + \psi_1)$ and $\theta_2 = (\Omega t + \psi_2)$, then

$$\frac{1}{T}\int_o^T e^{i2\theta_1}\, dt = \frac{1}{T}\int_o^T e^{i2(2\Omega t + \psi_1)} dt \to 0 \text{ as } T\to\infty$$

$$\frac{1}{T}\int_o^T e^{i(2\theta_2 - \theta_1)} dt = \frac{1}{T} e^{i(2\psi_2 - \psi_1)}\int_o^T e^{i(2\Omega t - 2\Omega t)} dt \to e^{i(2\psi_2 - \psi_1)} \text{ as } T\to\infty$$

$$\frac{1}{T}\int_o^T e^{i(2\Omega t - \theta_1)} dt = \frac{1}{T} e^{-i\psi_1}\int_o^T e^{i(2\Omega t - 2\Omega t)} dt \to e^{-i\psi_1} \text{ as } T\to\infty$$

Hence III.1.9 became,

$$\dot{a}_1 = -(\epsilon/4i\Omega)[-\tfrac{1}{2}R\Omega^2 a_2{}^2(-e^{i(2\psi_2 - \psi_1)} + e^{-i(2\psi_2 - \psi_1)}) +$$

$$+ \tfrac{1}{2}P(-e^{-i\psi_1} + e^{i\psi_1})]$$

$$a_1\dot{\psi}_1 = -(\epsilon/4\Omega)[\epsilon^{-1}(4\Omega^2 - \omega_1{}^2)a_1 - \tfrac{1}{2}R\Omega^2 a_2{}^2(e^{i(2\psi_2 - \psi_1)} + e^{-i(2\psi_2 - \psi_1)}) +$$

$$+ \tfrac{1}{2}P(e^{-i\psi_1} + e^{i\psi_1})]$$

$$\dot{a}_2 = -(\epsilon/2i\Omega)[-\Omega^2 a_1 a_2(e^{i(2\psi_2 - \psi_1)} - e^{-i(2\psi_2 - \psi_1)})]$$

$$a_2\dot{\psi}_2 = -(\epsilon/2\Omega)[\epsilon^{-1}(\Omega^2 - \omega_2{}^2)a_2 - \Omega^2 a_1 a_2(e^{i(2\psi_2 - \psi_1)} + e^{-i(2\psi_2 - \psi_1)})]$$

... III.1.14

It is now assumed that the condition of external resonance holds, namely that

$$\omega_1 = 2\omega_2$$

so that equations III.1.14 become, in trigonometric form,

$$\dot{a}_1 = -(\epsilon/2\omega_2)[\tfrac{1}{2}R\omega_2{}^2 a_2{}^2 \sin(2\psi_2 - \psi_1) + \tfrac{1}{2}P\sin\psi_1]$$

$$a_1\dot{\psi}_1 = -(\epsilon/2\omega_2)[2\epsilon^{-1}(\Omega^2 - \omega_2{}^2)a_1 - \tfrac{1}{2}R\omega_2{}^2 a_2{}^2\cos(2\psi_2 - \psi_1) + \tfrac{1}{2}P\cos\psi_1]$$

$$\dot{a}_2 = -(\epsilon/2\omega_2)[-2\omega_2{}^2 a_1 a_2 \sin(2\psi_2 - \psi_1)]$$

$$a_2\dot{\psi}_2 = -(\epsilon/2\omega_2)[\epsilon^{-1}(\Omega^2 - \omega_2{}^2)a_2 - 2\omega_2{}^2 a_1 a_2\cos(2\psi_2 - \psi_1)]$$

... III.1.15

Equations III.1.15 may now be transformed using the change of variables introduced in Chapter 2,

$$t = (4/\epsilon)\,(PR)^{-\frac{1}{2}}\tau \quad ; \quad \gamma = (1/\epsilon\omega_2)\,(PR)^{-\frac{1}{2}}\,(\omega_2{}^2 - \Omega^2) \quad ;$$

$$a_1 = (P/R)^{\frac{1}{2}}\,b_1/\omega_2 \quad ; \quad a_2 = (P/R)^{\frac{1}{2}}\,b_2/\omega_2 \qquad \text{III.1.16}$$

This provides the convenient form

$$b_1' = -b_2^2 \sin(2\psi_2 - \psi_1) - \sin\psi_1$$

$$b_1\psi_1' = 4\gamma b_1 + b_2^2 \cos(2\psi_2 - \psi_1) - \cos\psi_1$$

$$b_2' = (4/R) b_1 b_2 \sin(2\psi_2 - \psi_1)$$

$$b_2\psi_2' = 2\gamma b_2 + (4/R) b_1 b_2 \cos(2\psi_2 - \psi_1) \qquad \text{... III.1.17}$$

where primes denote differentiation with respect to slow time τ.

This completes the study of the method of averaging, it can be seen that equations III.1.17 are the same as equations 2.4.29 without the damping terms.

III.2 Two-Variable Expansion Procedure

The equations of motion for the undamped system are

$$\ddot{X} + 4\Omega^2 X = \epsilon[\epsilon^{-1}(4\Omega^2 - \omega_1^2)X + R(\dot{y}^2 + y\ddot{y}) + P\cos 2\Omega t]$$

$$\ddot{y} + \Omega^2 y = \epsilon[\epsilon^{-1}(\Omega^2 - \omega_2^2)y + \ddot{X}y] \qquad \text{III.2.1}$$

(Again ϵ^2 term in y equation has been omitted.)

It is suitable to rewrite these equations as follows,

$$4\Omega^2 X'' + 4\Omega^2 X = \epsilon[\epsilon^{-1}(4\Omega^2 - \omega_1^2)X + 4R\Omega^2(y'^2 + yy'') + P\cos t^*]$$

$$4\Omega^2 y'' + \Omega^2 y = \epsilon[\epsilon^{-1}(\Omega^2 - \omega_2^2)y + 4\Omega^2 X''y] \qquad \text{III.2.2}$$

where primes denote differentiation with respect to time $t^* = 2\Omega t$.

Exact internal resonance is assumed so that $\omega_1 = 2\omega_2$, and with $\omega_1/2\Omega = \omega_2/\Omega = Q$, $G = P/4\Omega^2$ equations III.2.2 become

$$\ddot{X} + X = \epsilon[\epsilon^{-1}(1 - Q^2)X + R(\dot{y}^2 + y\ddot{y}) + G\cos t^*]$$

$$\ddot{y} + \tfrac{1}{4} y = \epsilon[\tfrac{1}{4}\epsilon^{-1}(1 - Q^2)\, y + \ddot{X}y] \qquad \text{III.2.3}$$

Now choose two time scales t_1 and t_2 such that

$$t_1 = t^*(1 + \epsilon^2 \omega + ..)$$

$$t_2 = \epsilon t^* \qquad \text{III.2.4}$$

and write a solution in the form of an expansion in the two variables t_1 and t_2,

$$X(t^*, \epsilon) = F_o(t_1, t_2) + \epsilon F_1(t_1, t_2) + \epsilon^2 F_2(t_1, t_2) + \ldots$$

$$y(t^*, \epsilon) = E_o(t_1, t_2) + \epsilon E_1(t_1, t_2) + \epsilon^2 E_2(t_1, t_2) + \ldots \qquad \text{III.2.5}$$

Then

$$\dot{X} = \frac{\partial F_o}{\partial t_1}\frac{dt_1}{dt^*} + \frac{\partial F_o}{\partial t_2}\frac{dt_2}{dt^*} + \frac{\epsilon\partial F_1}{\partial t_1}\frac{dt_1}{dt^*} + \frac{\epsilon\partial F_1}{\partial t_2}\frac{dt_2}{dt^*} + \ldots$$

$$\ddot{X} = \frac{\partial}{\partial t_1}[\dot{X}]\frac{dt_1}{dt^*} + \frac{\partial}{\partial t_2}[\dot{X}]\frac{dt_2}{dt^*}$$

$$\dot{y} = \frac{\partial E_o}{\partial t_1}\frac{dt_1}{dt^*} + \frac{\partial E_o}{\partial t_2}\frac{dt_2}{dt^*} + \frac{\epsilon\partial E_1}{\partial t_1}\frac{dt_1}{dt^*} + \frac{\epsilon\partial E_1}{\partial t_2}\frac{dt_2}{dt^*} + \ldots$$

$$\ddot{y} = \frac{\partial}{\partial t_1}[\dot{y}]\frac{dt_1}{dt^*} + \frac{\partial}{\partial t_2}[\dot{y}]\frac{dt_2}{dt^*} \qquad \ldots \text{III.2.6}$$

Note that $\frac{dt_1}{dt^*} = 1$ and $\frac{dt_2}{dt^*} = \epsilon$ from III.2.4

Substituting the solution (III.2.5, III.2.6) into the equations III.2.3 provides sets of equations in the perturbation functions F_o, E_o, F_1, E_1, etc.

Thus to order ϵ^0,

$$\frac{\partial^2 F_0}{\partial t_1^2} + F_0 = 0 \quad ; \quad \frac{\partial^2 E_0}{\partial t_1^2} + \tfrac{1}{4} E_0 = 0$$

and the solutions for F_0 and E_0 have the form

$$F_0 = A_0(t_2)\cos(t_1 + B_0(t_2))$$

$$E_0 = C_0(t_2)\cos((t_1/2) + D_0(t_2)) \qquad \text{III.2.7}$$

To order ϵ^1

$$\frac{\partial^2 F_1}{\partial t_1^2} + F_1 = \epsilon^{-1}(1 - Q^2)F_0 - \frac{2\partial^2 F_0}{\partial t_1 \partial t_2} + R\left[\left(\frac{\partial E_0}{\partial t_1}\right)^2 + E_0 \frac{\partial^2 E_0}{\partial t_1^2}\right] + G\cos t_1$$

$$\frac{\partial^2 E_1}{\partial t_1^2} + \tfrac{1}{4} E_1 = \tfrac{1}{4}\epsilon^{-1}(1 - Q^2)E_0 - 2\frac{\partial^2 E_0}{\partial t_1 \partial t_2} + E_0 \frac{\partial^2 F_0}{\partial t_1^2} \qquad \text{III.2.8}$$

Substituting III.2.7 into III.2.8 and using the usual trigonometric identities, there results

$$\begin{aligned}\frac{\partial^2 F_1}{\partial t_1^2} + F_1 = {} & \epsilon^{-1}(1 - Q^2)A_0\cos(t_1 + B_0) + 2A_0' \sin(t_1 + B_0) \\ & + 2A_0 B_0' \cos(t_1 + B_0) - \tfrac{1}{4} RC_0^2 \cos(t_1 + B_0)\cos(2D_0 - B_0) \\ & + \tfrac{1}{4} RC_0^2 \sin(t_1 + B_0)\sin(2D_0 - B_0) \\ & + G\cos(t_1 + B_0)\cos B_0 + G\sin(t_1 + B_0)\sin B_0\end{aligned}$$

and

$$\begin{aligned}\frac{\partial^2 E_1}{\partial t_1^2} + \tfrac{1}{4} E_1 = {} & \tfrac{1}{4}\epsilon^{-1}(1 - Q^2)C_0 \cos((t_1/2) + D_0) + C_0' \sin((t_1/2) + D_0) \\ & + C_0 D_0' \cos((t_1/2) + D_0) - \tfrac{1}{2} A_0 C_0 \cos((t_1/2) + D_0)\cos(2D_0 - B_0) \\ & - \tfrac{1}{2} A_0 C_0 \sin((t_1/2) + D_0)\sin(2D_0 - B_0) - \tfrac{1}{2} A_0 C_0 \cos((3t_1/2) + \\ & + B_0 + D_0)\end{aligned}$$

where primes now denote differentiation with respect to t_2.

For F_1 and E_1 bounded the coefficients of $\cos(t_1 + B_o)$ give

$$\epsilon^{-1}(1 - Q^2)A_o + 2A_oB_o' - \tfrac{1}{4} RC_o^2\cos(2D_o - B_o) + G\cos B_o = 0$$

Similarly the coefficients of $\sin(t_1 + B_o)$ give

$$2A_o' + \tfrac{1}{4} RC_o^2\sin(2D_o - B_o) + G\sin B_o = 0$$

While coefficients of $\cos((t_1/2) + D_o)$ yield

$$\tfrac{1}{4}\epsilon^{-1}(1 - Q^2)C_o + C_oD_o' - \tfrac{1}{2} A_oC_o\cos(2D_o - B_o) = 0$$

and those of $\sin((t_1/2) + D_o)$ give

$$C_o' - \tfrac{1}{2} A_oC_o\sin(2D_o - B_o) = 0$$

... III.2.9

Equations III.2.9 may be transformed to real time t using

$$\frac{d}{dt_2} = \frac{1}{2\Omega\epsilon}\frac{d}{dt}$$

Thus, III.2.9 become

$$A_o\dot{B}_o = -(\epsilon/4\Omega)[\epsilon^{-1}(4\Omega^2 - \omega_1^2)A_o - R\,\Omega^2C_o^2\cos(2D_o - B_o) + P\cos B_o]$$

$$\dot{A}_o = -(\epsilon/4\Omega)[R\,\Omega^2C_o^2\sin(2D_o - B_o) + P\sin B_o]$$

$$C_o\dot{D}_o = -(\epsilon/2\Omega)[\epsilon^{-1}(\Omega^2 - \omega_2^2)C_o - 2\Omega^2A_oC_o\cos(2D_o - B_o)]$$

$$\dot{C}_o = -(\epsilon/2\Omega)[-2\Omega^2A_oC_o\sin(2D_o - B_o)]$$

... III.2.10

where dots denote differentiation with respect to t.

If the usual transformation of variables is made, namely

$$t = (4/\epsilon)(PR)^{\frac{1}{2}}\tau \quad ; \quad \gamma = (1/\epsilon\omega_2)(PR)^{-\frac{1}{2}}(\omega_2^2 - \Omega^2) \quad ;$$

$$A_o = (P/R)^{\frac{1}{2}} b_1/\omega_2 \quad ; \quad C_o = (P/R)^{\frac{1}{2}} b_2/\omega_2 \quad ; \quad B_o = \psi_1 \; ; \; D_o = \psi_2$$

III.2.11

then equations III.2.10 assume the familiar form

$$b_1\psi_1' = 4\gamma b_1 + b_2^2\cos(2\psi_2 - \psi_1) - \cos\psi_1$$

$$b_1' = -b_2^2\sin(2\psi_2 - \psi_1) - \sin\psi_1$$

$$b_2\psi_2' = 2\gamma b_2 + (4/R)b_1 b_2 \cos(2\psi_2 - \psi_1)$$

$$b_2' = (4/R)b_1 b_2 \sin(2\psi_2 - \psi_1)$$

... III.2.12

where primes denote differentiation with respect to τ.

Equations III.2.12, III.1.17 and 2.4.29 (without its damping terms) are the same equations, showing the equivalence of the two methods described here to that used in Chapter 2. It then becomes a matter of preference as to which method to use. The method of averaging involves lengthy transfers from trigonometric to complex functions and vice versa as well as considerable integration, while the two-variable technique does not provide the physical insight of the asymptotic method.

Thus the asymptotic method used in Chapter 2 emerges as the best technique both for its brevity and for the physical interpretation it lends during its application in that it highlights the important behaviour of the so-called resonant terms.

APPENDIX IV

A NOTE ON THE BEHAVIOUR OF THE AVA UNDER RANDOM EXCITATION

Although this present investigation has been limited to a study of the performance of the AVA under deterministic external excitation of the main mass system, its response to random excitation is of considerable interest. No attempt is made here to present a theoretical analysis of this particular aspect but a brief survey of the literature would suggest that a study of systems with randomly varying parameters under random excitation has been restricted to the linear case. (See, for example, the series of papers by Ariaratnam and Graefe). Such linear systems are governed by a stochastic differential equation of the form

$$d\left(\frac{d^{n-1}z}{dt^{n-1}}\right) + (a_n dt + d\beta_n)\frac{d^{n-1}z}{dt^{n-1}} + \ldots + (a_1 dt + d\beta_1)z = d\beta_o \qquad \text{IV.1}$$

where the coefficients $a_r (r = 1, 2, .., n)$ are deterministic constants and $\beta_o(t)$, $\beta_r(t)$ are random functions of time.

From equation IV.1, a second order system without damping would be represented by the equation

$$\ddot{z} + (a_1 + \frac{d\beta_1}{dt})z = \frac{d\beta_o}{dt}$$

The form of this equation may be compared with the corresponding AVA equations to the first order in ϵ,

$$\ddot{X} + \omega_1^2 X - \epsilon R(\dot{y}^2 + y\ddot{y}) = \frac{Q(t)}{X_o}$$

$$\ddot{y} + (\omega_2^2 - \epsilon\ddot{X})y = 0$$

where $Q(t)$ is a stationary random process.

Clearly the randomly varying nonlinear feedback term $\epsilon R(\dot{y}^2 + y\ddot{y})$, essential for the operation of the AVA, makes the solution of this set of equations difficult. However, it is possible to obtain some experimental data on the AVA's response to a random excitation of Gaussian distribution.

The AVA's ability to cope with random excitation was assessed experimentally by comparing the power spectral densities of the main mass response with and without absorber action. Basically the experimental set-up was similar to that described in Chapter 4. A Hewlett Packard noise generator (model 3722A) replaced the Muirhead decade oscillator and the output from the linear displacement transducer (which monitors the main mass response) was fed into a Fenlow spectrum analyser (SA2) which was coupled to an automatic plotter (MP1). The noise generator provides a random noise output which is a continuous analog waveform of approximately Gaussian amplitude distribution.

The response of the main mass system to this random excitation is plotted in the form of a spectral density by the Fenlow equipment, (see Fig. IV.1). Figure IV.2 compares the spectral density plots obtained for the absorber locked and with absorber action. It can be seen that there is a distinct decrease in the power density of the main mass response when the absorber is acting. While not in itself a startling result, it does suggest that the AVA does respond favourably to random excitation. It would be interesting to note how the AVA's performance compares with that of other types of absorber in this respect.

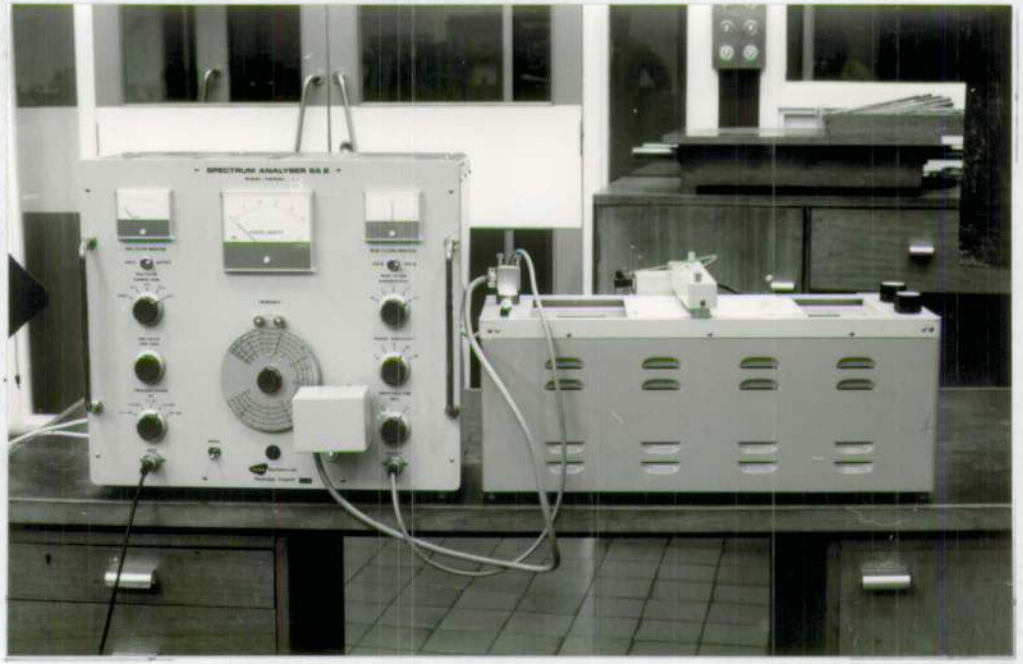

Fig. IV.1

Fenlow Spectrum Analyser SA2
and Automatic Plotter MP1.

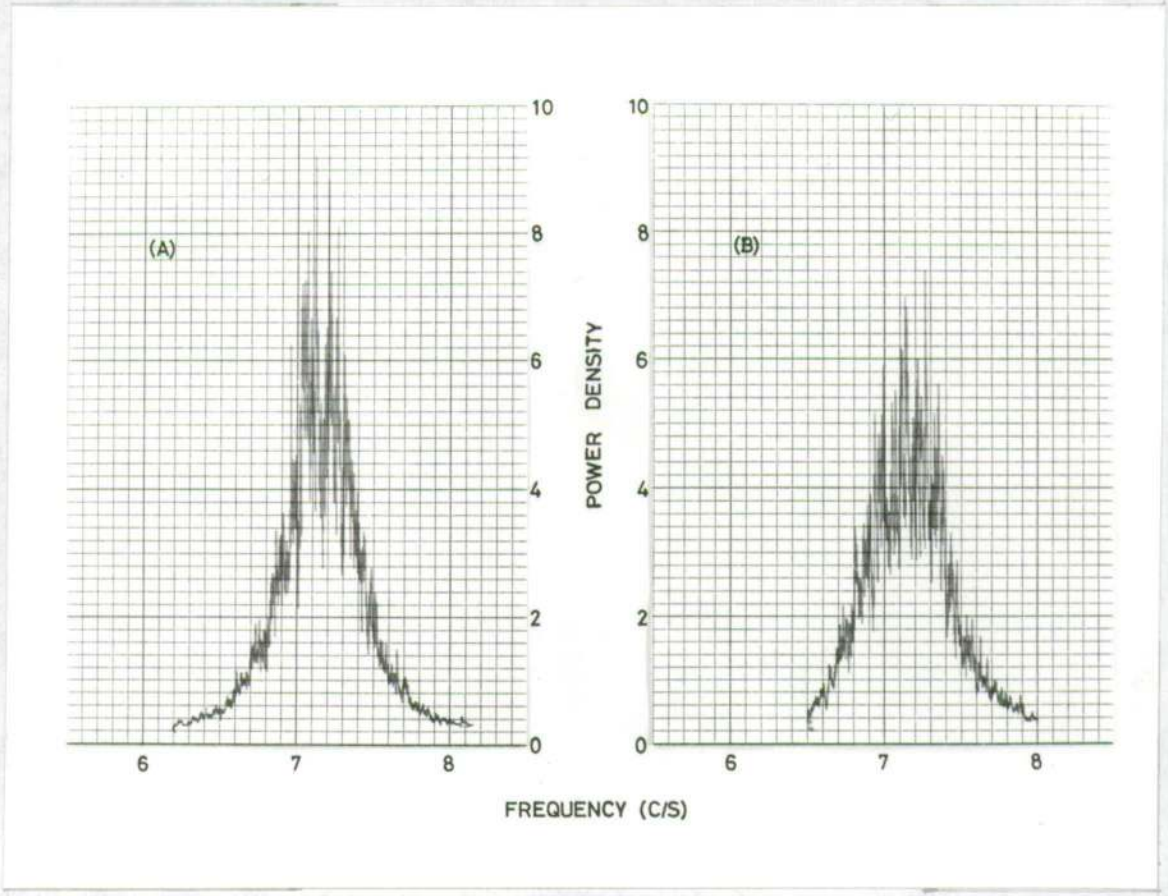

Fig. IV.2

Spectral Density of Main Mass Response

(A) absorber locked,

(B) absorber action.

APPENDIX V

THE AUTOPARAMETRIC VIBRATION ABSORBER

by

R.S. HAXTON AND A.D.S. BARR

A paper to be presented at the ASME Vibrations Conference in Toronto, September 1971.

The Autoparametric Vibration Absorber

by

R. S. Haxton[1] and A. D. S. Barr[2]

Postgraduate School of Applied Dynamics,
Department of Mechanical Engineering,
University of Edinburgh,
Mayfield Road,
Edinburgh EH9 3JL.
Scotland, U.K.

[1]Research Student [2]Senior Lecturer

Abstract

The paper presents the basic features of the steady-state performance of a two-degree of freedom system consisting of a main linear spring mass system under periodic forcing the motion of which acts parametrically on the motion of an attached absorber system. Terms, nonlinear in the absorber motion, act back on the main mass and with appropriate choice of tuning parameters, 'absorption' of the main mass response can be obtained.

Experimental results for this type of device are compared with a theoretical solution obtained from a first order asymptotic approximation. Comparison is also made with the performance of a linear tuned and damped absorber.

INTRODUCTION

Within the context of this paper, vibration absorbers are passive single degree of freedom systems which are designed for addition to some larger vibrating system with a view to reducing its resonant response under external harmonic excitation. Falling into this class are such devices as the tuned and damped absorber, the gyroscopic vibration absorber and the pendulum absorber and the effectiveness and response characteristics of these is well documented. They are basically linear devices because although in operation large amplitudes may introduce nonlinear stiffness or inertial effects the working of the device is not dependent on these.

The device described here however, which for reasons that will be made clear has been termed the 'autoparametric vibration absorber' (contracted to AVA), interacts in an essentially nonlinear manner with the main system to which it is attached. In the usual forms of absorber the motion of the main mass acts effectively as a 'forcing' term on the absorber motion. In the autoparametric absorber however, the main mass motion causes variations in the absorber spring stiffness, that is, it varies one of the parameters of the absorber. Now it is well known that timewise variation of a parameter or 'parametric excitation' of this kind can lead to large amplitudes in the excited system particularly when the time variation involved is periodic.

In this case however the time-variation, arising from the main mass motion, is not an explicit function of time, it is actually dependent on the absorber motion itself which acts back on the main system through nonlinear terms. The system is thus termed autoparametric, the adjective parametric being reserved for situations where there is an explicit time-variation of the parameters.

Mathematically the analysis of the autoparametric absorber under harmonic excitation of the main system is the study of two coupled nonhomogeneous equations of the second order with quadratic nonlinearities. A general study of this form of system using the averaging method has been given by Sethna [1], [2]. For the present particular problem, the asymptotic method described by Struble [3] has been used in preference but, for this problem at least, the results are the same.

The classical autoparametric problem is that of the elastic pendulum described by Minorsky [4] but mostly, this problem has been discussed as an antonomous (free-vibration) one. The paper by Sevin [5] and the related ones by Struble and Heinbockel [6] [7] for instance are in this category but the system they discuss of a vibrating beam interacting parametrically with its pendulous supports is very close, mathematically at least, to the system presently under consideration. The simple pendulum is one possible form of AVA.

The absorber-like response of an autoparametric system might have been anticipated from existing analysis. However in this instance it was first noticed in the laboratory when during tests on the parametric excitation of simple structures under foundation motion, it was observed that in a region of parametric instability the structure could have considerable effect back on the 'foundation'. The foundation was really another degree of freedom and autoparametric interaction was involved.

The question naturally arises as to whether the AVA has any advantages in application over the more conventional types of absorber. This is at present an open question but in most cases it can be anticipated that the answer will be negative. In normal operation the frequency of the AVA absorber motion is one-half of that of the main system and this might be beneficial from a fatigue point of view, however the AVA depends in its operation on having relatively large amplitudes

and the corresponding increased stresses involved will tend to nullify any such advantage. The steady-state performance of the AVA can be made comparable with that of a tuned and damped absorber of the same mass ratio but, with the configurations so far examined, a rather extreme geometry in the form of an extremely short absorber beam length in conjunction with a large amplitude of oscillation is required in order to do this.

The paper presents the essential steady-state operating characteristics of the AVA.

Basic System

A schematic drawing of an AVA mounted on a single degree of freedom system under external forcing $F(t)$ is shown in Fig. 1. The AVA consists of a weightless cantilever beam of length ℓ and flexural rigidity EI carrying a concentrated end mass m. The varying motion $X_d(t)$ (subscript d indicates 'dimensional', a nondimensional X is introduced later) of the main mass M brings about fluctuations in the effective lateral spring stiffness λ of the cantilever. The X-directed force back on the main mass from the absorber comes from the fact that the absorber mass m does not move purely laterally (y_d) but has an associated X-wise or axial displacement which can be related to y_d from the geometry, assuming for instance a static form of displacement curve for the cantilever. This relationship between the axial and lateral displacements is of prime importance in determining the effectiveness of the absorber.

It is not necessary that the absorber should be in the form of a cantilever beam. An alternative mechanisation for instance, would be a pendulum pivoted on the main mass and restrained to the axial position by springs.

Equations of Motion

The equations of motion are most readily derived via the Lagrangian formulation. Both the axial and lateral components of velocity of the absorber mass have to be included in the evaluation of the kinetic energy and using the static deformation curve of the cantilever these components are found to be in the ratio $(6y_d/5\ell)$.

In nondimensional form when the external forcing is harmonic $F(t) = F_o\cos 2\Omega t$ the equations are

$$\begin{aligned} \ddot{X} + 2\epsilon\zeta_1\omega_1\dot{X} + \omega_1^2 X - \epsilon R(\dot{y}^2 + y\ddot{y}) &= \omega_1^2\cos 2\Omega t \\ \ddot{y} + 2\epsilon\zeta_2\omega_2\dot{y} + (\omega_2^2 - \epsilon\ddot{X})y + \epsilon^2 y(\dot{y}^2 + y\ddot{y}) &= 0 \end{aligned} \qquad (1)$$

where dots indicate differentiation with respect to time t and

$$\begin{aligned} &X_o = F_o/k \;;\; X = X_d/X_o \;;\; y = y_d/X_o;\; \epsilon = 6X_o/5\ell \;; \\ &\omega_1^2 = k/(M+m) \;;\; \omega_2^2 = \lambda/m \;;\; \lambda = 3EI/\ell^3 \;;\; R = m/(M+m) \;; \\ &\epsilon\zeta_1 = c_1/2(M+m)\omega_1 \;;\; \epsilon\zeta_2 = c_2/2m\omega_2 \;. \end{aligned} \qquad (2)$$

The basis X_o of the nondimensionalisation is the static deflection of the main system under force amplitude F_o, ω_1 is the free undamped natural frequency of the entire system with the absorber locked ($y = 0$) and ω_2 is the free undamped natural frequency of the absorber. Viscous damping c_1 and c_2 are assumed to act on the main mass and absorber mass respectively, R is a mass ratio and ϵ a natural small parameter of the system. Gravitational effects have been ignored.

Steady-State Solution

An approximate solution to equations (1) can be found using the asymptotic procedure outlined by Struble [3]. For this purpose the equations are written in the form

$$\ddot{X} + 4\Omega^2 X = \epsilon[\epsilon^{-1}(4\Omega^2 - \omega_1^2)X - 2\zeta_1\omega_1\dot{X} + R(\dot{y}^2 + y\ddot{y}) + P\cos 2\Omega t]$$

$$\ddot{y} + \Omega^2 y = \epsilon[\epsilon^{-1}(\Omega^2 - \omega_2^2)y - 2\zeta_2\omega_2\dot{y} + \ddot{X}y - \epsilon y(\dot{y}^2 + y\ddot{y})] \qquad (3)$$

where associating the small parameter ϵ with the forcing term so that ϵP is written for ω_1^2, allows the detailed structure of the solution near external resonance to be obtained.

The solution of (3) is taken in the form

$$X = A(t)\cos[\omega_1 t + \phi(t)] + \epsilon X_1(t) + \epsilon^2 X_2(t) + ..$$

$$\text{and } y = B(t)\cos[\omega_2 t + \theta(t)] + \epsilon y_1(t) + \epsilon^2 y_2(t) + .. \qquad (4)$$

where A, B, ϕ and θ are slowly varying functions of t.

Substitution of this solution, to the second order in ϵ, into the equations of motion yields the following two equations

$$[\ddot{A} - A(\omega_1 + \dot{\phi})^2]\cos(\omega_1 t + \phi) - [A\ddot{\phi} + 2\dot{A}(\omega_1 + \dot{\phi})]\sin(\omega_1 t + \phi) + \epsilon\ddot{X}_1 + \epsilon^2\ddot{X}_2$$

$$+ 4\Omega^2 A\cos(\omega_1 t + \phi) + 4\Omega^2\epsilon X_1 + 4\Omega^2\epsilon^2 X_2$$

$$= \epsilon[\epsilon^{-1}(4\Omega^2 - \omega_1^2)\{A\cos(\omega_1 t + \phi) + \epsilon X_1 + \epsilon^2 X_2\}]$$

$$- \epsilon 2\zeta_1\omega_1[\dot{A}\cos(\omega_1 t + \phi) - A(\omega_1 + \dot{\phi})\sin(\omega_1 t + \phi) + \epsilon\dot{X}_1]$$

$$+ \epsilon R[(B\ddot{B} + \dot{B}^2)\cos^2(\omega_2 t + \theta) - B^2(\omega_2 + \dot{\theta})^2\{\cos^2(\omega_2 t + \theta) - \sin^2(\omega_2 t + \theta)\}$$

$$- \{B^2\ddot{\theta} + 4B\dot{B}(\omega_2 + \dot{\theta})\}\sin(\omega_2 t + \theta)\cos(\omega_2 t + \theta)]$$

$$+ \epsilon^2 R[\{B\ddot{y}_1 + 2\dot{B}\dot{y}_1 + (\ddot{B} - B(\omega_2 + \dot{\theta})^2)y_1\}\cos(\omega_2 t + \theta)$$

$$- \{2B\dot{y}_1(\omega_2 + \dot{\theta}) + (B\ddot{\theta} + 2\dot{B}(\omega_2 + \dot{\theta}))y_1\}\sin(\omega_2 t + \theta)]$$

$$+ \epsilon P\cos 2\Omega t \qquad (5)$$

and

$$[\ddot{B} - B(\omega_2 + \dot{\theta})^2]\cos(\omega_2 t + \theta) - [B\ddot{\theta} + 2\dot{B}(\omega_2 + \dot{\theta})]\sin(\omega_2 t + \theta) + \epsilon\ddot{y}_1$$

$$+ \epsilon^2\ddot{y}_2 + \Omega^2 B\cos(\omega_2 t + \theta) + \Omega^2\epsilon y_1 + \Omega^2\epsilon^2 y_2$$

$$= \epsilon[\ \epsilon^{-1}(\Omega^2 - \omega_2{}^2)\ \{B\cos(\omega_2 t + \theta) + \epsilon y_1 + \epsilon^2 y_2\}]$$

$$- \epsilon 2\zeta_2\omega_2[\dot{B}\cos(\omega_2 t + \theta) - B(\omega_2 + \dot{\theta})\sin(\omega_2 t + \theta) + \epsilon\dot{y}_1]$$

$$+ \epsilon[\{B\ddot{A} - AB(\omega_1 + \dot{\phi})^2\}\cos(\omega_1 t + \phi)\cos(\omega_2 t + \theta) - \{AB\ddot{\phi} + 2B\dot{A}(\omega_1 + \dot{\phi})\}\cdot$$

$$\cdot\sin(\omega_1 t + \phi)\cos(\omega_2 t + \theta)]$$

$$+ \epsilon^2[B\ddot{X}_1\cos(\omega_2 t + \theta) + y_1\{\ddot{A} - A(\omega_1 + \dot{\phi})^2\}\cos(\omega_1 t + \phi) - y_1\{A\ddot{\phi} +$$

$$+ 2\dot{A}(\omega_1 + \dot{\phi})\}\sin(\omega_1 t + \phi)]$$

$$- \epsilon^2[\{B^2\ddot{B} + B\dot{B}^2 - B^3(\omega_2 + \dot{\theta})^2\}\cos^3(\omega_2 t + \theta) + B^3(\omega_2 + \dot{\theta})^2\sin^2(\omega_2 t +$$

$$+ \theta)\cos(\omega_2 t + \theta) - \{B^3\ddot{\theta} + 4\ B^2\dot{B}(\omega_2 + \dot{\theta})\}\sin(\omega_2 t + \theta)\cos^2(\omega_2 t + \theta)] \qquad (6)$$

The terms of order zero in ϵ in equations (5) and (6) are referred to as variational terms and equating these appropriately on each side yields four variational equations. Higher order terms in ϵ give rise to perturbational equations and any of these having resonant solutions are transferred to the variational equations.

The first order terms in ϵ in (5) and (6) give the first order perturbation equations,

$$\ddot{X}_1 + \omega_1^2 X_1 = -2\zeta_1\omega_1[\dot{A}\cos(\omega_1 t + \phi) - A(\omega_1 + \dot{\phi})\sin(\omega_1 t + \phi)]$$
$$+ R\,[(B\ddot{B} + \dot{B}^2)\cos^2(\omega_2 t + \theta) - B^2(\omega_2+\dot{\theta})^2\{\cos^2(\omega_2 t +$$
$$+ \theta) - \sin^2(\omega_2 t + \theta)\}$$
$$- \{B^2\ddot{\theta} + 4B\dot{B}(\omega_2 + \dot{\theta})\}\sin(\omega_2 t + \theta)\cos(\omega_2 t + \theta)]$$
$$+ P\cos 2\Omega t \qquad (7)$$

$$\ddot{y}_1 + \omega_2^2 y_1 = -2\zeta_2\omega_2[\dot{B}\cos(\omega_2 t + \theta) - B(\omega_2 + \dot{\theta})\sin(\omega_2 t + \theta)]$$
$$+ [\{B\ddot{A} - AB(\omega_1 + \dot{\phi})^2\}\cos(\omega_1 t + \phi)\cos(\omega_2 t + \theta) -$$
$$- \{AB\ddot{\phi} + 2B\dot{A}(\omega_1 + \dot{\phi})\}\sin(\omega_1 t + \phi)\cos(\omega_2 t + \theta)] \qquad (8)$$

The periodic external forcing will have most effect when the frequency 2Ω is close to the system frequency ω_1, accordingly we assume that the condition of external resonance holds $(2\Omega/\omega_1) = 1 + O(\epsilon)$. Further, to ensure that the absorber is excited parametrically in its principal region of instability the internal resonance or tuning condition $\omega_1 = 2\omega_2$ is imposed. Consequently such terms as $\cos\{(\omega_1 - \omega_2)t + (\phi - \theta)\}$ in (7) and (8) are resonant and must be removed to the variational equations.

The resulting first order perturbation equations are

$$\ddot{X}_1 + \omega_1^2 X_1 = \tfrac{1}{2} R\,(B\ddot{B} + \dot{B}^2)$$
$$\ddot{y}_1 + \omega_2^2 y_1 = \tfrac{1}{2}[B\ddot{A} - AB(\omega_1 + \dot{\phi})^2]\cos\{(\omega_1 + \omega_2)t + (\phi + \theta)\}$$
$$- \tfrac{1}{2}[AB\ddot{\phi} + 2B\dot{A}(\omega_1 + \dot{\phi})]\sin\{(\omega_1 + \omega_2)t + (\phi + \theta)\}$$

Now as previously stated A, B, ϕ and θ are slowly varying functions of time so that their first and second derivatives with respect to time are assumed small. This means that these perturbation equations need not be treated precisely and the particular integral solutions can be taken as

$$X_1 = 0$$

$$y_1 = \frac{AB\omega_1}{2(\omega_1 + 2\omega_2)} \cos\left\{(\omega_1 + \omega_2)t + (\phi + \theta)\right\}$$

With these solutions for X_1 and y_1 the second order perturbation equations may be written, once again any 'resonant' terms are removed to the variational equations.

The Variational Equations

Returning to equations (5) and (6), the variational equations comprise the coefficients of the fundamental harmonic terms together with the coefficients of the resonant terms brought up from the perturbation equations.

Thus the coefficients of $\cos(\omega_1 t + \phi)$ give

$$\ddot{A} - A(\omega_1 + \dot{\phi})^2 + 4\Omega^2 A = \epsilon[\bar{\epsilon}^{-1}(4\Omega^2 - \omega_1^2)A] - \epsilon 2\zeta_1\omega_1\dot{A}$$
$$+ \epsilon R[\tfrac{1}{2}(B\ddot{B} + \dot{B}^2) - B^2(\omega_2 + \dot{\theta})^2]\cos(2\theta - \phi)$$
$$- \epsilon R[\tfrac{1}{2}B^2\ddot{\theta} + 2B\dot{B}(\omega_2 + \dot{\theta})]\sin(2\theta - \phi) + \epsilon P\cos\phi$$
$$+ \epsilon^2[R\omega_1 AB/4(\omega_1 + 2\omega_2)][\ddot{B} - B(\omega_2 + \dot{\theta})^2 + 2B(\omega_2 +$$
$$+ \dot{\theta})(\omega_1 + \omega_2)]$$

The coefficients of $\sin(\omega_1 t + \phi)$ give

$$-A\ddot{\phi} - 2\dot{A}(\omega_1 + \dot{\phi}) = \epsilon 2\eta_1\omega_1 A(\omega_1 + \dot{\phi}) - \epsilon R[\tfrac{1}{2}B^2\ddot{\theta} + 2B\dot{B}(\omega_2 + \dot{\theta})]\cos(2\theta - \phi)$$

$$- \epsilon R[\tfrac{1}{2}(B\ddot{B} + \dot{B}^2) - B^2(\omega_2 + \dot{\theta})^2]\sin(2\theta - \phi)$$

$$+ \epsilon P\sin\phi + \epsilon^2[R\omega_1 AB/4(\omega_1 + 2\omega_2)][B\ddot{\theta} + 2\dot{B}(\omega_2 + \dot{\theta})]$$

The coefficients of $\cos(\omega_2 t + \theta)$ give

$$\ddot{B} - B(\omega_2 + \dot{\theta})^2 + \Omega^2 B = \epsilon[\epsilon^{-1}(\Omega^2 - \omega_2^2)B] - \epsilon 2\eta_2\omega_2\dot{B}$$

$$+ \epsilon[\tfrac{1}{2}B\ddot{A} - \tfrac{1}{2}AB(\omega_1 + \dot{\phi})^2]\cos(2\theta - \phi)$$

$$+ \epsilon[\tfrac{1}{2}AB\ddot{\phi} + B\dot{A}(\omega_1 + \dot{\phi})]\sin(2\theta - \phi)$$

$$+ \epsilon^2[\omega_1 AB/4(\omega_1 + 2\omega_2)][\ddot{A} - A(\omega_1 + \dot{\phi})^2]$$

$$- \tfrac{1}{4}\epsilon^2[3B^2\ddot{B} + 3B\dot{B}^2 - 2B^3(\omega_2 + \dot{\theta})^2]$$

Finally, the coefficients of $\sin(\omega_2 t + \theta)$ yield

$$-B\ddot{\theta} - 2\dot{B}(\omega_2 + \dot{\theta}) = \epsilon 2\eta_2\omega_2 B(\omega_2 + \dot{\theta}) - \epsilon[\tfrac{1}{2}AB\ddot{\phi} + B\dot{A}(\omega_1 + \dot{\phi})]\cos(2\theta - \phi)$$

$$+ \epsilon[\tfrac{1}{2}B\ddot{A} - \tfrac{1}{2}AB(\omega_1 + \dot{\phi})^2]\sin(2\theta - \phi)$$

$$+ \epsilon^2[\omega_1 AB/4(\omega_1 + 2\omega_2)][A\ddot{\phi} + 2\dot{A}(\omega_1 + \dot{\phi})]$$

$$+ \tfrac{1}{4}\epsilon^2[B^3\ddot{\theta} + 4B^2\dot{B}(\omega_2 + \dot{\theta})]$$

Again, taking into account the assumed slow variation of A, B, ϕ and θ, these variational equations can be simplified.

The resulting reduced equations are,

$$-A\dot{\phi} = (\epsilon/2\omega_2)[2\,\bar{\epsilon}^{-1}(\Omega^2 - \omega_2^2)A - \gamma_1\omega_1\dot{A} - \tfrac{1}{2}RB^2\omega_2^2\cos(2\theta - \phi) + \tfrac{1}{2}P\cos\phi + \epsilon(RAB^2\omega_1\omega_2(2\omega_1 + \omega_2)/8(\omega_1 + 2\omega_2))] \tag{9}$$

$$-\dot{A} = (\epsilon/2\omega_2)[\gamma_1\omega_1^2 A + \tfrac{1}{2}RB^2\omega_2^2\sin(2\theta - \phi) + \tfrac{1}{2}P\sin\phi] \tag{10}$$

$$-B\dot{\theta} = (\epsilon/2\omega_2)[\bar{\epsilon}^{-1}(\Omega^2 - \omega_2^2)B - 2\gamma_2\omega_2\dot{B} - 2AB\omega_2^2\cos(2\theta - \phi) - \epsilon(A^2B\,\omega_1^3/2(\omega_1 + 2\omega_2)) + \epsilon\tfrac{1}{2}B^3\omega_2^2] \tag{11}$$

$$-\dot{B} = (\epsilon/2\omega_2)[2\gamma_2\omega_2^2 B - 2AB\omega_2^2\sin(2\theta - \phi)] \tag{12}$$

The term in $\dot{A}$ in equation (9) and that in $\dot{B}$ in (11) can be eliminated using equations (10) and (12). It is also convenient to transform the variables as follows,

$$t = 4\tau/\epsilon\sqrt{PR}\ ;\ \gamma = (\omega_2^2 - \Omega^2)/\epsilon\omega_2\sqrt{PR}\ ;$$
$$A = b_1\sqrt{P}/\omega_2\sqrt{R}\ ;\ B = b_2\sqrt{P}/\omega_2\sqrt{R}\ ;\ \phi = \psi_1\ ;\ \theta = \psi_2\ . \tag{13}$$

The resulting variational equations are,

$$b_1\psi_1' = 4\gamma b_1 + b_2^2\cos(2\psi_2 - \psi_1) - \cos\psi_1 + \epsilon\gamma_1[-4\gamma_1(\epsilon/R)^{\frac{1}{2}}b_1 - b_2^2\sin(2\psi_2 - \psi_1) - \sin\psi_1] - \frac{5}{4}(\epsilon/R)^{\frac{1}{2}}b_1b_2^2 \tag{14}$$

$$b_1' = -4\gamma_1(\epsilon/R)^{\frac{1}{2}}b_1 - b_2^2\sin(2\psi_2 - \psi_1) - \sin\psi_1 \tag{15}$$

$$b_2\psi_2' = 2\gamma b_2 + (4/R)b_1b_2\cos(2\psi_2 - \psi_1) + \epsilon\gamma_2[-2\gamma_2(\epsilon/R)^{\frac{1}{2}}b_2 + (4/R)b_1b_2\sin(2\psi_2 - \psi_1)] + (2/R)(\epsilon/R)^{\frac{1}{2}}[2b_1^2b_2 - b_2^3] \tag{16}$$

and

$$b_2' = -2\zeta_2(\epsilon/R)^{\frac{1}{2}} b_2 + (4/R)b_1 b_2 \sin(2\psi_2 - \psi_1) \tag{17}$$

where primes denote differentiation with respect to the slow time τ.

In this analysis a solution to the first order variational equations only will be sought. These are

$$b_1 \psi_1' = 4\gamma b_1 + b_2^2 \cos(2\psi_2 - \psi_1) - \cos\psi_1 \tag{18}$$

$$b_1' = -4\zeta_1(\epsilon/R)^{\frac{1}{2}} b_1 - b_2^2 \sin(2\psi_2 - \psi_1) - \sin\psi_1 \tag{19}$$

$$b_2 \psi_2' = 2\gamma b_2 + (4/R)\, b_1 b_2 \cos(2\psi_2 - \psi_1) \tag{20}$$

$$b_2' = -2\zeta_2(\epsilon/R)^{\frac{1}{2}} b_2 + (4/R)\, b_1 b_2 \sin(2\psi_2 - \psi_1) \tag{21}$$

The steady-state solutions for b_1, b_2, ψ_1 and ψ_2 are found by equating the right hand sides of equations (18) to (21) to zero.

Thus $b_1' = b_2' = b_1\psi_1' = b_2\psi_2' = 0$ and after some algebra, eliminating ψ_1 and ψ_2,

$$b_1 = \pm\tfrac{1}{2}(R)^{\frac{1}{2}}[\epsilon\zeta_2^2 + \gamma^2 R]^{\frac{1}{2}} \tag{22}$$

and

$$b_2^2 = 2[\gamma^2 R - \epsilon\zeta_1\zeta_2] \pm [1 - 4\gamma^2\epsilon R(\zeta_1 + \zeta_2)^2]^{\frac{1}{2}} \tag{23}$$

By transformation the two nondimensional expressions for the X and y amplitudes are

$$|X_d/X_o| = \pm[\zeta_2^2 + (1 - n^2)^2/4\epsilon^2]^{\frac{1}{2}} \tag{24}$$

and

$$|(y_d/X_o)^2| = (8/\epsilon R)[((1 - n^2)^2/4\epsilon) - \epsilon\zeta_1\zeta_2] \pm (4/\epsilon R)[1 - (1 - n^2)^2(\zeta_1 + \zeta_2)^2]^{\frac{1}{2}} \tag{25}$$

Stability of Steady-State Solutions

Case 1 b_1, b_2 nonzero.

By observing the behaviour of the parameters b_1, b_2, ψ_1, ψ_2 when given small displacements about their equilibrium position it is possible to determine the stability of the steady-state solutions.

The following substitutions

$$b_1 = b_1^{\,o} + \delta b_1 ; \; b_2 = b_2^{\,o} + \delta b_2 ; \; \psi_1 = \psi_1^{\,o} + \delta\psi_1 ; \; \psi_2 = \psi_2^{\,o} + \delta\psi_2$$

are made in the variational equations (18) thro' (21) where b_1^o, b_2^o, $\psi_1^{\,o}$, $\psi_2^{\,o}$ are the equilibrium solutions. Retaining the linear terms in δb_1, δb_2, $\delta\psi_1$ and $\delta\psi_2$ gives a set of four first order equations.

Following the usual procedure, the stability determinant provides a characteristic equation of the form

$$J_4 \lambda^4 + J_3\lambda^3 + J_2\lambda^2 + J_1\lambda + J_o = 0$$

The Routh-Hurwitz criteria are, J_i positive and $H \equiv J_1J_2J_3 - J_1^{\,2}J_4 - J_oJ_3^{\,2}$ positive for stability.

Now by inspection J_1, J_2, J_3 and J_4 are positive and by calculation H is also positive. The only condition to be considered is thus $J_o > 0$

$$\text{i.e.} \quad (b_2^{\,o})^2 > 2[\gamma^2 R - \epsilon\beta_1\beta_2]$$

is the required stability condition, (c.f. first part of equation (23)).

This means that the steady-state solutions for b_1 and b_2 both nonzero, are stable over the frequency range spanned by the upper branches of the b_2 response curves, and are bounded by the points of vertical tangency on these curves.

Case 2 b_1 nonzero, b_2 zero.

Here $b_1^{\,o} = \pm \dfrac{1}{4[\gamma^2 + (\epsilon/R)\beta_1^{\,2}]^{\frac{1}{2}}}$, $b_2^{\,o} = 0$

The characteristic equation is cubic of the form

$$J_3\lambda^3 + J_2\lambda^2 + J_1\lambda + J_o = 0$$

and the stability criteria are J_i positive and $J_1J_2 > J_o$

The condition that emerges is that

$$\zeta_2(\epsilon/R)^{\frac{1}{2}} \geq [(2b_1{}^o/R)^2 - \gamma^2]^{\frac{1}{2}}$$

for stability.

Substituting for $b_1{}^o$, the solution is unstable within the frequency range defined by

$$\gamma^2 = -(\epsilon/2R)(\zeta_1{}^2 + \zeta_2{}^2) \pm (1/2R)[\epsilon^2(\zeta_1{}^2 - \zeta_2{}^2)^2 + 1]^{\frac{1}{2}} \qquad (26)$$

Again from equation (23) it is seen that for $b_2 = 0$ this same expression (26) is obtained and that $\frac{db_2}{d\gamma}$ is infinite. Therefore the bounds of zero b_2 stability coincide with the points of vertical tangency in the b_2 response curves.

One further aspect which emerges is that the 'cross-over' points found by equating the one-degree of freedom solution ($b_2{}^o = 0$) to the two-degree of freedom solution (equation (22)) thus

$$\frac{1}{16[\gamma^2 + (\epsilon/R)\zeta_1{}^2]} = (R/4)[\epsilon\zeta_2{}^2 + \gamma^2 R]$$

provides the same frequency expression (26). This means that the 'cross-over' points are the entry points for the absorber system.

The Theoretical Response Curves

It is now possible to draw a set of theoretical amplitude response curves for the quantities (X_d/X_o) and (y_d/X_o) using equations (24) and (25), together with the stability conditions just derived. These nondimensional amplitudes are plotted against the forced frequency ratio, $n = 2\Omega/\omega_1$, for various values of viscous damping $\epsilon\zeta_1$ and $\epsilon\zeta_2$.

To establish a comparison with experimental results known experimental values are assigned to ζ_1, ζ_2 and the constants X_o, ϵ and R. ($X_o = 0.0029$ in, $\epsilon = 0.0005$, $R = 0.0196$).

Fig. 2 shows the theoretical response curves for the amplitude of the main mass. Included are the one-degree of freedom responses (absorber locked, $y_d = 0$) for $\epsilon\zeta_1 = 0$ and $\epsilon\zeta_1 = 0.0035$ and four response curves showing the effect of absorber action, for

(a) $\epsilon\zeta_1 = 0, \epsilon\zeta_2 = 0$; (b) $\epsilon\zeta_1 = 0.0035, \epsilon\zeta_2 = 0.0035$

(c) $\epsilon\zeta_1 = 0.0035, \epsilon\zeta_2 = 0.0110$; (d) $\epsilon\zeta_1 = 0.0035, \epsilon\zeta_2 = 0.0184$

The corresponding response curves for the absorber system are shown in Fig. 3. It should be noted that the lower branches of these curves are unstable as indicated by the broken lines.

The points of vertical tangency on the absorber response curves are important as they define the boundaries of the region of parametric instability of the absorber. They coincide with the discontinuities and jumps observed in the main mass displacement of Fig. 2. The forcing frequency at which a nonzero absorber amplitude becomes unstable will be referred to as a 'collapse frequency' and the associated main mass amplitude just prior to this will be referred to as its 'collapse amplitude'.

In Fig. 2 the locus of the collapse amplitude for $\epsilon\zeta_1 = 0.0035$ is shown for varying ζ_2 by the broken line. This locus has as asymptotes the one-degree of freedom response for $\epsilon\zeta_1 = 0$ and the two-degree of freedom response for $\epsilon\zeta_1 = 0$ and $\epsilon\zeta_2 = 0$. It is seen to have a minimum value which defines that value of $\epsilon\zeta_2$ for a given $\epsilon\zeta_1$ which will produce the minimum collapse amplitude.

To follow the details of the action of the AVA consider the set of curves (c) from Figs. 2 and 3 for $\epsilon\zeta_1 = 0.0035$ and $\epsilon\zeta_2 = 0.0110$.

From Fig. 2, it is seen that following the path of increasing frequency (indicated by arrows) the system behaves as a normal one-degree of freedom system (region A) until it reaches the cross-over point (point B) previously discussed. This corresponds to a point of vertical tangency in the absorber solution (b_2^o = 0 solution unstable) and so absorber action begins. The main mass system then follows the two-degree of freedom solution (region C), its amplitude reaching a minimum value at n = 1. It then climbs steadily until the collapse amplitude is reached (point D). This corresponds to a vertical tangency in the absorber solution which marks the bound of absorber action. The result is that absorber action ceases and the main mass amplitude drops to its one-degree of freedom level (point E).

Following a path of decreasing frequency (again arrowed) the main system behaves in a similar fashion tracing the path F, G (absorber entry point), C, H (collapse amplitude), K, and A.

Fig. 3 shows the corresponding regions and points on the absorber response curve, the jumps BB and GG coinciding with the entry points B and G on the main mass response.

Experimental Apparatus and Procedure

The experimental apparatus was designed to give a one-degree of freedom main mass system with low damping. Fig. 4 shows the basic layout.

The main mass is a solid steel block supported and restrained to horizontal motion by four spring steel legs. A coil spring provides the necessary horizontal stiffness giving a natural frequency of 6.92 Hz. The absorber system consists of a spring steel beam 0.020 in. thick by $\frac{3}{4}$ in. wide with an adjustable end-mass. This system is attached to the main mass by means of a light clamping block.

The complete system is mounted on an angle bracket which is strapped to the head of an electromagnetic shaker. To prevent a bending moment on the shaker head, the deadweight is taken by suspending the whole assembly on elastic ropes connected to the four support points of the angle bracket.

The shaker was excited through a power amplifier from an accurate decade oscillator.

Viscous damping could be introduced to both main mass and absorber systems by the addition of light vanes operating in oil baths.

Thus the experimental rig is basically a spring-mass system on a moving support (shaker head). Keeping the amplitude of the support constant ensures a constant exciting force on the system.

The instrumentation incorporated in the set-up consisted of

(a) a proximity probe to monitor shaker head amplitude.

(b) a linear displacement transducer to measure main mass amplitude (coupled to an oscilloscope).

(c) strain gauges at the root of the absorber cantilever to measure absorber end-mass amplitude (coupled to an ultraviolet recorder).

The oscilloscope and ultraviolet recorder provided monitoring and recording facilities. The instrumentation was initially calibrated and appropriate damping rates decided.

The typical test procedure involved the step-wise increase and decrease of the forcing frequency through the resonance region. At each setting of frequency the shaker head amplitude was held at a constant, predetermined level by means of a potentiometer in the power amplifier output and the steady-state amplitudes of the main mass and absorber systems were noted.

The Experimental Response Curves

Fig. 5 shows four response curves for the main mass system labelled (a), (b), (c) and (d). Curve (a) is the response with the absorber locked ($b_2 = 0$) for $\epsilon\eta_1 = 0.0035$. Curves (b), (c) and (d) are the amplitude responses under absorber action for the following damping ratios,

(b) $\epsilon\eta_1 = 0.0035, \epsilon\eta_2 = 0.0035$; (c) $\epsilon\eta_1 = 0.0035, \epsilon\eta_2 = 0.0110$;

(d) $\epsilon\eta_1 = 0.0035, \epsilon\eta_2 = 0.0184$.

Fig. 6 shows the corresponding response curves for the absorber system.

Interpretation of these experimental curves follows the same pattern as outlined for the theoretical case.

Comparison of Theoretical and Experimental Response Curves

Direct comparison between the theoretical and experimental response curves can be made using Figs. 2, 3, 5 and 6. The experimental curves (b), (c), (d) in Fig. 5 compare directly with curves (b), (c), (d) in Fig. 2. Similarly curves (b), (c), (d) in Fig. 6 have their counterparts (b), (c), (d) in Fig. 3.

The comparison is seen to be quite reasonable although the experimental amplitudes of the main mass are, in general, greater than those predicted theoretically. It is, of course, difficult to tune the absorber precisely to the condition $\omega_1 = 2\omega_2$, and as a result the experimental curves lack the symmetry displayed by the theoretical curves about the n = 1.0 axis.

This may also in part be attributable to the neglect in the theory of the nonlinearity in the spring force of the cantilever which, with the relatively large amplitudes involved, was quite significant.

The main mass experimental curves of Fig. 5 can also be seen to exhibit jumps at the points of entry of the absorber which are not predicted by the first order theory used.

Comparison of AVA with LTDA

It can be shown from the analysis that a more powerful absorber action is achieved when the value of the parameter $\epsilon (= 6X_o/5\ell)$ is increased. This implies an increase in the ratio of axial motion to lateral motion of the absorber mass. In practice this can be achieved by dimensioning the absorber cantilever beam to provide the same natural frequency (ω_2) with the same mass (m) while decreasing the length (ℓ).

Experiments were carried out using an absorber whose length was one-fifth of that of the system already discussed. This increased the value of ϵ by a factor of five. Fig. 7 compares a set of theoretical and experimental main mass responses for such an absorber, where $\epsilon_{\gamma_1} = 0.0030$ and $\epsilon_{\gamma_2} = 0.0338$. Studying Figs. 2, 5 and 7, it can be seen that a general improvement in the performance of the absorber has been obtained by shortening its length but this improvement is obtained at the expense of greater strain amplitudes in the absorber.

To provide a measure of the effectiveness of this improved AVA system it was decided to effect a theoretical comparison with the linear tuned and damped absorber (contracted to LTDA). The theory of the LTDA is given in reference [8].

The experimental mass ratio $(m/M) = 0.02$ is chosen for both AVA and LTDA systems.

Since this ratio is small compared with unity, the LTDA natural frequency ratio is taken as unity and the optimum damping between its two mass systems is found to be 0.09.

Fig. 8 compares the resulting LTDA main mass response (a) with two AVA response curves (b) and (c). Response (b) is for $\epsilon\gamma_1 = 0$ and $\epsilon\gamma_2 = 0.0208$, while response (c) is for $\epsilon\gamma_1 = 0$ and $\epsilon\gamma_2 = 0.0360$. Also shown is the one-degree of freedom response (d) for the absorber locked. The AVA response (c) represents the minimum collapse amplitude attainable for the stated parameters but this $\epsilon\gamma_2$ value does not produce good absorber action near resonance. Response (b) for a smaller $\epsilon\gamma_2$ value compares more favourably with the LTDA near resonance but the consequent widening of the parametric instability zone results in much higher collapse amplitudes.

Conclusions

The basic absorbing action of the autoparametric system described has been shown experimentally and the first order asymptotic theory developed has effectively predicted most of the principal features of the steady-state response. The transient response of the absorber is currently under investigation.

The comparison described between an autoparametric absorber and a linear tuned and damped absorber of the same mass ratio is not favourable towards the former. However there is a great deal of development of the autoparametric device which might still be carried out and it may prove advantageous in some applications. It is for instance in principle possible to design an absorber which will act simultaneously as an autoparametric and a tuned and damped absorber. If the input consists of a fundamental frequency (Ω) and its first overtone (2Ω) then the fundamental component would be absorbed by the tuned and damped action while the overtone would stimulate the autoparametric action.

Acknowledgements

The Studentship support of one of the authors (R.S.H.) by the Science Research Council, London, during the course of the investigation described in this paper is gratefully acknowledged.

References

[1.] P.R. Sethna, "Transients in Certain Autonomous Multiple-Degree-of-Freedom Nonlinear Vibrating Systems", Journal of Applied Mechanics, Vol. 30, Trans. ASME, Vol. 85, Series E, 1963, pp. 44-50.

[2.] P.R. Sethna, "Vibrations of Dynamical Systems With Quadratic Nonlinearities", Journal of Applied Mechanics, Vol. 32, Trans. ASME, Vol. 87, Series E, 1965, pp. 576-582.

[3.] R.A. Struble, "Nonlinear Differential Equations," McGraw-Hill Book Company, New York, N.Y., 1962, pp. 220-260.

[4.] N. Minorsky, "Nonlinear Oscillations," D.Van Nostrand Company, New York, N.Y., 1962.

[5.] E. Sevin, "On the Parametric Excitation of Pendulum-Type Vibration Absorber", Journal of Applied Mechanics, Vol. 28, Trans. ASME, Vol. 83, Series E, 1961, pp. 330-334.

[6.] R.A. Struble and J.H. Heinbockel, "Energy Transfer in a Beam-Pendulum System", Journal of Applied Mechanics, Vol. 29, Trans. ASME, Vol. 84, Series E, 1962, pp. 590-592.

[7.] R.A. Struble and J.H. Heinbockel, "Resonant Oscillations of a Beam-Pendulum System", Journal of Applied Mechanics, Vol. 30, Trans, ASME, Vol. 85, Series E, 1963, pp. 181-188.

[8.] J.P. Den Hartog, "Mechanical Vibrations", McGraw-Hill Book Company, New York, N.Y., Fourth edition, 1956, pp. 93-102.

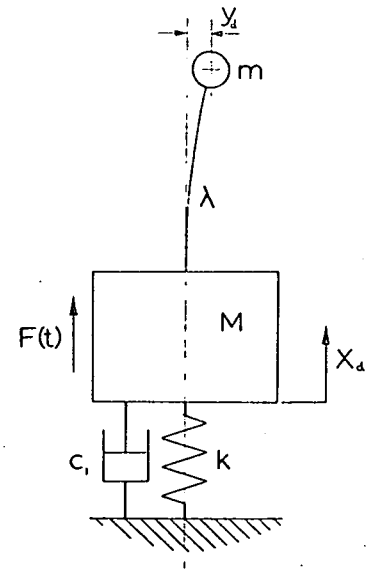

Fig. 1

Schematic diagram of autoparametric absorber system.

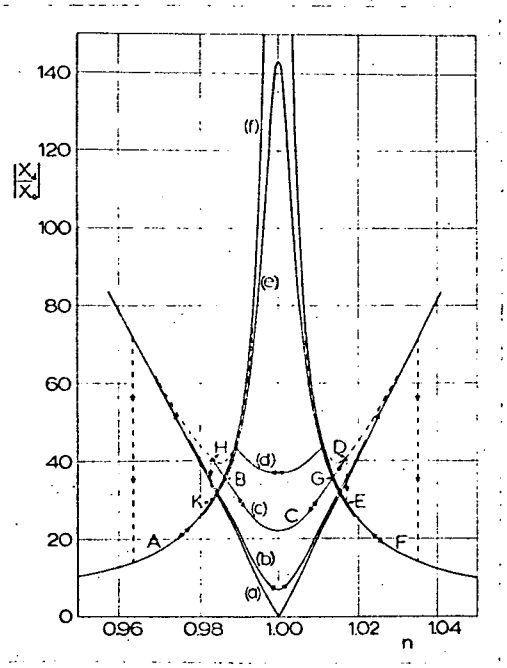

Fig. 2

Theoretical response amplitude of main mass under the action of the AVA for various values of the damping ratios.

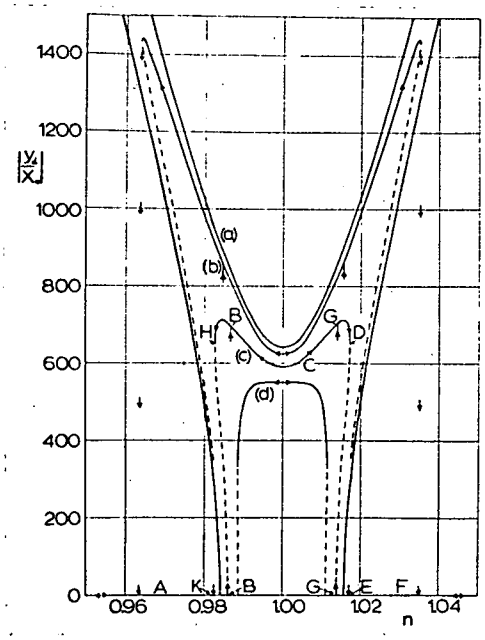

Fig. 3

Theoretical response amplitude of the absorber for various values of the damping ratios.

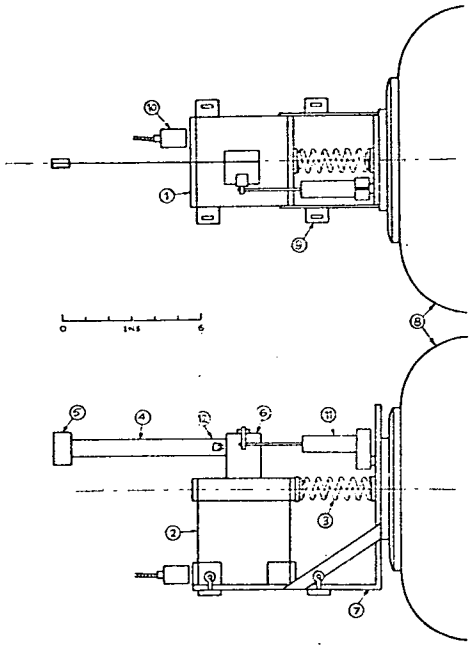

Fig. 4

Experimental Apparatus

1. main mass, 2. Spring steel legs,
3. coil spring, 4. absorber cantilever spring,
5. absorber end-mass, 6. absorber clamping block,
7. angle bracket, 8. shaker,
9. support points, 10. proximity probe,
11. linear displacement transducer, 12. strain gauges.

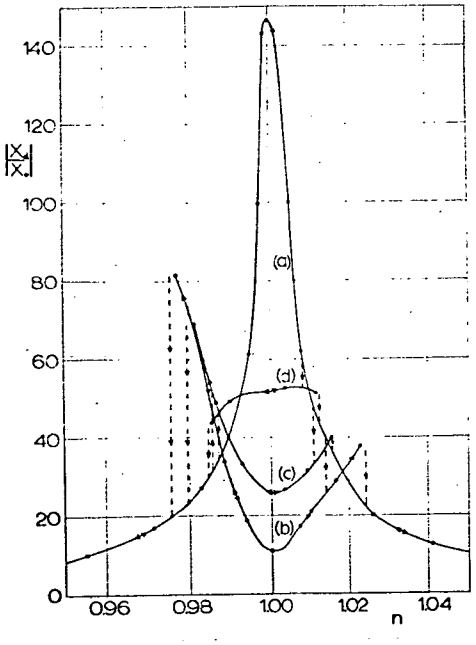

Fig. 5

Experimental response amplitude of main mass under the action of the AVA.

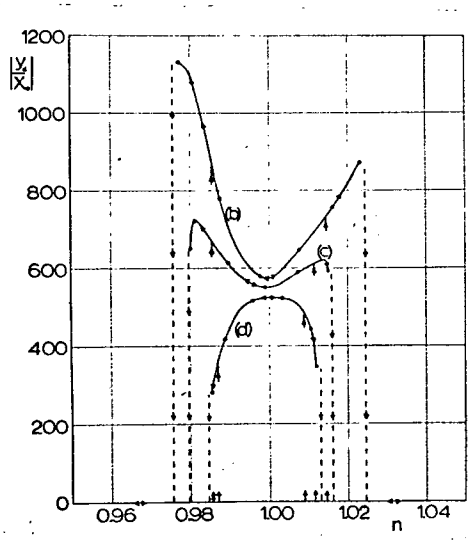

Fig. 6

Experimental response amplitude of absorber.

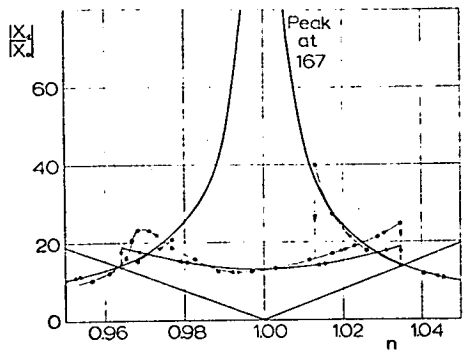

Fig. 7

Comparison of theoretical and experimental main mass response amplitude under the action of small length AVA. The legend —o———o— represents experimental data.

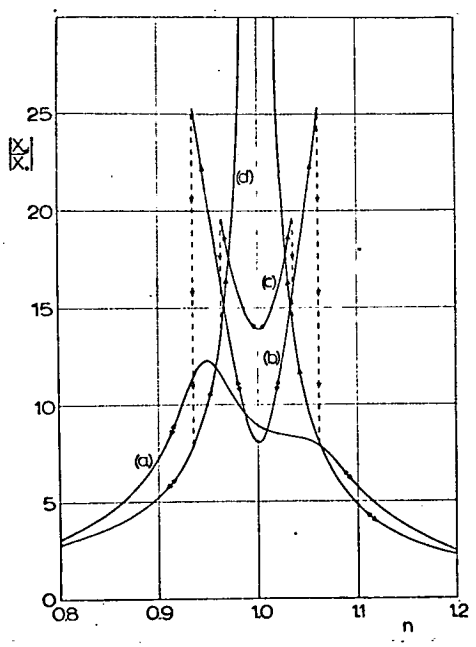

Fig. 8

Comparison of main mass response amplitude of the LTDA with that of the small length AVA.